

**Seismic performance assessment of reinforced concrete structures:  
quantifying the effects of damage and informal construction**

by

**Polly B. Murray**

B.S., Tufts University, 2014

M.S., University of Colorado Boulder, 2018

A thesis submitted to the  
Faculty of the Graduate School of the  
University of Colorado in partial fulfillment  
of the requirements for the degree of  
Doctor of Philosophy

Department of Civil, Environmental, and Architectural Engineering

2021

This thesis entitled:  
Seismic performance assessment of reinforced concrete structures: quantifying the effects of  
damage and informal construction  
written by Polly B. Murray  
has been approved for the Department of Civil, Environmental, and Architectural Engineering

---

Abbie B. Liel

---

Amy Javernick-Will

---

Shideh Dashti

---

Kenneth J. Elwood

---

Orlando Arroyo

---

Siamak Sattar

Date \_\_\_\_\_

The final copy of this thesis has been examined by the signatories, and we find that both the content and the form meet acceptable presentation standards of scholarly work in the above mentioned discipline.

IRB protocol #19-0337

Murray, Polly B. (Ph.D., Civil Engineering)

Seismic performance assessment of reinforced concrete structures: quantifying the effects of damage  
and informal construction

Thesis directed by Professor Abbie B. Liel

Earthquakes have led to extensive loss of human life, destruction of the built environment, displacement of residents from their homes, and high economic costs in many parts of the world. These impacts largely stem from building collapse and damage, and reinforced concrete (RC) structures are a significant contributor. The behavior of RC buildings in earthquakes is highly uncertain, particularly when a building has been damaged or built informally. The goal of this research is to develop improved assessment techniques of RC buildings that increase the understanding of the seismic performance of RC structures in order to improve community outcomes in major earthquakes. This dissertation is a compilation of two studies that each present a new methodology for assessing seismic performance. In each, the methodology is also exercised for a set of archetype structures. These frameworks employ nonlinear simulation models and computationally efficient analysis methods.

In a post-earthquake environment, repair and demolition decision making play a significant role in community recovery. These decisions are made based on a number of factors, including the future seismic performance of buildings. The connection between the extent of damage—and how best to evaluate damage—and the change in performance is not well understood. *Chapter 2* of this dissertation presents a new computationally-efficient framework for evaluating future seismic performance based on damage. This relationship is affected by building characteristics: short period buildings are more sensitive to damage and highly ductile buildings are capable of withstanding higher levels of damage. The framework and the findings in this study can be used in conjunction with component-level assessments and visual inspection to guide post-earthquake decision making about repair and demolition.

Informally-constructed houses have had devastating consequences in recent earthquakes. Informally constructed homes are those that are built without explicit engineering design or code-compliance, and may be built with low-quality materials. Despite the ubiquity of this type of construction, few seismic performance assessments have been conducted. *Chapter 3* presents a methodology for evaluating the collapse risk of informally-built RC houses. This framework is exercised for houses in Puerto Rico, where informal construction is prevalent. This work revealed which building components and characteristics are most critical for seismic safety. Open-ground-story houses are most vulnerable to collapse, but can be improved through improved column detailing or retrofit. One-story houses are generally safer than two-story houses, heavier buildings generate larger seismic forces on building components. Confined masonry construction is safer than infilled masonry. These findings are used to provide recommendations for homeowners, builders, and local organizations that will improve seismic safety. The methods outlined in this study can be applied more broadly to areas where informal construction is common and seismic hazard is high.

## Acknowledgements

I am so grateful for the support of mentors, family, and friends on my journey to complete graduate school. This Ph.D. has challenged me in innumerable ways, and I am deeply grateful for the team who helped me complete it.

First, I must express my deep gratitude to my advisor, Dr. Abbie Liel. I feel so lucky to have been your student. You have gone above and beyond on countless occasions to help me achieve my research goals. It is clear to me, and all members of Liel Nation, how invested you are in our work and our success. Beyond research, I'm grateful for your advice on navigating this male-dominated field and the example you set for balancing a career with parenthood.

To my committee members: Dr. Ken Elwood, Dr. Siamak Sattar, Dr. Orlando Arroyo, Dr. Amy Javernick-Will, and Dr. Shideh Dashti, thank you for your insight on this work. I feel so lucky to have worked closely with many of you over the last few years, and am a much better researcher because of your guidance and thoughtful discussions. I look forward to continued collaboration.

To the members of the ATC 145 Project committee, thank you for your feedback on the development of the repair framework. The opportunity to collaborate with so many accomplished researchers was very beneficial to my development as a researcher. To the Puerto Rico research team: Briar, Yare, Junelis, and Dirsar, I'm so grateful for our collaboration and (mis)adventures in Puerto Rico. We could not have completed this work without your translation efforts, your connections to the community, and your insight. Thank you for accommodating my inane requests, for breaking concrete blocks, and for your attempts to teach me Spanish. To the project team at NIST: Dr. Chris Segura and Dr. Siamak Sattar, thank you for bringing me on to this project, and

your feedback as I worked through modeling challenges. Thank you to NIST for supporting the final years of my graduate studies.

To the members of Liel Nation and friends: Dustin, Jakub, Zach, Eric, Casie, Rob, Sam, Sarah, Cody, Hailey-Rae, Lianne, Maria-Jose, Amir, Janice, and Briar, thank you for the research advice and the office camaraderie. Dustin, I'm grateful for our concurrent studies, your work ethic is inspiring, and I'm so appreciative of your efforts to bring yuletide joy to the office. Jakub, thank you for teaching me the ways of *OpenSees*, and for your constant willingness to talk through modeling challenges. Zach, your insight on machine learning, statistics, and data processing was invaluable, and I'm deeply grateful for your help in this work. Eric, I'm glad our paths crossed here. Your sly humor brightened our windowless basement. Casie, I thoroughly enjoyed our discussions of life, fashion, and typefaces. Your capacity to present and disseminate information is inspiring. Rob, I'm grateful to have had the company of another New Englander in a sea of Californians. Sam, our regular Costco visits bring me so much joy. Sharing the first two years of grad school with you made those years so much more fun. Becca, you inspire me with your work ethic and sense of humor, and I'm so glad we overlapped here.

To the Lunch Bunch: Johnny, Shane, Mike, Aman, Guillermo, Jan, Charlie, and Mikaela, our midday lunch breaks were a highlight of grad school for me. I'm thankful, too, for our adventures skiing, biking, and climbing, and for your help when those adventures ended with broken bones. To Emma and Christine, our bike rides, trips to Dunkin', and movie nights have really brightened this stressful and sorrowful year. I'm so glad for your friendship as we celebrate our successes and mourn our losses.

To the Kelly Road house: Phil, Dan, Melissa, Sarah, Rob, and Matt, thank you for the life advice and the potlucks. I'm so grateful you took a chance on fresh-out-of-college me as your roommate, and that the roommate bond has not fractured as we moved across state lines. Dan and Melissa, thank you for lending me your dog so frequently. To my Boulder roommates, thanks for making this such a fun place to live. Isabel, living with you was a true highlight of my time in Boulder. I miss our (bad) music playing, our collaborative crossword efforts, and the endless chats.

Jan, I'm so glad you moved in, and shared your love of bikes and excellent cooking skills with me.

To my Tufts pals: Tony, Will, Gabe, Strandy, and Orli, our time in Utah's desert, New England's waterways, and mountains near and far has brought me so much joy. To Britt, Christine, and Lauren, I'm so grateful that our friendships have held strong as we dispersed across the country. To Jenna, thank you for teaching me the importance of a calendar invite and your willingness to proofread. To my SG friends: Suzy, Julia, Courtney, Molly, Jesse, Laura, Hannah, and Charlotte, I'm thrilled that our friendship has persevered long after we left high school. It has been a delight to celebrate life's milestones with you all.

To my family: Betts, Wisner, Francis, and Grandpa, I'm so appreciative for your support of my efforts to pursue engineering. From the early days where I hoarded the family tupperware supply to build structures in my room, to your reviews of the chapters in this dissertation, I have always felt so supported by you.

In loving memory of Daniel, Ginger, and Alec.

Contents

Chapter

**1** Introduction 1

1.1 Motivation . . . . . 1

1.2 Research scope and gaps . . . . . 3

1.3 Overview of research questions . . . . . 7

1.4 Organization . . . . . 8

**2** A framework for assessing impaired seismic performance as a trigger for repair 10

2.1 Introduction . . . . . 10

2.2 Related previous work . . . . . 12

2.3 Methods . . . . . 15

2.4 SDOF study to isolate effects of building characteristics . . . . . 22

2.5 RC frame buildings of interest . . . . . 26

2.6 Reparability of RC frame buildings . . . . . 30

2.7 Conclusions . . . . . 35

**3** Seismic safety assessment of informally-constructed houses in Puerto Rico 38

3.1 Introduction . . . . . 38

3.2 Background . . . . . 39

3.3 Methods . . . . . 47

3.4 Nonlinear simulation models . . . . . 59



3.5	Seismic performance assessment methods . . . . .	67
3.6	Seismic performance results for informally-constructed houses . . . . .	69
3.7	Comparison with reconnaissance data . . . . .	78
3.8	Limitations and future work . . . . .	79
3.9	Conclusions and recommendations . . . . .	80
4	Conclusions	84
4.1	A framework for assessing impaired seismic performance as a trigger for repair . . .	84
4.2	Seismic safety assessment of informally-constructed houses in Puerto Rico . . . . .	87
4.3	Proposed future work . . . . .	90
	<b>References</b>	92
	<b>Appendix</b>	
A	Interview questions for informal construction data collection	103
B	Multi-axial column material	107

Tables

Table

1.1 Summary of studies collected in this dissertation, including research gaps, questions, and supplementary information . . . . . 9

2.1 Range of values for each SDOF model parameter. . . . . 23

2.2 RC frame buildings assessed for reparability in this study . . . . . 27

3.1 Archetype design variations and assumptions . . . . . 51

3.2 Open-ground-story houses, including design parameters and performance measures . 56

3.3 One- and two-story houses with masonry walls and their seismic design parameters . 57

3.4 Archetype houses used to assess effects of incremental construction . . . . . 58

3.5 Recommendations for improved seismic safety in new and existing houses . . . . . 82

4.1 Summary of studies collected in this dissertation, including research gaps and contributions . . . . . 85

## Figures

### Figure

2.1	Framework for assessing the level of damage at which a building's seismic performance is impaired . . . . .	16
2.2	Set of damage conditions for a code-conforming RC frame, showing how peak story drift and the period of the damaged structure vary with ground motion intensity ( $Sa(T_1)$ ). The damaged period is calculated using eigenvalue analysis at the end of the analysis; $T_1$ for this undamaged building is 1.0 sec. . . . .	18
2.3	Set of damage conditions, and the selected conditions, for a code-conforming structure. The distribution of damage conditions along each axis are also shown. . . . .	19
2.4	Story drift time history of analyses for one damage condition and one $MCE_R$ -level performance assessment motion. . . . .	20
2.5	Median drift amplification ratios over a moving window for one building model subjected to 50 damage conditions and 15 $MCE_R$ -level motions. . . . .	21
2.6	Static pushover response of SDOF models with (a) varied deformation capacity ( $\theta_p$ ) and constant strength and stiffness, and (b) varied strength and stiffness with constant yield and capping drifts, and (c) $P - \Delta$ effects. . . . .	23
2.7	Drift histories of SDOF models with varied deformation capacities ( $\theta_p$ ) subjected to a back-to-back ground motion. . . . .	24

2.8	SDOF models with variation in deformation capacity (defined as $\theta_p$ ) showing (a) moving window medians, and (b) hysteretic response during one damage condition and performance assessment. . . . .	25
2.9	SDOF models with variation in $P - \Delta$ showing (a) moving window medians, and (b) hysteretic response during one damage condition and performance assessment. . . .	25
2.10	Median drift amplifications for SDOF models with variation in (a) stiffness and period, and (b) stiffness only. . . . .	26
2.11	Median drift amplifications for SDOF models with variation strength and a first mode period (a) $T = 0.5$ s, and (b) $T = 1.0$ s. . . . .	27
2.12	Diagram of geometry and modeling of exterior frames, with three-bay seismic-resisting bays perimeter frame and two gravity frame bays. Typical column backbones for perimeter frame in 4-story buildings definition are shown. . . . .	28
2.13	Response of RC frame buildings under static pushover loading. Base shear is normalized by building weight. . . . .	30
2.14	Reparability of 4-story RC frame buildings, showing the change in response of (a) code-conforming (Bldg C4) and (b) non-conforming (Bldg N4) frames in $MCE_R$ -level motions, as a function of peak story drift in a damaging motion. . . . .	32
2.15	Reparability of 1-story code-conforming RC frame (Bldg C1) building, showing the change in response of in $MCE_R$ -level motions, as a function of peak story drift in a damaging motion. . . . .	33
2.16	Reparability of 12-story RC frame buildings, showing the change in response of (a) code-conforming (Bldg C12) (b) non-conforming (Bldg N12) buildings in $MCE_R$ -level motions, as a function of peak story drift in a damaging motion. . . . .	33
2.17	Relationship between drift amplifications and (a) period elongation and (b) residual drift in a 1-story, code-conforming building. . . . .	35

2.18 (a) Relationship between the the duration of the damaging motion and associated peak drift for selected damage conditions in a 1-story, code-conforming structure (Bldg C1). (b) Reparability of Bldg C1 for long and short duration ground motions.	36
3.1 Shaking intensity during January 7, 2020 earthquake . . . . .	41
3.2 Damage to RC houses in Guánica with (a) an open ground story, showing loss of the first open story, and (b) masonry walls between columns at the first story, showing shear cracking in walls and columns. [Photos: Polly B. Murray] . . . . .	41
3.3 (a) Puerto Rican home with exposed reinforcing bars to facilitate house expansion. (b) Home with RC first story and wood frame second story (Yabucoa, Puerto Rico)[Photos: Polly B. Murray] . . . . .	42
3.4 Commonly available concrete materials, including coarse and fine aggregate and cement, at a hardware store in San Juan, Puerto Rico. [Photos: Polly B. Murray] . .	49
3.5 Typical RC houses in Guánica and Humacao, Puerto Rico. [Photos: Polly B. Murray]	49
3.6 Typical floor plan (showing building frame of interest) and elevation views for archetype houses. The infill configuration and the number of stories are two of the variations considered. . . . .	50
3.7 Houses in Guánica that were damaged during the January 7, 2020 earthquake. (a) failure in first story columns, (b) shear cracks in masonry walls. [Photos: Polly B. Murray] . . . . .	50
3.8 Masonry wall configurations with and without openings . . . . .	51
3.9 Baseline column configuration, and two variations (PVC gutter and RC jacket) . . .	52
3.10 Column damaged during the January 7, 2020 earthquake (Guánica, Puerto Rico) . .	53
3.11 Steel reinforcing bars used in home construction. Transverse ties are sold in pre-defined bent shapes; the 6 x 12 in bars are most common. The most common longitudinal bars are no. 4 and no. 5, and are often stored outside (Humacao, Puerto Rico). [Photos: Polly B. Murray] . . . . .	53

3.12 Masonry blocks used in home construction available at a hardware store in Puerto Rico. [Photos: Polly B. Murray] . . . . . 54

3.13 Diagram of models of a two-story, two-bay house with infilled or confined masonry walls. . . . . 60

3.14 Diagram of models of the open-ground-story houses. The lumped masses account for the weight of a second story with masonry walls. . . . . 61

3.15 Static pushover response of columns configurations. . . . . 63

3.16 (a) Diagram of the model of a single bay with RC columns and a concrete masonry panel, illustrating the adopted modeling approach; and (b) analytical backbone and static pushover response of one bay calibrated for infilled and confined construction. 64

3.17 (a) IDA results for a single-story house with infilled and confined construction, and (b) corresponding fragility curves (both empirical and fitted distribution). . . . . 68

3.18 (a) Summary of collapse fragilities for all archetype houses; (b) distribution of median collapse capacities for informally-constructed RC open-ground-story houses and houses with masonry walls. . . . . 70

3.19 Collapse fragilities of open-ground-story houses with variation in weight, induced by floor and roof slab thicknesses listed in the legend. . . . . 71

3.20 Collapse fragilities of open-ground-story houses with variation in weight, induced by floor and roof slab thicknesses listed in the legend. . . . . 71

3.21 Collapse fragilities of open-ground-story houses with (a) longitudinal PVC gutter, and (b) corroded reinforcing steel. Corroded reinforcing steel in vulnerable columns reduces collapse capacity. . . . . 73

3.22 Collapse fragilities of open-ground-story house retrofit with full or partial RC jackets, one, and two bays of infill, illustrating the largest reduction in collapse capacity is provided by two bays of infill . . . . . 74

3.23 Collapse fragilities for one- and two-story houses with infilled and confined masonry walls, showing the large benefit from the confined construction technique. . . . . 75

3.24 (a) Damage states, defined by the level of peak story drift. (b) Probability of exceedance for slight, moderate, extensive, and collapsed damage states in a two-story house with infilled (I) and confined (C) masonry walls. . . . . 75

3.25 Collapse fragilities two-story houses with variation in masonry unit strength. Stronger masonry units reduce collapse risk. . . . . 76

3.26 Collapse fragilities for walls with openings . . . . . 77

3.27 Collapse fragilities for one- and two-story houses. The addition of an RC second story drastically increases collapse risk, while a wood frame second story, which does not increase building weight significantly, does not. . . . . 77

B.1 Hinge response history (a) before and (b) after error generating discontinuity in the hinge was addressed . . . . . 109

## Chapter 1

### Introduction

#### 1.1 Motivation

Earthquakes have caused extensive loss of human life, destruction of the built environment, displacement of residents from their homes, and high economic costs in many parts of the world. These impacts are largely a result of building collapse and damage, and reinforced concrete (RC) buildings are a significant contributor [1, 2, 3, 4, 5]. RC buildings are common worldwide, as the necessary materials are relatively inexpensive and widely available [6, 7]. These buildings typically perform well under gravity and wind loading [8, 9], but can be vulnerable to damage or collapse in earthquakes if not designed and detailed for seismic design [10, 11].

In areas where seismic loads are considered in design and construction, RC buildings are generally able to withstand damage without compromising life safety, by dissipating the energy introduced by the ground motion [12]. However, this damage may be extensive and its effect on the future performance of the building is uncertain [13], and post-earthquake decision making about repairs and building occupancy tends to be conservative as a result. Presently, visual inspection and post-earthquake capacity assessments—typically based on static pushover analysis—are used to inform repair or demolition decisions [14, 15, 16]. Conservative decision making can lead to excessive repair or demolition costs, downtime, and socioeconomic stagnation, which impede community recovery [17]. For example, following the 2011 Christchurch, New Zealand earthquake, 65% of “significant” buildings (defined as those with more than five stories) were demolished in the central business district [2]. Safety cordons to mitigate risk to public safety from damaged buildings



remained in Christchurch for up to 28 months [18]. Excessive demolition contributed significantly to the enormous economic costs, with an estimated NZ\$5 billion in repair and reconstruction costs in Christchurch [19]. Conversely, if decision making is not conservative, severely damaged buildings may be at higher risk of collapse in a future earthquake or aftershock if insufficient repair actions are taken [20, 21]. Particularly in dense urban areas, collapse risk of damaged buildings can halt social and economic activity, displace residents from their homes, and lead to adverse mental health among the population [22, 17]. Researchers who studied mental health following the Christchurch Earthquake attributed the increase in stress and depression among residents to the continuing disruption and feelings of fear “maintained by environmental cues” (*i.e.*, lingering unrepaired and demolished buildings) [22]. Decisions about repair and demolition depend on an interdependent set of factors, including extent of damage, risk perceptions, insurance, and regulations [2].

In regions where construction is largely unregulated and built without consideration of seismic loads, earthquakes can have devastating consequences. During the earthquake sequence that began in December 2019, thousands of houses in Puerto Rico were damaged or collapsed, mostly from the moment magnitude (Mw) 5.8 and 6.4 earthquakes in early January 2020 [23, 24]. Reconnaissance efforts by the Structural Extreme Events Reconnaissance (StEER) team revealed that, among the collapsed buildings, most were open-ground-story houses, where failure of first-story columns led to a soft story mechanism. Masonry walls, particularly those with openings, developed large shear cracks during the earthquakes [24]. Residents who believed their houses were vulnerable to earthquakes opted to sleep outside, in cars, or at a neighbor’s houses (Personal correspondence and [25, 26]). The risk of building collapse, along with lost access to water and electricity, contributed to an environment of fear and anxiety on the island [25].

More than half of residential construction in Puerto Rico is classified as informal [27], which contributed to widespread damage and collapse during the earthquakes [24]. These informally-constructed houses are self-managed, built by homeowners or builders without formal construction training, and built without explicit permitting, adherence to building codes or input from architects or engineers; they may also be on land for which the resident does not have land tenure [28, 27, 29].

The prevalence of informal construction—up to 90% of construction in some areas worldwide [30]—has been cited as contributing to a disproportionate effect of disasters on residents in low- and middle-income countries [31, 32]. In particular, areas where informal construction is common have suffered extensive damage, injury and loss of life in recent earthquakes. For example, approximately 316,000 people lost their lives due to a Mw 7.0 earthquake in Haiti in 2010; another 300,000 were injured and 1.3 million were displaced [33]. This devastating outcome is largely attributed to building collapse among informally-constructed RC houses there, which were often built without consideration of seismic forces, had insufficient column detailing and connections, or used low-quality materials [10, 4, 34]. Similarly, in Nepal, lack of compliance with building codes contributed to the extensive damage to over 500,000 buildings in Nepal in the 2015 Mw 7.8 earthquake [3].

Through interviews with residents and those who work in construction in Puerto Rico, Goldwyn et al. [35] found that the informal and RC-dominant nature of residential construction stems from the safety of RC houses in hurricanes, material costs and availability (concrete and masonry are relatively inexpensive and widely available), and a lack of understanding of the need for seismic design [29, 36]. Before the damaging January 2020 earthquakes, informally-constructed houses were predominantly designed to withstand high winds and flooding in frequent hurricanes. After the earthquakes, however, interest in earthquake preparedness workshops organized by local organizations had increased and the number of residents who reported a preference for concrete construction decreased substantially [35].

## 1.2 Research scope and gaps

This dissertation examines two barriers to seismic performance assessments for RC buildings. First, the extent to which damage affects performance in future earthquakes is not well understood and this relationship is critical in post-earthquake decision making. I address this by developing a framework for quantifying the relationship between damage and impaired future performance. I demonstrate the use of this framework, provide results for a set of archetype RC frame buildings, and link these results to decision making about post-earthquake repair. Second, extensive damage

has been observed in informally-constructed RC buildings, and especially houses, but there has been limited study on the effect of specific building design, construction, and retrofit decisions on collapse risk. In this dissertation, I demonstrate the capacity for mitigating seismic risk of RC houses through modifications to construction methods, materials, and seismic detailing. I assess RC houses in Puerto Rico, but the methods described here can be applied broadly to regions where informal construction is prevalent.

### **1.2.1 Post-earthquake assessment of RC buildings**

In practice, post-earthquake assessments seek to understand the impact of damage on the future performance of a building, relying on visual inspection, and in some cases instrumentation, to understand the effects of shaking [16, 37, 38]. There is uncertainty associated with future seismic performance implications of this damage, in part because the damage to RC structures can manifest as cracking, reinforcing bar buckling and yielding, and plastic hinge formation, and is not always visible. Component-level analysis has been used to determine repair using visual inspection [37], but there is not presently a widely used method for system-level analysis [39].

Researchers have studied the effects of mainshock-aftershock sequences on buildings, and found that, for example, the future collapse risk of well-detailed RC frame buildings is not negatively affected by an earthquake in which story drift demands do not exceed 2% [21, 40, 41, 42]. However, the level of damage and the threshold at which future performance is impaired remains unclear and has a significant impact on repair decisions. There is also uncertainty relating to the measure of damage that best indicates future performance. Engineers have quantified damage in terms of residual drift [42], peak story drifts [21, 43], and lost strength and stiffness, but none of these measures are widely used to inform repair decisions.

Recovery time and cost depend on which buildings require repair, a central question in the aftermath of an earthquake. In the United States, we lack a general seismic repair guideline, but some communities have identified criteria for when repair is needed; in Oakland, California, a 10% loss of lateral capacity triggers repair; in nearby San Francisco, a 20% loss of capacity indicates

repair is needed [44, 14]. In other municipalities, damaged and repaired buildings were required to comply with the 1970 Uniform Building Code [44]. These criteria are inconsistent between municipalities and lack guidance on how to assess the loss of capacity. In the United States, FEMA 306 [45] provides guidelines for determining the change in capacity, which indicates a need for repair, but this document only applies to a subset of building types (RC and masonry wall buildings) and predates many advancements in seismic analysis, including in simulation models and probabilistic performance assessment. Computational models can aid in determining the damage a building has incurred, but more work is needed to link visible indicators of damage to numerical analyses and repair decisions.

Recognizing this need, other researchers have worked to develop frameworks for reparability (*i.e.*, when repair is needed). Polese et al. [14] developed a post-earthquake repair and demolition framework that considers building repair costs and change in the probability of failure for decision making based on RC buildings in Italy. This method uses static pushover analysis of damaged buildings to relate damage on residual capacity. Similarly, Safiey et al. [15] proposed a performance-based earthquake engineering model to consider what buildings cannot be repaired. Their model considers building characteristics and external factors (*e.g.*, insurance, legislation) in determining irreparability.

There is a need for post-earthquake repair guidelines in the United States [39], which require methods for assessing post-earthquake performance. Current methods for assessing reparability do not provide a consistent, well-defined methodology for system-level analysis, which is needed to understand the effect of damage and inform repair decisions. Many of the current methods rely on simplified analysis methods that are computationally-efficient but may not capture the full extent of the seismic response, and do not incorporate the latest strategies for earthquake assessment.

### **1.2.2 Collapse risk of informally-constructed houses**

Despite the ubiquity of informal construction, little seismic assessment has been conducted, limiting the understanding of collapse risk and mechanisms for improving performance in this

resource-constrained context. Most work to assess the seismic performance of these houses occurs after earthquakes, where researchers work to identified vulnerabilities that made structures more susceptible to collapse through reconnaissance (*e.g.*, Brando et al. [46]; Lang and Marshall [4]). In Haiti, where informal construction is common, a Mw 7.0 earthquake caused extensive damage and collapse to 40% of houses, according to one study [47]. Researchers assessed housing following a seismic vulnerability model developed by Hassan and Sozen [48], and found that 90% of houses were at risk of damage [47]. Holliday and Kang [7] observed similar deficiencies among non-engineered houses in Nicaragua, identifying shear critical short columns, soft-story configurations, and brittle masonry walls as seismic vulnerabilities. They hypothesized that the excessively heavy roofs generated large inertial earthquake forces that increased demands on under-designed building components. In Nepal, researchers attributed damage to buildings in the 2015 Ghorka earthquake to weak materials, poor construction, and non-compliance with building codes [49, 50].

Collapse risk assessments of informal construction have been limited, in part due to the difficulty of modeling and analyzing these buildings. Nonductile building components, such as shear critical columns and masonry walls, are difficult to accurately represent in nonlinear models [51, 52]. These components dictate response, especially in informally-constructed houses, due to the lack of seismic design and detailing. Numerical modeling requires engineers to make assumptions that introduce uncertainty to the assessment [53]. Efforts to improve numerical modeling have focused on the development of more accurate models of building components (*e.g.*, columns and walls [54, 55, 56]). These component models typically rely on databases of experimental testing to develop empirical equations, and require engineers to a priori assess, for example, failure mechanism and the interaction of forces within the element.

Prior work to assess behavior of informally-constructed houses has typically focused on individual building components, such as infilled walls or retrofit methods. Much of the work has employed static pushover analysis, which may not capture the dynamic loading effects induced by an earthquake [57, 58] and may not focus on collapse or life safety. There has been some study of the collapse capacity of informally-constructed houses, but it has typically not focused on improving

seismic resilience on a community-wide level. This work combines prior collapse risk assessment methods, such as those employed by Sattar and Liel [59], who studied the collapse risk clay-brick infilled RC frames, with assessments of individual building components. Thorough parametric study of location-specific archetype houses using dynamic analysis is needed to understand the performance, and potential improvements, of informally-constructed houses.

### 1.3 Overview of research questions

Through this work, summarized in Table 1.1, I sought to improve methods for the seismic performance assessment of RC structures, with a particular focus on buildings that have been damaged and houses that were built informally. In two studies, I developed frameworks that can be used by other researchers to assess the seismic performance of buildings and presented results of those frameworks applied to a set of archetype structures.

In *Chapter 2*, I seek to answer the questions: When does damage matter in terms of impaired future seismic performance? How do building characteristics affect how damage changes building performance in a future earthquake? How can the computational efficiency of these assessments be improved? I compare the performance of RC buildings with varying levels of damage to the same buildings in an undamaged state to understand the relationship between the extent of damage and impaired performance. This study includes 50 single-degree-of-freedom (SDOF) systems and five modern RC buildings to capture the effects of building characteristics on repeated earthquake performance. Using a nonlinear model of each building, I assess the drift demands during maximum considered earthquake ( $MCE_R$ ) level ground motions as a proxy for collapse safety. Repair is triggered when the performance of the damaged building in  $MCE_R$ -level motions is impaired by damage in a prior motion. This study illustrated when a building requires safety repair as a result of damage in an earthquake, and which building characteristics (*e.g.*, deformation capacity and building period) influence the need for repair. This work seeks to improve post-earthquake performance assessment methods, which primarily rely on visual inspection, by providing a system-level assessment framework.

The work detailed in *Chapter 3* is guided by the following questions: How vulnerable are informally-constructed RC houses in earthquakes? What building elements affect the earthquake vulnerability of informally-constructed houses? What improvements could be incorporated to reduce the collapse risk of RC houses? This study assesses collapse risk of informally-constructed houses with variation in material quality, construction method, and gravity loading. The focus of this work is on Puerto Rico, where informal construction is common and seismic hazard is high, but many of the construction practices are found in other regions of the world. I began by collecting information through interviews and field work to develop 50 archetype buildings representing RC informal construction in Puerto Rico. I then model each house archetype in *OpenSees*, and assess performance through incremental dynamic analysis. For each building, I determine the collapse capacity and the relative effect of building elements and construction methods on seismic performance. These findings are intended to guide construction and retrofit recommendations to be disseminated to local organizations.

## 1.4 Organization

This dissertation is organized in a journal article format. Chapters 2 and 3 present the two studies, summarized in Table 1.1. These are standalone studies, but each seeks to increase the understanding of the seismic performance of RC structures to improve community outcomes in major earthquakes.

Table 1.1: Summary of studies collected in this dissertation, including research gaps, questions, and supplementary information

Chapter	Research Gaps	Research Questions
<b>Chapter 2.</b> Murray, P.B., Liel, A.B., and Elwood, K.J. (Under review) “A framework for assessing impaired seismic performance as a trigger for repair.”	Post-earthquake assessments of buildings rely on inconsistent and poorly defined analysis methods. Estimating the future performance of RC buildings through numerical analysis is computationally-expensive	When does damage matter? How do building characteristics affect how damage changes future performance? How can the computational efficiency of these assessments be improved?
<b>Chapter 3.</b> Murray, P.B., Feliciano, D.M., Goldwyn, B.H., Liel, A.B., and Arroyo, O., and Javernick-Will, A (In preparation) “Seismic safety assessment of informally-constructed houses in Puerto Rico”	Informal RC construction is common worldwide, and potentially increases vulnerability in disasters. There is a dearth of seismic performance assessments of informally-constructed houses.	How does informal construction affect the earthquake risk of houses? What building elements most influence seismic performance? What improvements could be made to houses to reduce collapse risk?



## Chapter 2

### A framework for assessing impaired seismic performance as a trigger for repair

This chapter is the journal paper “A framework for assessing impaired seismic performance as a trigger for repair” co-authored by Dr. Abbie B. Liel and Dr. Kenneth J. Elwood. It has been submitted and is under review.

#### 2.1 Introduction

Decisions about repair of buildings after an earthquake can be consequential, and depend on a complex set of factors including damage, cost to repair, insurance, regulations, and risk perceptions [2]. On one hand, buildings that are not repaired may be at risk of collapse in a future earthquake. On the other hand, the cost and time of unnecessary repair—and in some cases demolition—can impede community recovery and resilience. For example, following the 2011 Canterbury (New Zealand) Earthquake sequence, 65% of “significant” buildings (*i.e.*, buildings with more than five stories) were demolished in Christchurch’s central business district [2]. Even before the demolition, the process of evaluating which structures could or should be repaired exacerbated downtime and socioeconomic impacts [1]. Among communities around the world, there has been significant variation in the criteria used to identify when repairs of earthquake-damaged buildings are necessary; I refer to these criteria as “repair triggers”. Following the 1989 Loma Prieta (California) Earthquake, for example, the repair trigger in San Francisco was 20% loss of capacity [14]; in Oakland, the trigger was a 10% loss of lateral capacity; and, in Santa Cruz, all damaged or repaired buildings were required to comply with the 1970 Uniform Building Code [44]. There is also uncertainty about

how to consistently and effectively assess this loss of capacity in the post-earthquake environment. In the U.S., the FEMA 306 [45] guidelines for repair of earthquake-damaged buildings define a procedure for comparing (through pushover) earthquake demands and capacities that account for reduction of component stiffness and strength. Yet, this document is more than 20 years old, and applies only to reinforced concrete and masonry wall buildings. Seismic repair decisions are becoming increasingly scrutinized with a growing emphasis on community resilience and functional recovery [60].

There has also been increased interest in reparability among researchers in recent years. For example, Polese et al. [14] developed a tool for estimating the loss in performance of earthquake-damaged reinforced concrete (RC) buildings. A database of repair costs for such buildings was calibrated to costs associated with repair of buildings damaged in the 2009 L'Aquila (Italy) Earthquake, and the change in lateral capacity was determined through mechanism-based and static pushover analyses [14]. Expanding on this work and the framework presented in FEMA 306 [45], Polese et al. [61] proposed a method for repair/demolish decisions that considers reconstruction costs and change in performance, quantified as probability of failure. The researchers applied this methodology to a municipality in Italy to determine the effect of repair and retrofit thresholds on the safety of the entire building stock. Safiey and Pang [15] likewise proposed a performance-based earthquake engineering model to consider irreparability (*i.e.*, damage to the structure cannot be remediated). They account for both endogenous (building characteristics, such as structural system and building size) and exogenous (insurance, legislation, etc.) factors in determining irreparability.

In this study, I propose a framework that quantifies reparability by estimating the level of damage at which a building's future performance is impaired. Performance is deemed not impaired if the assessed performance in a maximum considered earthquake ground motion, or  $MCE_R$ , level motion remain essentially unchanged after a damaging earthquake. I measure performance in terms of drift demands, which are taken as a conservative proxy for residual collapse capacity [62, 21], meaning drift demands are likely to be affected by seismic damage before collapse capacity. The framework involves developing nonlinear simulation models of a building to assess drift demands

of a (pre-earthquake) undamaged building, and comparing these to drift demands in a (post-earthquake) damaged building at the same level of shaking. I identify impaired performance by an increase in the median drift demands under rare  $MCE_R$ -level ground motions. To reduce the computational expense of hundreds of back-to-back simulations to represent damaged buildings, I propose a method for selecting a representative subset of analyses. The trends in reparability, if assessed for multiple types of buildings, could be used as part of guidelines for seismic repair, such as those being considered in the FEMA-funded ATC 145 project that seeks to identify drift limits for system and component checks to determine if repair is needed, from a safety and serviceability perspective, after an earthquake [39].

The framework is first applied to 50 single-degree-of-freedom (SDOF) structures and then to a set of RC moment frame buildings that represent modern code-conforming and non-conforming buildings in the U.S. to explore how building characteristics affect the repair trigger. Damage to even well-detailed RC frame buildings, including, in the Christchurch Earthquake, plastic hinging in beams and columns and damage to floor slabs [1], is common during intense ground shaking, and repair decisions can be consequential for community recovery.

## 2.2 Related previous work

The consequences of earthquake damage on future seismic performance of buildings have been examined by a number of researchers investigating performance of buildings in aftershocks or repeated shaking. As part of the FEMA 307 report [63], analytical studies of SDOF models showed that prior damage does not significantly affect displacement demands (-3% to +10%) unless the strength of the system is significantly reduced by the damage. However, prior damage was shown to affect the variability in response. More recently, a number of researchers have assessed the change in collapse capacity and drift demands of damaged, modern RC frame buildings in comparison to an undamaged building. For example, Raghunandan et al. [21] found that, for modern well-detailed ductile RC frame buildings, drift demands in subsequent events do not increase until the mainshock (or first event) peak story drift demand exceeds 2%. That study also showed peak

story drift demands in the mainshock event to be a robust indicator of residual collapse capacity. Abdelnaby and Elnashai [64] assessed the seismic performance of RC frame buildings subjected to repeated motions to determine the effects of different modeling and analysis decisions on outcomes. They concluded that complex models (*i.e.*, those that consider gravity systems, degradation and  $P - \Delta$  effects), and the influence gravity systems are needed. They also found that simplified analysis methods (*i.e.*, static pushover or component level analysis) could not adequately capture the effects of damage. Hosseinpour and Abdelnaby [20] observed a 20% change in median collapse capacity if the building has previously experienced demands at “life safety” levels in a first event. This study focused on 8-story RC frame buildings designed by Hatzigeorgiou and Liolios [65], who studied the multiple-earthquake behavior of structures designed for gravity only, and gravity and seismic loading. They observed an increase in seismic demands in repeated earthquake sequences [65]. Zhang et al. [66] also quantified changes in collapse capacity of a 4-story RC special moment frame building associated with drift demands in a first (damaging) motion showing a 7% reduction in collapse capacity for a building damaged at 1% drift and a 40% reduction when the building was damaged at 3% drift. For comparison, in a study of aftershock collapse fragilities of older, less ductile, RC buildings, Jeon et al. [67] assessed several RC frames, relating a damage state following an initial motion with a change in damage state and collapse fragility in an aftershock. They found that buildings were more likely to reach a higher damage state in an aftershock when they were more severely damaged in a first motion defined as drifts exceeding 3%. The change in aftershock vulnerability was minimal in structures where the initial damage state was slight or moderate (below 1% drift). Uma et al. [68] reached similar conclusions and found that aftershock effects are heavily influenced by the detailing of RC components. Through review of numerous experimental studies on components, Elwood et al. [13] showed that the deformation capacity of ductile (modern detailing) RC frame components is largely unaffected by cyclic loading that does not exceed 2% drift. Taken together, these studies indicate that seismic damage can significantly impair the future performance of a building when the damage exceeds some threshold, but the threshold is not well-defined and depends on factors including the detailing of RC components.

Studies of mainshock-aftershock performance of modern steel frame buildings have led to similar observations as to when damage significantly impairs seismic performance. For example, Ruiz-García and Aguilar [42] studied the change in performance as a function of the residual drift demands from the first motion, and showed that the median spectral acceleration ( $S_a$ ) at which a demolition threshold (defined by 2% residual drift) is reached is reduced by 10% if the building retained residual drifts exceeding 1.4%. Li et al. [69] found that “moderate damage”, consistent with approximately 2.5% peak story drifts, leads to a 20% reduction in collapse capacity for modern steel buildings.

Studies of ground motion duration and its influence on performance are also pertinent here, as these explore how seismic response may become impaired with more cycles of shaking. For example, Fairhurst et al. [70] observed that modern RC shear wall buildings experienced comparable peak displacement and peak force demands during ground motions with longer durations, but saw higher energy demands (*i.e.*, cyclic dissipation of energy) when compared with shorter duration motions. Similarly, Raghunandan and Liel [71] studied the change in collapse capacity of modern RC frame structures under long duration shaking and found that long duration motions decrease the collapse capacity of these buildings by 20 to 60%; the magnitude of the decrease increased with deformation capacity, but decreased the period of the structure. Belejo et al. [72] modeled a 3-story, non-ductile, torsionally irregular RC frame building and subjected it to both long and short duration motions. They quantified damage in terms of peak displacement, drift response, and the Park and Ang [73] damage index, and found that ground motion duration does not significantly affect deformation demands, but does increase the energy dissipation demands [72]. Chandramohan et al. [74] also quantified a decrease in collapse capacity of about 20% in steel moment frame buildings subjected to long duration motions compared to a set of spectrally-equivalent shorter duration motions. Using the same set of motions, Hwang et al. [75] quantified the effect of ground motion duration on economic losses in steel moment frame buildings and found that the most significant increase in loss results from duration’s role in increasing collapse risk for mid- and high-rise buildings.

In addition to deformation capacity, prior work has also indicated what characteristics of

buildings may influence these conclusions. Based on SDOF models, Mahin [76] found that structures that were relatively weak and with shorter periods were more likely to be more vulnerable to amplified drift demands to subsequent events. Amadio et al. [77] found that highly ductile structures do not see a significant “penalty” when subjected to repeated events, though structures with less deformation capacity do. Raghunandan et al. [21] showed that buildings that were more susceptible to  $P - \Delta$  effects were more sensitive to mainshock damage in terms of their aftershock performance. Similarly, in a study of SDOF models, Liapopoulou et al. [78] found that collapse capacity is lower in long-duration motions and—crucially—that this response is more pronounced in structures that are susceptible to  $P - \Delta$  effects. Systems in this study with longer first-mode periods had higher collapse capacities than those with short periods [78]. The effect of structure period diminished as  $P - \Delta$  effects increased, as collapse tended to occur as the building entered the post-capping region. Deformation capacity, particularly in cases where the effect of  $P - \Delta$  is small, increased the collapse capacity of the structure [78]. Recently, Ji et al. [79] assessed a suite of SDOF structures, showing that weaker and stiffer systems had larger inelastic demands for the same residual displacement from a first earthquake, indicating that damage will impair subsequent performance earlier. Polese et al.’s [14] model for performance loss of RC structures suggests ductility (deformation capacity) as a critical parameter.

## 2.3 Methods

As summarized in Figure 2.1, the framework for quantifying reparability involves, first, assessing the performance, in terms of drift demands, of an **undamaged** building in a set of  $MCE_R$ -level ground motions. This intensity level is the basis for U.S. seismic design, and was chosen to quantify drift demands under rare ground motions as a proxy for life safety performance. Drift demands have been shown to be a reliable indicator of future performance [21]. I then assess the performance of the **damaged** building in the same  $MCE_R$ -level motions and quantify the change in drift demands of the damaged building relative to the undamaged building. I relate this change to the level of damage, quantified by the peak story drift in the damaging motion, to identify the effect of prior

damage on future performance. This relationship can be used to determine when major structural repairs are needed to prevent performance being impaired. These assessments require the development of a nonlinear simulation model for the buildings of interest that is capable of capturing seismic performance of the system well into the nonlinear range, as described subsequently.

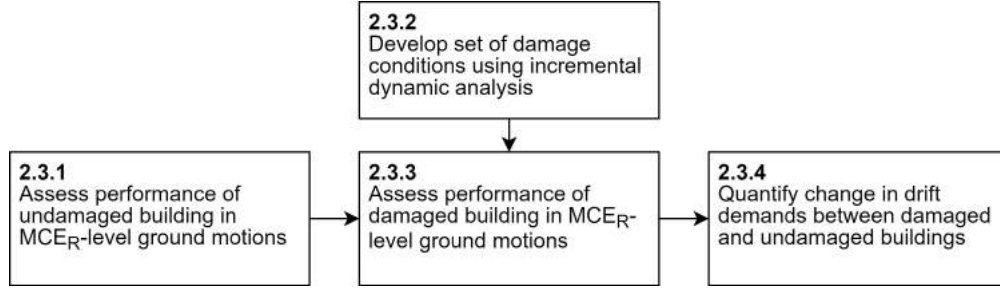


Figure 2.1: Framework for assessing the level of damage at which a building’s seismic performance is impaired

### 2.3.1 Assess performance of undamaged building

The performance of the undamaged structure is assessed under  $MCE_R$ -level ground motions. Here, 15 of these so-called “performance assessment” motions, or 15 orthogonal motion pairs for 3D analysis, are selected from the PEER NGA-West2 database [80] to represent the  $MCE_R$ -level at a site of interest. These motions were selected based on the conditional mean spectrum considering the building of interest’s first-mode period, using the tool developed by Baker [81], to capture expected spectral shape (and variability therein). For the buildings studied here and described in Sections 4 and 5, I assume that they are located at a high seismic site with  $S_{M1} = 0.91$  g in Oakland, California (site class C) [82]. The hazard deaggregation needed to do the conditional mean spectrum calculations was obtained from the USGS Unified Hazard Tool [83], consistent with ASCE/SEI 7-16 [84]. If story drifts in the undamaged building exceed 10% in any story during the  $MCE_R$ -level motion, the record is not considered in the determination of drift amplifications, but is considered in determining median peak story drifts for the undamaged building. In non-conforming buildings, if any records caused story drifts to exceed 10% in the undamaged building,

I selected additional  $MCE_R$ -level motions so 15 drift amplifications could be considered.

### 2.3.2 Develop set of damage conditions

In order to understand how damage impairs future performance, I develop a varied set of potential damage conditions for each building. This is accomplished by subjecting the structure to incremental dynamic analysis (IDA) [85]. In IDA, a suite of ground motion records are scaled to a range of ground motion intensities to capture the effects of intensity and record to record variability on response [85]. The IDA employed here uses 22 (pairs of) motions in the FEMA P-695 [86] Far-Field set and (for some buildings) 22 long-duration motions selected by [74]. The long-duration motions are spectrally matched to the FEMA P-695 set. The Far-Field set are intended to be representative of ground motion records for significant events recorded farther than 10 km from the fault rupture [86]. Each input motion is scaled at increasing intensities, quantified as the geomean  $Sa(T_1)$  for each building, until 10% story drift limit is reached. For 2D analysis, I applied one component from each record pair; for 3D analysis, the record pair was applied simultaneously in each orthogonal building direction.

Each analysis in the IDA (**i.e.**, ground motion record and intensity) creates a damage condition in the building. This damage condition is defined in terms of peak story drift, residual drift, and damaged period. The set of damage conditions produced by this set of ground motions is intended to represent the range of possible damage outcomes for a building. Figure 2.2 shows the set of damage conditions generated through IDA for one building.

#### 2.3.2.1 Selection of damaging ground motions for use in subsequent analysis

From all generated damage conditions, I developed a selection algorithm to select a subset of cases for further analysis. With this selection, I aim to represent the entire set of damage conditions, while minimizing the number of analyses conducted subsequently in the framework, thereby greatly reducing computational time from back-to-back nonlinear analyses. To that end, I use stratified random sampling [87] to select points. Stratified random sampling is appropriate when



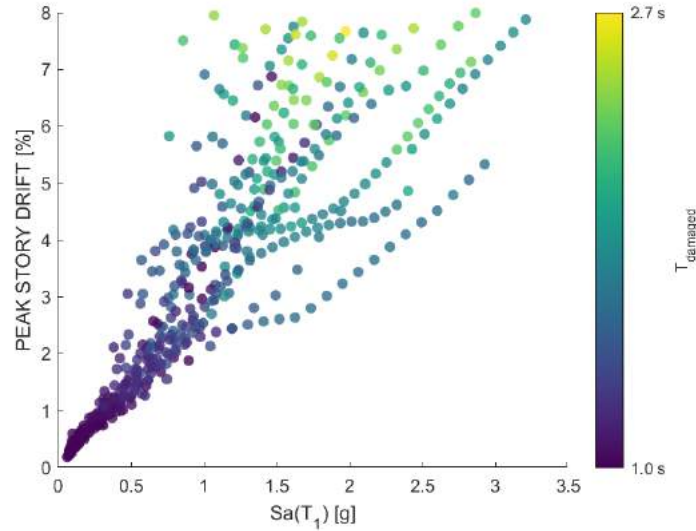


Figure 2.2: Set of damage conditions for a code-conforming RC frame, showing how peak story drift and the period of the damaged structure vary with ground motion intensity ( $Sa(T_1)$ ). The damaged period is calculated using eigenvalue analysis at the end of the analysis;  $T_1$  for this undamaged building is 1.0 sec.

a proportional, representative sample of a data set is sought. I stratify here based on peak story drift. I primarily quantify damage in terms of the peak story drift, which is strongly correlated with seismic performance metrics, including economic losses (**e.g.**, Ramirez et al. [43]) and aftershock performance (**e.g.**, Raghunandan et al. [21]). The discrepancy between the distributions of selected damage conditions and all the damage conditions is quantified by the KL divergence [88]. When the KL divergence is sufficiently small (less than 0.5), and no more than two damage conditions have been selected from the same ground motion record, the iterative selection process ends. Figure 2.3 illustrates the result of this selection process for one of the buildings. While I selected motions based on peak story drifts only, the distribution of ground motion intensities is also well represented by the selected set. I start with 15 damage conditions for each structure, adding conditions as needed to capture trends in performance.

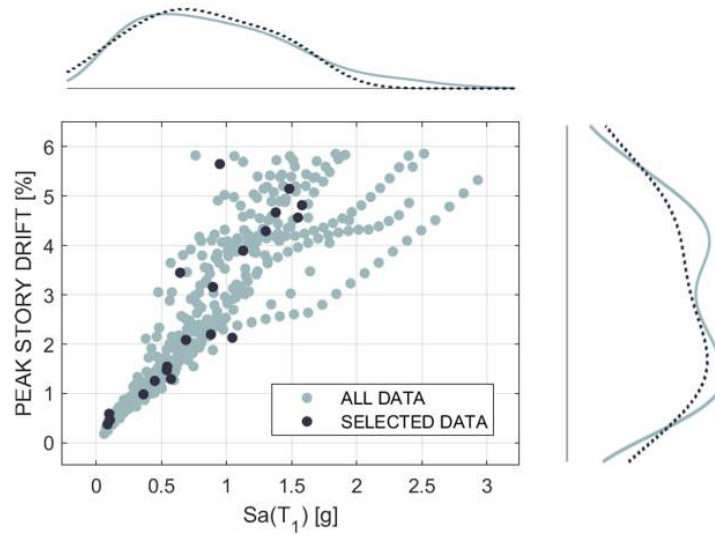


Figure 2.3: Set of damage conditions, and the selected conditions, for a code-conforming structure. The distribution of damage conditions along each axis are also shown.

### 2.3.3 Assess performance of damaged building

In the next step of the framework, I aim to quantify the change in drift demands on a building when it has been damaged. I compare the response of the building to each of the performance assessment motions defined in Section 2.3.1 when the building has and has not experienced prior damage. The prior damage is represented by the selected damage conditions (defined in Section 2.3.2.1).

To quantify drift demands in the damaged building, analyses for each of the performance assessment motions are run for each selected damage condition. In each analysis, the building model is subjected to two ground motions: the damaging motion, which replicates the damage condition, and one of the performance assessment ( $MCE_R$ -level) motions. Figure 2.4 shows the set of drift histories from the analyses for one damage condition and one  $MCE_R$ -level motion. If story drifts exceed 10% in the performance assessment motion, I consider the structure collapsed, and set the peak story drift to 10% in determining drift amplifications.

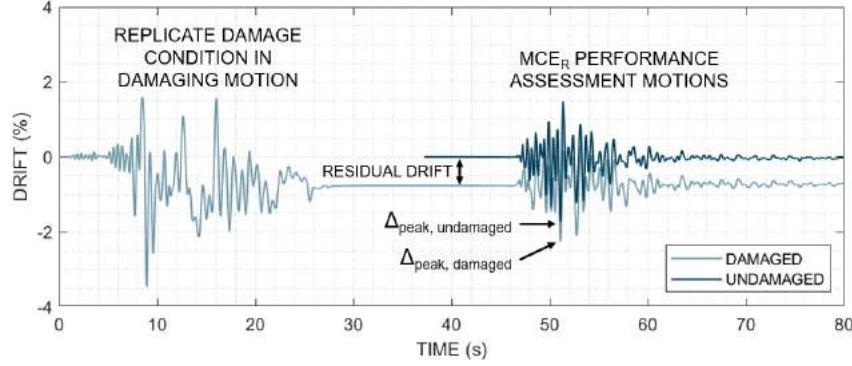


Figure 2.4: Story drift time history of analyses for one damage condition and one  $MCE_R$ -level performance assessment motion.

### 2.3.4 Quantify change in drift demands between damaged and undamaged buildings

The response of the undamaged structure in each of the performance assessment motions is compared to the damaged structure in Equation 2.1, as a ratio of peak story drift,  $\Delta_{peak}$ , in the damaged structure to the peak story drift in the undamaged structure in the same  $MCE_R$ -level performance assessment motion. For each damage condition, there are therefore 15 such drift amplification ratios. The peak drift may occur in any story, and in either orthogonal direction. If the building collapsed during the second motion, I assumed a damaged peak story drift value of 10% in determining the drift amplification ratio.

$$\text{Drift amplification ratio} = \frac{\Delta_{peak,damaged}}{\Delta_{peak,undamaged}} \quad (2.1)$$

I plotted the drift amplification ratio against the peak story drift in the damaging motion. The results for one case are shown in Figure 2.5. I also calculated the moving median value to capture the trend in drift amplifications as damage (quantified as peak story drift) increases. I took the median value for all drift amplifications within each 1% drift bin at increments of 0.25% drift (*i.e.*, 0 - 1% drift, 0.25 - 1.25% drift, etc.). In each bin, I computed the 10<sup>th</sup> and 90<sup>th</sup> percentile to quantify the dispersion of drift amplifications.

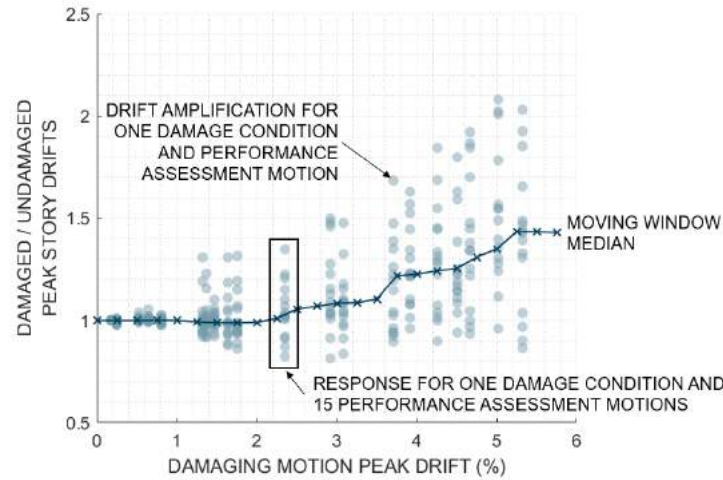


Figure 2.5: Median drift amplification ratios over a moving window for one building model subjected to 50 damage conditions and 15 MCE<sub>R</sub>-level motions.

This moving median illustrates the increase in demands associated with damage, and can be used to assess building reparability. This assessment reveals damage (drift) levels below which performance is largely not impaired, when compared to the same building in an undamaged state. However, it is important to note that the denominator of the drift amplification ratio is based on the existing undamaged building, and may differ greatly from building to building, with implications discussed in the results. In this study, I identify a repair trigger as the level of damage at which the 90<sup>th</sup> percentile indicates a 15% increase in drifts has occurred relative to the undamaged building. Municipalities have implemented repair triggers based on 10 and 20% losses of lateral capacity following major earthquakes [14]; I use 15% as a typical threshold for a notable change in performance. The 90<sup>th</sup> percentile of amplifications is selected conservatively, as repair guidelines should err on the side of identifying too many rather than too few buildings as needing repair. This range and threshold are somewhat arbitrary, but used here to illustrate the selection of a repair trigger. Further study into appropriate limits should be selected by the judgment of a committee.

## 2.4 SDOF study to isolate effects of building characteristics

In this section, I employ nonlinear SDOF models of buildings to explore how building characteristics such as deformation capacity, strength, stiffness, period, deterioration, post-yield slope and sensitivity to  $P - \Delta$  effects affect the reparability assessment. In the subsequent section, I apply the framework to assess reparability of more realistic multi-DOF building models for RC frames.

### 2.4.1 SDOF building models

I modeled the SDOF structures using open source structural analysis software *OpenSees* [89] with a fixed base, a zero-length tri-linear Ibarra-Medina-Krawinkler IMK hinge [90], and an elastic element. The IMK hinge captures the nonlinear behavior and stiffness and strength degradation as the model undergoes shaking. The models have a lumped mass and axial load applied at the top of the SDOF model. Table 2.1 lists the range of values used for each structure parameter considered in this study. The median drifts during 15  $MCE_R$ -level motions ranged from 0.9 % to 3.24 % for the SDOF structures. These values were selected to develop SDOF models that capture the range of characteristics of real buildings, and isolate the effects of these characteristics with 50 different models. The baseline SDOF model is representative of a 4-story, code-conforming perimeter moment frame building, with a first mode period,  $T = 1.0$ s, strength,  $V_{max}/W = 0.35$ , deformation capacity,  $(\theta_p) = 0.06$  rad, and total gravity load equivalent to the seismic weight of the 4-story building,  $P$ . Figure 2.6 shows the static pushover (backbone) response for models with variation in deformation capacity, strength, and  $P - \Delta$  effects. The median drifts during 15  $MCE_R$ -level motions ranged from 0.9 to 3.2% for the undamaged SDOF building models.

### 2.4.2 Reparability assessment results

I applied the framework for assessing reparability, described in Section 2.3, to all 50 SDOF models. I considered 50 damage conditions, with 15 performance assessment ( $MCE_R$ -level) motions.

Table 2.1: Range of values for each SDOF model parameter.

Parameter	Values considered
Strength, $V_{max}/W$	0.2 - 0.7
Stiffness, $T$ (s)	0.5 - 1.5
$P - \Delta$ effects	$0.25P - 4.0P$
Post-yield slope, $M_c/M_y^1$	1.0 - 1.5
Yield drift <sup>2</sup> (%)	0.1 - 2.8
Deformation capacity ( $\theta_p$ ) <sup>3</sup>	0.0001 - 0.08
Cyclic deterioration	low-high

<sup>1</sup> Typical value is  $M_c = 1.13M_y$  [54]

<sup>2</sup> Drift is calculated assuming an effective height,  $h = 0.7L$

<sup>3</sup> Defined as rotation capacity between yield and capping drifts

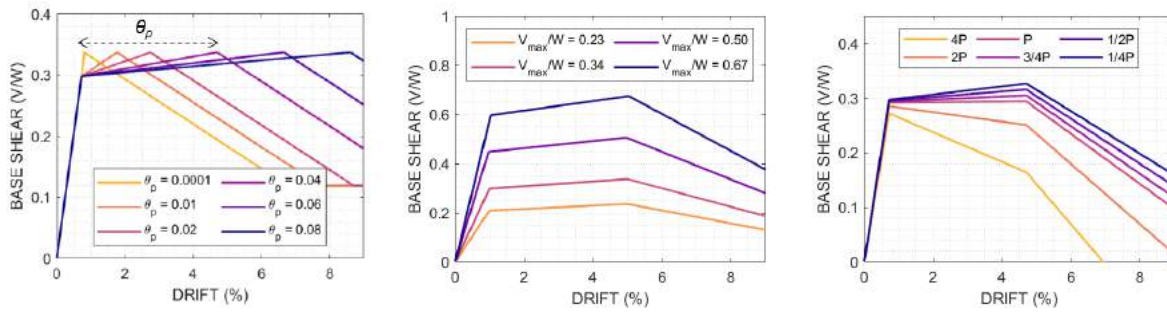


Figure 2.6: Static pushover response of SDOF models with (a) varied deformation capacity ( $\theta_p$ ) and constant strength and stiffness, and (b) varied strength and stiffness with constant yield and capping drifts, and (c)  $P - \Delta$  effects.

Figure 2.7 shows the response of five models with variation in deformation capacity (Figure 6a) in a selected damaging motion, and subsequent performance assessment motion. The reparability assessment compares the drift demands in damaged and undamaged models, with the same 15  $MCE_R$ -level motions. Subsequent plots (Figures 2.8 to 2.11) report the median drift amplification, relative to the undamaged building, as a function of the drift demands in the damaging motion.

First, I analyzed how deformation capacity affects future seismic performance and reparability in Figure 2.8a. For relatively small damaging motion drifts, *i.e.* relatively less damage, the ratio of drifts in the damaged and undamaged SDOF models is 1, indicating performance has not been impaired. Figure 2.8a shows, however, the steeper increase in drift amplifications in structures with

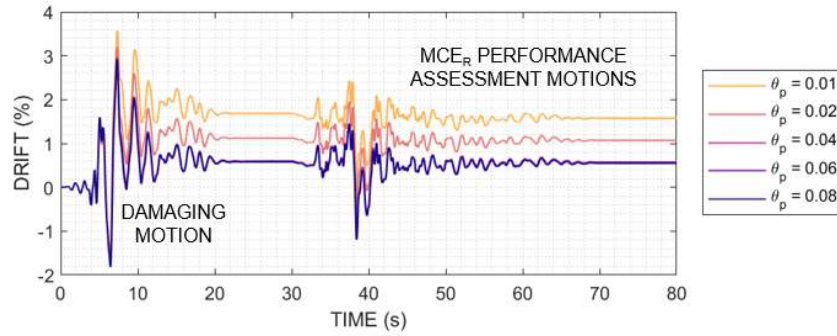


Figure 2.7: Drift histories of SDOF models with varied deformation capacities ( $\theta_p$ ) subjected to a back-to-back ground motion.

less deformation capacity. Those structures with less deformation capacity have more deteriorated strength and stiffness, largely due to in-cycle deterioration, such that they tend to see larger drifts (relatively to the same undamaged oscillator) in the performance assessment motion. The less ductile structures also have larger residual drifts after the damaging motions, as illustrated by the hysteretic response of each of these models in the same set of damaging and performance assessment motions shown in Figure 2.8b, which contribute to the drift amplifications. The jaggedness in the curves in Figure 2.8a also reflects the complexity of the structural responses; with larger drifts in the damaging motion, the period of the building tends to elongate and increase effective damping, and decreasing spectral demand. Results of analyses not shown indicated that cyclic deterioration in the hysteresis model did not have a large effect on reparability outcomes.

I also isolated the effect of increased  $P - \Delta$  effects, with results shown in Figure 2.9. These results show that models with higher  $P - \Delta$ , and lower effective deformation capacity, see bigger amplifications at lower damage. However, even structures with the most extreme  $P - \Delta$ , the drift amplifications do not become significant until there is significant residual drift.

Figure 2.10 shows the effect of stiffness,  $k$ , and first mode period,  $T$ , on drift amplifications. Stiffness alone (Figure 2.10b) does not strongly influence response, in terms of when damage impairs performance. However, period matters (Figure 2.10a) with shorter period structures seeing higher drift amplifications at lower levels of damage (drift). This trend is pronounced for  $T < 1.0s$ , where



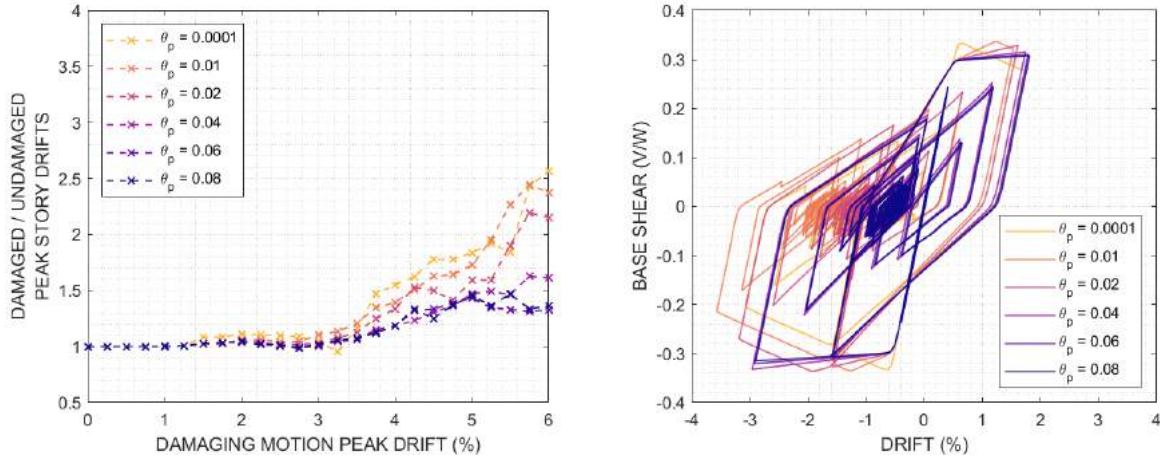


Figure 2.8: SDOF models with variation in deformation capacity (defined as  $\theta_p$ ) showing (a) moving window medians, and (b) hysteretic response during one damage condition and performance assessment.

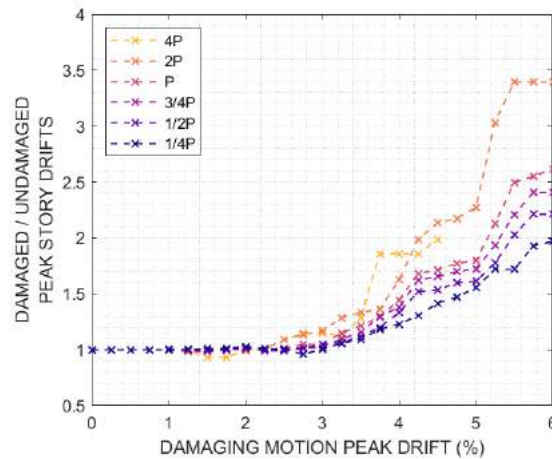


Figure 2.9: SDOF models with variation in  $P - \Delta$  showing (a) moving window medians, and (b) hysteretic response during one damage condition and performance assessment.

the equal displacement “rule” is known to break down [91].

Structure strength does not significantly affect a building’s capacity to withstand damage, particularly in longer period structures ( $T > 1.0s$ ), as illustrated by Figure 2.11. In the short period case, drifts in the undamaged oscillators were strongly inversely correlated with strength and the drift amplification ratios were controlled by the small denominator in Equation 2.1. Stronger buildings had smaller drifts in the undamaged case, which is consistent with the equal displacement



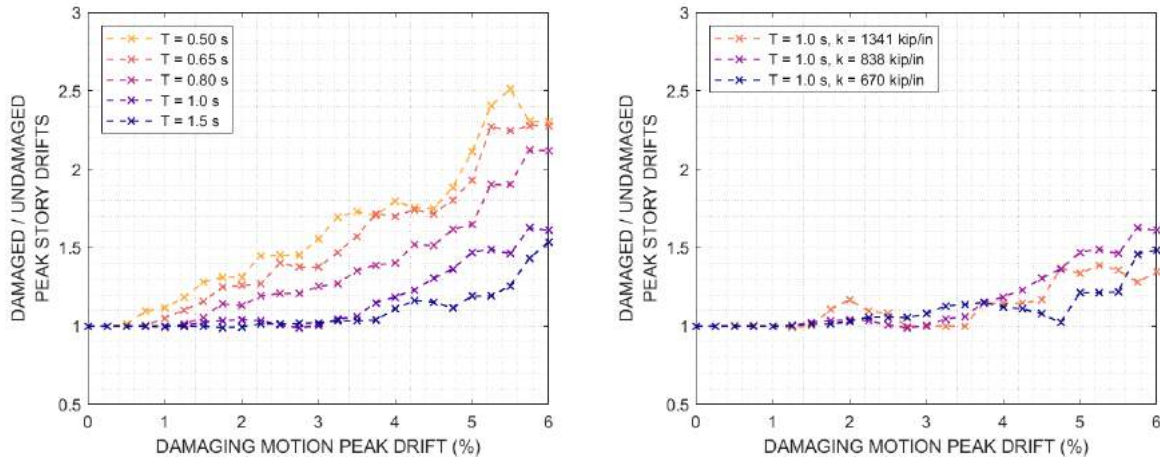


Figure 2.10: Median drift amplifications for SDOF models with variation in (a) stiffness and period, and (b) stiffness only.

“rule” [91].

## 2.5 RC frame buildings of interest

### 2.5.1 Building selection and design

I then applied this framework to five RC frame buildings that are based on Haselton et al. [92], and were updated in FEMA P-695 [93]. The code-conforming buildings follow ASCE/SEI 7-16 [84] standards, and were designed for seismic design category (SDC) D with design and detailing provisions for special moment frames (SMF). The non-conforming, less ductile, buildings are based on the ordinary moment frames (OMF) described in FEMA P-695 [93] (see also FEMA P-695 [86]) and originally designed for SDC B; these designs were also assessed in SDC D as examples of non-conforming buildings. Based on the building characteristics identified as potentially significant through review of previous work, I selected buildings for this study that represented a variation in height, building period, sensitivity to  $P - \Delta$  effects, detailing and deformation capacity to quantify the difference in reparability associated with these characteristics. Table 2.2 lists these buildings and key design parameters: Building C4 is a 4-story code-conforming RC frame building. Building N4 is the same height, but non-conforming, and is weaker and less ductile. Building C1 is a

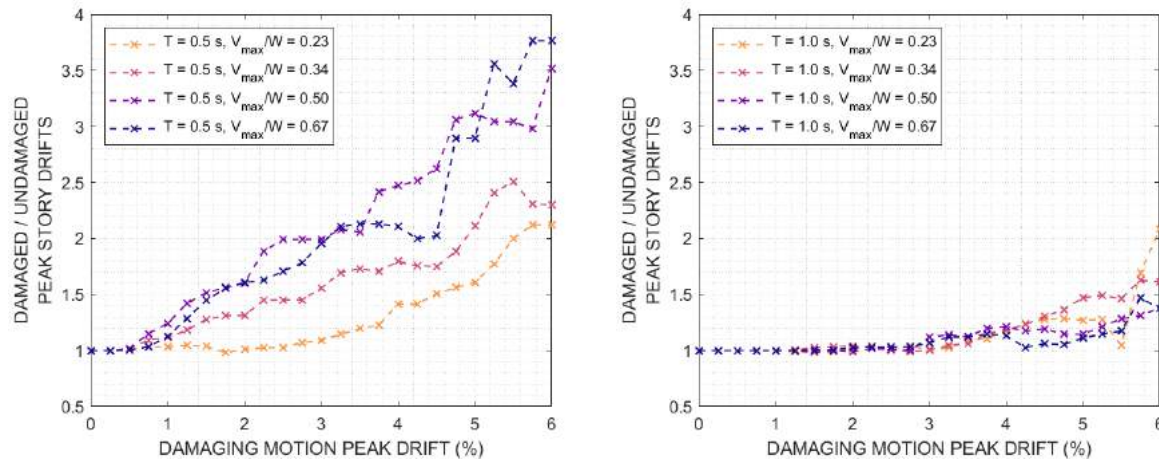


Figure 2.11: Median drift amplifications for SDOF models with variation strength and a first mode period (a)  $T = 0.5$  s, and (b)  $T = 1.0$  s.

single-story, code-conforming structure. Buildings C12 and N12 are 12-story buildings where C12 is code-conforming, and N12 is non-conforming.

Table 2.2: RC frame buildings assessed for reparability in this study

ID	Stories	Design	$T(s)^1$	$V_{max}/W^2$	Ultimate story drift (%) <sup>3</sup>	$MCE_R$ story drifts (%) <sup>4</sup>	Repair trigger (% drift) <sup>5</sup>
C4	4	Code-conforming	1.0	0.33	4.9	2.7	2.2
N4	4	Non-conforming	1.4	0.24	3.0	3.6	1.8
C12	12	Code-conforming	2.4	0.16	5.8	3.4	2.0
N12	12	Non-conforming	3.5	0.12	3.9	3.8	2.8
C1	1	Code-conforming	0.4	0.68	5.0	1.5	1.5

<sup>1</sup> Measured using eigenvalue analysis, with elements modeled with cracked sections

<sup>2</sup> Peak strength from static pushover analysis, normalized by building weight

<sup>3</sup> Drift at capping (onset of negative slope) in controlling story during pushover

<sup>4</sup> Median peak drifts of undamaged building in performance assessment motions

<sup>5</sup> Level of drift at which the 90<sup>th</sup> percentile of drift amplifications exceeds 1.15, representing a 15% increase relative to the undamaged building

Figure 2.12 shows one exterior frame of the 4-story RC frame building, indicating typical building geometry. In all of the buildings, seismic loads are resisted by three-bay perimeter moment frames. Interior beams and columns are designed only for gravity loading. Column spacing is 20 ft

in both (orthogonal plan) directions. The first story height is 15 ft; upper story heights are 13 ft. All buildings have a floor system consisting of a 6 in RC floor slab. Each of the buildings was designed for this geometry and dead, live, and seismic loads [93] and other requirements from ASCE/SEI 7-16 [84]. For the 4-story code-conforming building (Bldg C4), for example, in the perimeter frame, beam sizes range from 20 x 34 in to 18 x 24 in, and column sizes range from 22 x 30 in to 22 x 26 in. In columns, reinforcement ratios ( $\rho$ ) are typically around 1.7% and ties spaced at 2.5 - 3.5 in in the hinge regions ( $\rho_s = 0.011$ ). The perimeter frames were designed by [93, 86], and reviewed by practicing engineers. I also designed a beam-column gravity frame system following ASCE/SEI 7-16 [84] requirements. Typical gravity-system beams are 12 x 18 in and columns are 14 x 14 in.

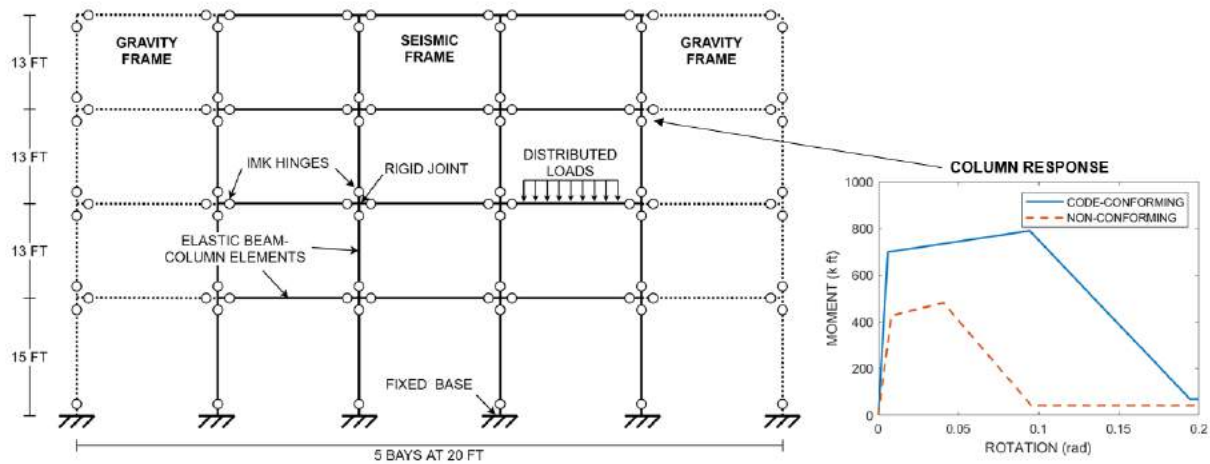


Figure 2.12: Diagram of geometry and modeling of exterior frames, with three-bay seismic-resisting bays perimeter frame and two gravity frame bays. Typical column backbones for perimeter frame in 4-story buildings definition are shown.

### 2.5.2 Nonlinear modeling of RC frame buildings

I developed a three-dimensional (3D) nonlinear model of each building in the open source structural analysis software *OpenSees* [89]. This model employs lumped plasticity for beam and column elements, with zero-length hinges at both ends of each element, as shown in Figure 2.12. I chose this approach for computational efficiency and for its advantages in capturing, phenomenologically, softening behavior of flexurally-controlled elements in the severely nonlinear range due

to spalling and rebar buckling [94]. All beams and columns are flexure or flexure-shear critical, such that the response can be captured with a rotational spring. Here, the zero-length moment-rotation hinges were modeled using the IMK peak-oriented hysteretic model [90] to represent beam and column flexural behavior. Figure 2.12 shows backbone curves for perimeter frame first-story columns in two buildings; backbone and cyclic deterioration parameters were determined using the empirical calibration equations developed by Haselton et al. [54], based on each building's design details. According to these equations, even the non-conforming buildings in this study have significant plastic rotation capacity due to their design detailing.

The model assumes cracked stiffness properties for beams and columns based on Haselton et al. [54]. Columns are assumed to be fixed at the base. At the beam-column joint, the finite size panel zone was modeled with nearly rigid, elastic elements. The floor slab is not explicitly modeled; rather a rigid diaphragm condition and corresponding loads and mass are incorporated into the model.  $P - \Delta$  effects are considered with the PDelta geometric transformation [89]. Distributed loads representative of an office building [93] are applied to beams before dynamic analysis, considering unfactored dead load and the expected (small) fraction of live load [58]. Masses are based on these distributed loads and are applied at all model nodes. Three-percent Rayleigh damping [95] is applied at the first and third lateral modes (because the building is symmetric, the modes are the same in both orthogonal directions). Damping is based on current stiffness, and is updated throughout the analysis.

I used eigenvalue analysis to determine the building periods, and static pushover analysis to quantify building strength and deformation capacity to summarize building characteristics in Table 2.2. The static pushover responses of the buildings under inverted triangular loading used in this study are shown in Figure 2.13. These results indicate that the strength of the buildings and range of periods are typical of RC frame structures, and shows variation among the buildings.

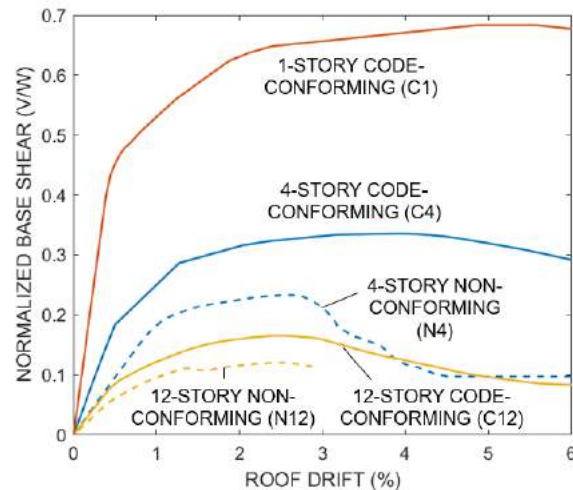


Figure 2.13: Response of RC frame buildings under static pushover loading. Base shear is normalized by building weight.

## 2.6 Reparability of RC frame buildings

Through this framework, I assess reparability, quantifying the relationship between damage and impaired performance in a  $MCE_R$ -level event for the RC frame buildings of interest. These results are summarized in Figures 2.14, 2.15, and 2.16. These figures illustrate the range of drift amplifications, as well as the level of damage at which the range of amplifications increase drift demands by 15%. This level of damage can be used, with limitations, to determine reparability.

### 2.6.1 Effect of building deformation capacity

I studied the two 4-story RC moment frame structures, Buildings C4 and N4, with variation in strength and deformation capacity (see Table 2.2). These differences in deformation capacity are partially due to component detailing differences (typical column tie spacing,  $s/d$ , is of 0.1 vs. 0.4 in in C4 and N4, respectively), and partially due to system effects (stronger columns relative to beams in Bldg C4: typical beam-column strength ratios,  $\frac{\sum M_c}{\sum M_b}$ , are 1.4 and 1.1 in Bldg C4 and Bldg N4, respectively). Figure 2.14 shows the median drift amplification ratio over a moving window in these two buildings, along with the 10<sup>th</sup> to 90<sup>th</sup> percentiles of each window. The upper end

of this range can be compared to a 15% increase in drift demands to identify a building-specific repair trigger. The repair triggers for these buildings are 2.0% and 1.7% for Bldgs C4 and N4, respectively. I see larger drift amplifications in the non-conforming structure (Bldg N4), though in both structures, damage does not significantly impair performance until the building experiences story drifts in excess of 1.5% in a damaging motion. I attribute the worse performance of Bldg N4 primarily to its smaller deformation capacity because the SDOF study found that strength and stiffness are not critical for  $T > 1.0$ s. Further, drift demands in Bldg N4 are larger in both the undamaged and damaged cases, as reported in Table 2.2. In Bldg N4, higher damage is associated with larger drift amplifications and increased scatter.

In some analyses, the drift amplification is less than one, indicating that peak drifts were smaller in the damaged building. Buildings often experience period elongation as a result of shaking, which can lead to changes in the intensity of shaking felt by the damaged building. I scaled ground motions to the period of the undamaged building, considering a cracked initial stiffness assumption, such that damaged and undamaged cases are subjected to the same motions. If a building is then oscillating at a longer period, it may not be as affected by a motion scaled for a shorter period. In addition, the motions selected according to the conditional mean spectrum slightly underestimated the demand at the elongated period.

### 2.6.2 Effect of building period and $P - \Delta$ sensitivity

I also compared the performance of three code-conforming buildings with different heights and as a result, periods. These buildings include a 1-story structure (Bldg C1) with an initial period of 0.4 s, a 4-story structure (Bldg C4) with an initial period of 1.0 s, and a 12-story structure (Bldg C12) with an initial period of 2.4 s. Figure 2.15 shows the responses of the 1-story building, Figure 2.14a shows the 4-story response, and Figure 2.16 shows the 12-story response. The 1-story structure sees drift amplifications earlier than the 4- and 12-story counterparts, consistent with results of short-period SDOF structures. The repair trigger (*i.e.*, level of damaging motion drift at which the 90<sup>th</sup> percentile exceeds a 15% increase in demands) is 1.5% in the one-story building,

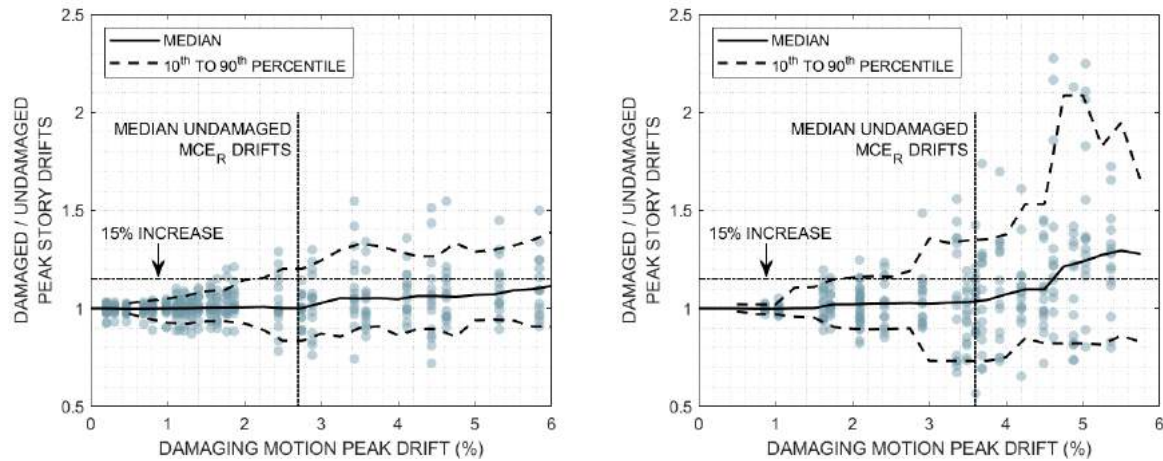


Figure 2.14: Reparability of 4-story RC frame buildings, showing the change in response of (a) code-conforming (Bldg C4) and (b) non-conforming (Bldg N4) frames in  $MCE_R$ -level motions, as a function of peak story drift in a damaging motion.

and 2% in the 12-story building. These values indicate the increase in demands relative to demands in an undamaged building, and should be considered along with design limits. Bldg C12 is more susceptible to  $P - \Delta$  effects than Bldgs C1 or C4 because of its longer period and additional stories. While this likely contributed to the higher drift demands experienced by Bldg C12 when it was undamaged (when compared to the other code-conforming structures, as reported in Table 2.2),  $P - \Delta$  has not amplified the effect of damage on drift demands. Although I find significant effects of  $P - \Delta$  in the SDOF study, modern seismic design procedures mitigate these effects through drift limits,  $P - \Delta$  design; the presence of gravity system also reduces the effect.

I analyzed two 12-story buildings in this study: Bldg C12 is code-conforming, Bldg N12 is non-conforming. The reparability results for these buildings are compared in Figure 2.16. Bldg N12 is somewhat weaker and saw larger drifts in the  $MCE_R$ -level motions in its undamaged state than the stronger Bldg C12. Both 12-story buildings have relatively similar deformation capacities (see Figure 2.13) as a result of similar gravity systems through which load is distributed, and this is reflected in the repair trigger. Also, denominator of the drift amplification ratio, defined in Equation 2.1, depends on the magnitude of drift in the undamaged building during the performance assessment motions, which is relatively high in both 12-story buildings (see Table 2.2) and greater



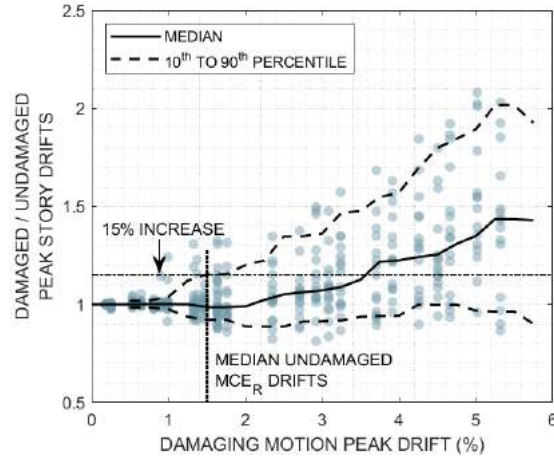


Figure 2.15: Reparability of 1-story code-conforming RC frame (Bldg C1) building, showing the change in response of in  $MCE_R$ -level motions, as a function of peak story drift in a damaging motion.

for Bldg N12 than C12.

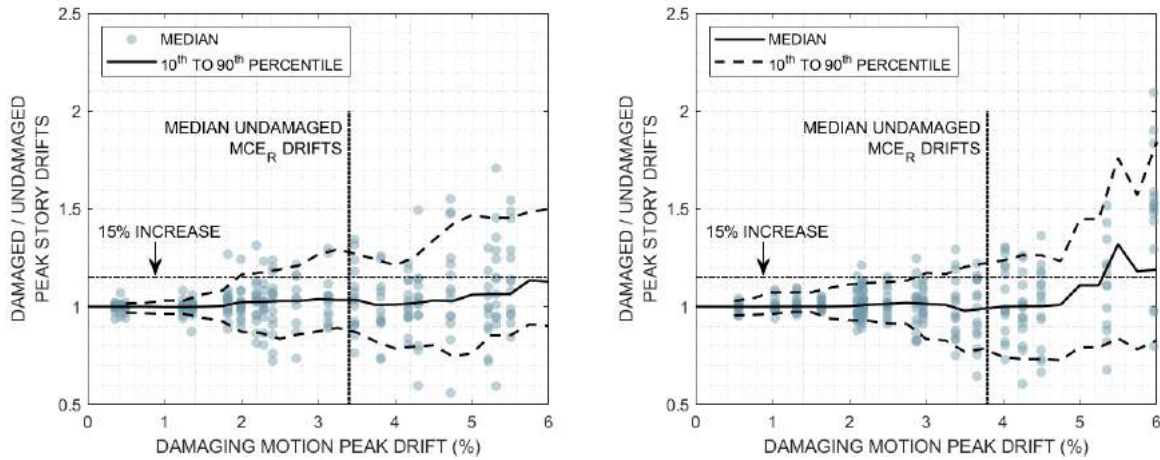


Figure 2.16: Reparability of 12-story RC frame buildings, showing the change in response of (a) code-conforming (Bldg C12) (b) non-conforming (Bldg N12) buildings in  $MCE_R$ -level motions, as a function of peak story drift in a damaging motion.

### 2.6.3 Other measures of damage

I considered other damage measures as predictors of drift amplification, namely period elongation and residual drift. Figure 2.17 shows the relationship between drift amplifications and these



damage measures for the 1-story, code-conforming building (Bldg C1). Period elongation, which indicates lost stiffness, is strongly correlated with drift amplification, as shown in Figure 2.17a, especially once period elongates by a factor of approximately 2. The damaged building period is determined using eigenvalue analysis of the numerical model following the damaging ground motion, but is difficult to determine in a real building without instrumentation. Figure 2.17b illustrates the relationship between residual drift and drift amplifications, showing significant amplifications where residual drifts exceed about 0.5% drift. Residual drift, while straightforward to measure in a real building, is difficult to accurately capture in an analysis model [96].

For these reasons, and because peak story drifts have been shown to capture damage well (*e.g.*, Elwood and Moehle [51], Ruiz-García and Aguilar [42], Jeon et al. [41], Paal et al. [97]) and are relatively more predictable [96], I primarily quantify damage in terms of peak story drifts in this study. However, I do consider the effects of residual drift in my quantifying of peak drifts. I considered both “total” drifts (*i.e.*, peak drift relative to the initial, undamaged state), and “in-run” (*i.e.*, peak drift in the second motion, relative to the building state at the end of the damaging motion). In some cases, the second motion counteracted the residual drift, and peak drifts appeared to be smaller as a result, but in others, the residual drift amplified the displacement in the second motion. Overall, I found that trends in drift amplification were largely the same when calculated as total and in-run drifts, though there was variation within individual drift amplification ratios.

#### **2.6.4 Effect of damaging ground motion duration**

Several studies have shown that collapse performance of buildings is worsened if they are subjected to longer duration shaking by increasing the number of cycles and cyclic energy dissipation demands (see Section 2.2). In this section, I explore whether the ground motion duration affects reparability. If so, the repair trigger may be sensitive to the seismic environment, and, specifically, the contribution of subduction motions to the hazard [74]. Recall that for some of the buildings (specifically, Bldgs C1 and C4), I considered some subduction longer duration motions in the development of set of damage conditions. Long duration motions are those for which the 5 - 75%

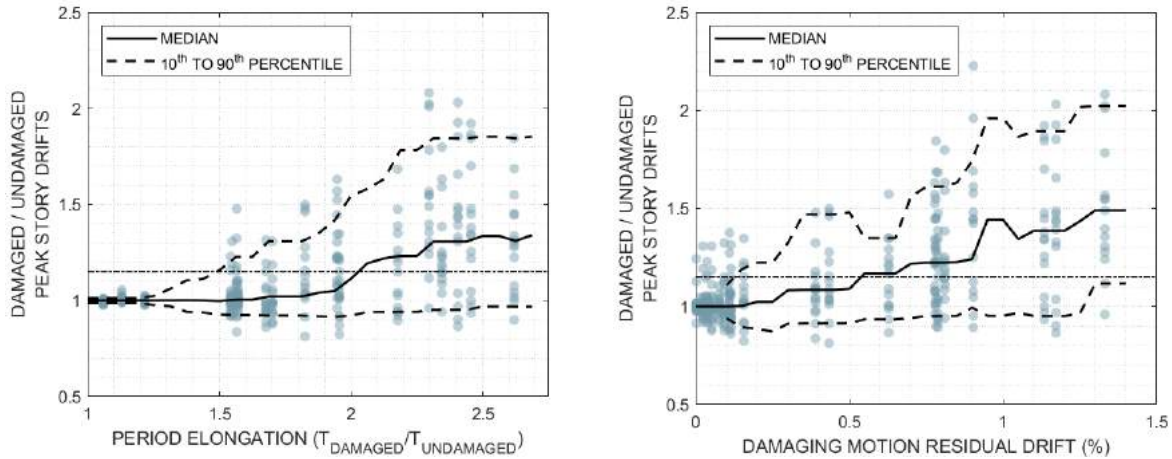


Figure 2.17: Relationship between drift amplifications and (a) period elongation and (b) residual drift in a 1-story, code-conforming building.

significant duration [98],  $D_{5-75}$ , is greater than 20 seconds.

To interrogate the effect of the duration of the damaging ground motion, I considered the effect of duration on peak story drift and on reparability. Figure 2.18a shows the relationship between duration and peak story drift in the damaging motion; the two are not correlated ( $R^2$  is 0.02). I also considered separately median drift amplifications for the long and short duration motion damage conditions. Figure 2.18 illustrates a nearly-identical trend in reparability between damage conditions that result from long and short duration motions. These results indicate that duration is not a significant ground motion for reparability.

## 2.7 Conclusions

This paper presents and exercises a framework for quantifying the change in building response that results from earthquake-induced damage with the intent of identifying limits that indicate when major structural repairs are needed for safety. The framework involves first assessing drift demands at the  $MCE_R$ -level in the undamaged building of interest. Then, drift demands in a damaged building are assessed, and the effect of the level of building damage is considered through a set of varied damage conditions. Damaged building response is simulated through back-to-back analyses,

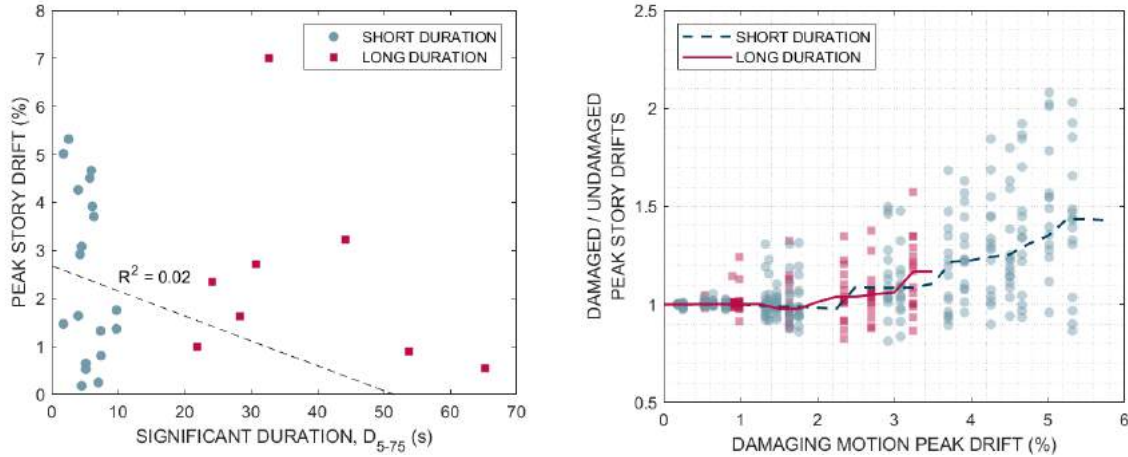


Figure 2.18: (a) Relationship between the the duration of the damaging motion and associated peak drift for selected damage conditions in a 1-story, code-conforming structure (Bldg C1). (b) Reparability of Bldg C1 for long and short duration ground motions.

using machine learning strategies in selecting damaging motions for computational efficiency. The framework is applied to 50 SDOF structures and five RC frame buildings, selected to capture variation in building characteristics representing modern, RC frame structures, which have been modeled for nonlinear dynamic analysis in *OpenSees*.

In longer-period, code-conforming structures, ground motions in which story drifts did not exceed 2% did not significantly increase drift demands in a  $MCE_R$ -level motion, when compared to the building's response in the  $MCE_R$ -level motion in its an undamaged state. The most important building characteristic determining when performance was impaired was deformation capacity. Stiffer structures (especially with  $T < 1.0s$ ) tended to be more sensitive to damage than more flexible structures, and saw a larger increase in drift amplification. Building strength did not critically change reparability performance, though it did influence drift demands in the undamaged buildings.

There are some limitations to this work. First, I focused on modern RC frame buildings, even for the non-conforming design, and did not consider especially non-ductile frames. These older RC frames are more likely to experience larger drifts during an earthquake, and are more likely to be demolished as a result [99]. The focus of this study is on the future performance of buildings, so I focused more on ductile structures for which repair—rather than demolition—is a likely post-

earthquake alternative. I considered only drift amplifications in  $MCE_R$ -level motions as an indicator of seismic repairs, focusing on safety motivations for repairs. Buildings may need serviceability or durability repairs at earlier damage levels. Further, in this study I assessed building performance on a system-level. Assessment of component-level response, *e.g.*, low cycle fatigue, is important in determining the extent of damage and repair strategy. Finally, several elements of this framework require judgment. I quantified drift amplifications relative to drift demands for an undamaged building, but this can obscure the actual seismic performance of a building when the undamaged building has poor performance. In using this framework to guide post-earthquake decision-making, it is important to consider how amplified drift demands relate to design limits. More discussion is needed to determine whether the limits chosen are appropriate for other structural systems.

Despite these limitations, this framework can be used to show when damage begins to impair performance in future earthquakes, an important consideration for post-earthquake decision making. These relationships can be used to inform thresholds for repair, in combination with inspection and component-based checks, as part of guidelines for earthquake repair being funded by FEMA [39].

## Chapter 3

### Seismic safety assessment of informally-constructed houses in Puerto Rico

This work is a collaborative effort with Dirsá Feliciano, Briar H. Goldwyn, Dr. Abbie B. Liel, Dr. Orlando Arroyo, Dr. Amy Javernick-Will. It is in preparation.

#### 3.1 Introduction

Worldwide, more than 1.6 billion people live in informally-constructed houses [100], which comprise 50-90% of residential construction in low- and middle-income countries [30]. These informally-constructed houses are self-managed, built by homeowners or builders without formal construction training, and without explicit permitting, adherence to building codes or input from architects or engineers; they may also be on land for which the resident does not have land tenure [28, 27, 29]. Informal construction is common in communities worldwide; this definition is based on residential construction in Puerto Rico. Informally-built houses are often reinforced concrete (RC) structures because the materials—cement, aggregate, steel reinforcing bars, and masonry blocks—are relatively inexpensive and widely available. Informally-built RC houses may be vulnerable to severe damage or collapse in an earthquake. Reconnaissance in the aftermath of recent major earthquakes has revealed a high incidence of collapse in houses that were built informally in—for example—Turkey, Nepal, Haiti, and Puerto Rico [46, 34, 11, 24]. Among other places, this mode of construction is common throughout the Caribbean, where frequent hurricanes, rather than seismic design, are the primary concern of informal builders [35]. While informal construction is prevalent throughout the world, seismic performance assessments of informally-constructed houses

are extremely limited.

In this study, I develop a framework to identify common housing characteristics and potential seismic vulnerabilities associated with informal construction in an effort to provide local organizations and builders with recommendations for safer construction, focusing on identifying and testing feasible, locally-available, and practical recommendations [101]. Housing and construction practices are first assessed through fieldwork, involving interviews with local builders, hardware store owners, and homeowners, and observations of damage from past earthquakes. These characteristics are used to define a set of informally-constructed RC houses representative of those found in the communities of interest, which are analyzed through nonlinear incremental dynamic analysis (IDA) [85] to assess seismic collapse capacity and damage limit states as a measure of seismic safety. These archetype houses vary in terms of material strengths and detailing, component sizes, presence, the configuration of masonry walls, and roof system/weight. I also examine the effects of window and door openings, including partial height infill walls, and the effects of incremental construction, in which a house is expanded over time.

I focus here on the Caribbean island of Puerto Rico, where hurricanes are frequent and have caused extensive damage [8], and where the January 2020 earthquake near Guánica have brought the high seismic hazard (design SS values range from 0.9 to 1.2 g and S1 range from 0.4 to 0.5 g, *i.e.*, Seismic Design Category or SDC D [84]) to the forefront of residents' minds [25, 35]. An estimated 55% of Puerto Rican houses were built informally [27]. Since the earthquakes, there has been an increased interest in workshops for earthquake safety on island [35], motivating the timing of this study.

## **3.2 Background**

### **3.2.1 Hazard and recent earthquakes**

Seismic hazard in Puerto Rico is a result of its location on the boundary between the North America and Caribbean tectonic plates, as well as interactions of microplates within the boundary

zone [102]. Seismic activity has generated significant ground shaking in recorded history [103, 102]. Notably, a damaging earthquake sequence began in late December 2019 and continued through January 2020. The largest of this series—moment magnitude (Mw) 5.8 and 6.4 earthquakes—occurred on January 6 and 7, 2020. Figure 3.1 shows the intensity of shaking during the latter event, which exceeded peak ground acceleration (PGA) of 0.5 g in the southern part of the island [23]. These earthquakes caused an estimated 3.1 billion USD in damage [23]. Preliminary reports note the collapse of at least 80 structures and damage to more than 10,000 houses [24]. Figure 3.2 shows typical damage in RC and masonry houses in Guánica. An estimated 8,000 people were displaced from their houses; either as a result of damage or fear of collapse in aftershocks, many sought shelter in tents, cars, or large temporary base camps [104, 26]. Thousands of residents were displaced for months, and many people were unable to afford repairs or the cost to replace a collapsed house [26, 105]. Similarly, in the aftermath of Hurricane Maria, many families struggled to rebuild damaged or destroyed homes due to a lack of resources [29]. In particular, those who live in informally-constructed houses and may not have land tenure were ineligible for financial assistance from FEMA, which delayed community recovery [29].

### **3.2.2 Residential construction in Puerto Rico**

More than half of houses in Puerto Rico are informally constructed [27], and RC construction is preferred by many residents because of its good performance in hurricanes [35]. Goldwyn et al. [35] conducted interviews with homeowners and those involved in the construction industry in Puerto Rico, and found that, before the early 2020 earthquakes, a “majority of people want a concrete house”, according to one hardware store manager. However, in the aftermath of the 2019-2020 earthquakes, the number of interviewees who report a preference for concrete construction dropped from 83 to 36% [35].

Informally-constructed RC houses in Puerto Rico and elsewhere are often built of weak concrete (due to, for example, high water-cement ratios, poor mixing or a lack of vibration, and large or smooth aggregate), or have deficient reinforcement detailing in beam, column, slabs and other

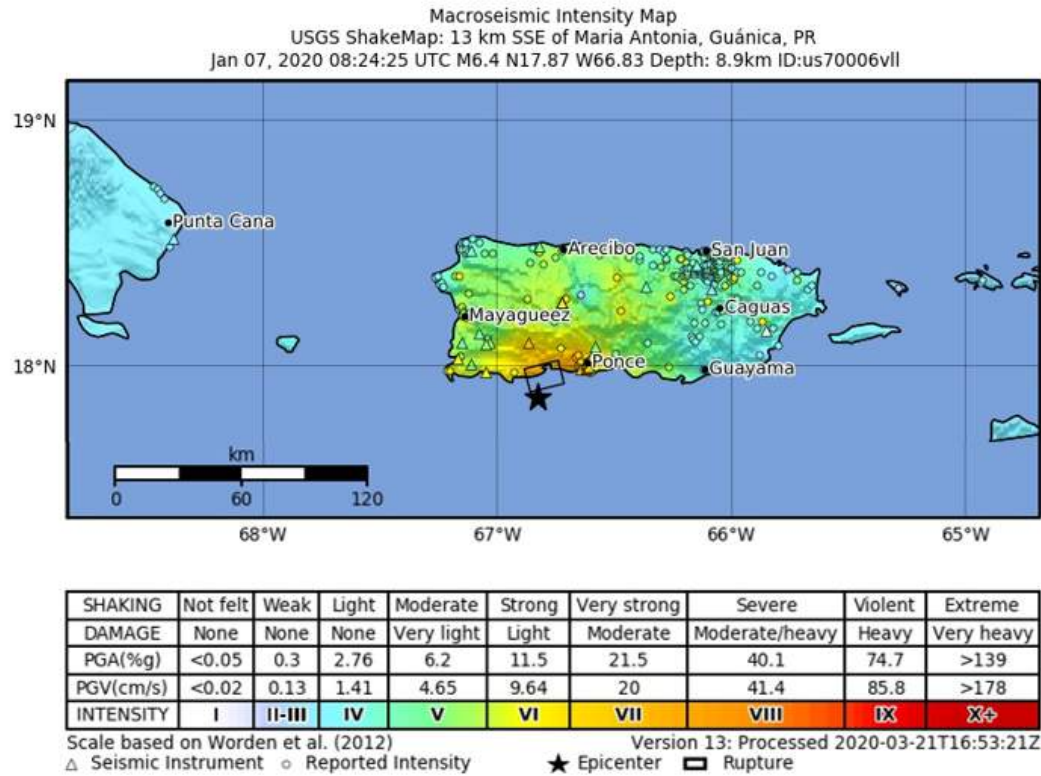


Figure 3.1: Shaking intensity during January 7, 2020 earthquake [23]



Figure 3.2: Damage to RC houses in Guánica with (a) an open ground story, showing loss of the first open story, and (b) masonry walls between columns at the first story, showing shear cracking in walls and columns. [Photos: Polly B. Murray]

RC elements (*e.g.*, large lateral tie spacing or insufficiently-sized longitudinal bars) [50, 10, 34, 106]. Masonry walls—both infilled and confined—are common in informal construction [4, 10]. In infilled construction, RC frame elements are built first and are intended to carry the loads on the building.



Masonry, which is almost always concrete blocks in Puerto Rico, typically unreinforced, is added to fill in the frame and create a wall. Conversely, in confined masonry construction, walls are built first, and confined with tie-columns and tie-beams [49].

I also observed a lack of access to high-quality materials on the island, either due to costs or availability, and a conflict between seismic and hurricane design considerations that may contribute to seismic vulnerabilities [35]. For example, reinforcing bars may be corroded from storage outside, and my team's drop tests led to brittle failure indicative of weak concrete masonry blocks [107]. For many homeowners, these lower-quality materials may be the only available option. Additionally, interviews with homeowners and hardware store workers revealed a prioritization of hurricane risk mitigation in residential construction. This can increase seismic vulnerability, as many of the features that are beneficial from the perspective of hurricane safety may create problems in earthquakes, such as the heavy roof construction or an open ground story [24].



Figure 3.3: (a) Puerto Rican home with exposed reinforcing bars to facilitate house expansion. (b) Home with RC first story and wood frame second story (Yabucoa, Puerto Rico)[Photos: Polly B. Murray]

### 3.2.3 Post-earthquake reconnaissance of informally-constructed houses

Post-earthquake reconnaissance studies have repeatedly demonstrated poor performance of informal and incremental construction (*e.g.*, Arslan and Korkmaz [11]; Barakat [108]; Brando et al. [46]; Chen et al. [109]; Lang and Marshall [4]; Marshall et al. [10]; Mix et al.[34]). Damage and collapse are of particular concern in RC houses with weak materials, inadequate detailing of

reinforcing bars (*i.e.*, large transverse tie spacing or an insufficient number of longitudinal bars), or with building designs that lead to excessive deformations in under-designed members (*e.g.*, soft stories or partial height infill walls that induce a short column with high shear demands) [11, 110, 109, 50, 4]. Large shear cracks formed in masonry walls during earthquakes are common [24, 4].

In the recent Puerto Rico earthquakes, damage was more extensive in houses with large, heavy roof and floor slabs, which generate large inertial forces that act on under-designed walls and columns [24]. There were also a number of soft-story collapses in RC houses with open ground stories [24]. Similarly, weak materials, under-designed lateral load systems, and heavy buildings contributed to extensive damage and collapse during the 2010 Mw 7.0 Haiti earthquake that killed more than 300,000 people [4, 10, 34]. In Haiti, engineers attributed damage to brittle unreinforced masonry construction, a lack of consideration of seismic forces, particularly in column detailing and lateral system connections, poor material quality, including the use of river rocks as aggregate, which reduces the bond strength in concrete mixes, and partially infilled walls that resulted in shear-critical short columns [4, 10, 34]. In a reconnaissance effort following the Haiti earthquake, Lang and Marshall [4] observed the effects of material quality and construction methods on seismic performance of houses in Haiti, finding that houses built “wall-first” (reminiscent of confined construction) withstood the shaking better than the “column-first”, or infilled, construction. In Nepal, weak materials or poor construction contributed to the poor seismic performance of buildings in the 2015 Ghorka earthquake [111]. Lack of compliance with building codes also contributed to the extensive damage to over 500,000 buildings in Nepal in a 2015 Mw 7.8 earthquake [3]; more than 50% of houses in the Kathmandu valley were built without consideration of building codes [112, 111, 113]. Likewise, Pokharel and Goldsworthy [5] attributed earthquake damage in Nepal to soft and weak story effects, short, shear-critical columns, and poor-quality materials.

Incremental construction is also thought to negatively affect seismic performance through weak connections, corroded rebar’s reduced strength and deformation capacity, and increased demand on structural systems as building progresses [114]. In Nepal, damage in the earthquake was

attributed to home expansion that led to increased demands in lower stories [46].

### 3.2.4 Past seismic assessment studies of informally-constructed houses

Despite their ubiquity and potential vulnerabilities, seismic performance assessments of informally-constructed RC houses have been extremely limited. Among the existing studies, Blondet et al. [106] compared lateral strength of informally-constructed RC frame houses with clay-brick masonry walls in Peru to expected earthquake demand and found that nearly 50% of structures would have deficient performance in a design-level earthquake. Holliday and Kang [7] likewise analyzed non-engineered RC houses in Nicaragua using static pushover procedures and identified seismic deficiencies including: shear failure in short columns, soft-story failures, poor-quality connections, inadequate steel bar detailing, excessively heavy roofs, and poor performance of masonry walls that influenced the behavior of the building.

Lallemant et al. [114] studied incremental construction in Nepal using analytical *OpenSees* models and IDA [85], and found that earthquake vulnerability increases over time when buildings are incrementally expanded, particularly when expansions add significant weight and upper stories. The largest increase in risk for an individual building occurs when a second story is added Lallemant et al. [114]. Reinforcing bar corrosion can also impair seismic performance in incrementally-constructed houses; Yu et al. [115] assessed the change in seismic collapse fragility of RC frames in China that results from corrosion using *OpenSees* fiber models with modified material definitions and additional bond slip through IDA, and found a moderate increase (6 – 8%) in collapse probability in RC frame buildings with corrosion damage. Similarly, McKee et al. [116] assessed the effect of steel corrosion on the seismic performance of RC frame buildings. They modeled RC frames using *OpenSees* fiber models that capture lost bar area and identified a decrease in peak base shear, deformation capacity, and drift and other engineering demands during design earthquake and  $MCE_R$ -level ground motions. These results are based on laboratory testing of individual building components and numerical simulation of full building frames.

Masonry walls, which are prevalent in informal construction in Puerto Rico and elsewhere,

have been studied through experimental testing and analytical modeling. Infill walls influence the stiffness, strength, and deformation capacity of frames [52]. Infill wall failure tends to be brittle, though the mechanism of failure depends on the relative stiffness and strength of the infill panels and neighboring columns [117]. Sattar and Liel [59] developed simulation models of nonductile RC frame buildings with clay-brick infilled walls, and found, through IDA, that infill in this building type increases collapse risk despite the increased lateral strength. Han and Lee [118] assessed the seismic performance of a bare frame, a frame with partial height infill, and a frame solid infill panels using experimental testing and analytical modeling. They found that, among the three, collapse capacity is highest in the solid infill case and lowest in the partial height infill case [118] because columns adjacent to the openings are prone to brittle shear failure. These vulnerable, or “captive”, columns are common in buildings where the opening provides lighting or ventilation [119]. In another study, Duran et al. [120] assessed, through field study, two adjacent buildings in Turkey with similar construction, but one had partial height masonry walls. The building with partial height walls collapsed, and through field investigation and analytical models, the authors determined that the partial height walls contributed to the collapse of the building [120]. The authors further attributed the collapsed building’s poor performance to low-strength concrete, corrosion in reinforcing bars, inadequate detailing, and strong-beam-weak-column configurations [120].

Confined masonry wall systems tend to be stronger and more ductile than RC frames infilled with masonry blocks, though the behavior is dependent on the detailing of the tie columns [121]. Confined masonry walls have performed well in recent earthquakes, and researchers have attributed this to the distribution of gravity loads in walls, which increases lateral strength, and the ability for confined masonry walls to act as a shear wall [122, 121, 4]. Confined masonry construction was widely adopted in Chile after its superior performance (compared to infilled construction) was demonstrated during the 1939 Chillán earthquake [121].

Other researchers have aimed to quantify the overall seismic risk to communities from informally-constructed housing, considering population density, building stock, and seismic hazard, though this

work often lacks specific seismic assessment of individual buildings, relying on general risk assessments. For example, Yepes-Estrada et al. [123] developed a model for seismic risk assessment of the residential building stock in South America, distinguishing between houses constructed of unreinforced masonry, confined masonry, cast-in-place RC frames, and RC walls. They found that RC wall systems are common in major urban areas; these buildings are generally assumed to have better seismic performance, which reduced the overall vulnerability in the regions assessed [123]. Similarly, Calderon and Silva [124] have categorized the building stock in Costa Rica, considering construction type, building height, ductility, and year of construction. They found masonry and RC houses to be most prevalent. These studies rely on assumptions about population distribution, building type, and seismic vulnerability in assessing community risk, but lack specific assessments of individual buildings.

### **3.2.5 Improvements to informally-constructed houses**

Several studies have sought to improve the seismic performance of informally-constructed RC buildings through retrofit. Antonopoulos and Anagnostopoulos [125] evaluated weak RC buildings with open ground stories in Greece, which have historically performed poorly in earthquakes. They assessed the seismic performance—quantified by the force-deformation based demand-to-capacity ratio—of buildings with and without diagonal steel braces in the open ground story and found that this retrofit reduced the ratio to an acceptable level (*i.e.*, below design level). Sahoo and Rai [126] assessed the benefit of adding steel jackets or diagonal steel braces with energy-dissipating connectors to RC frames with soft ground stories. Both retrofits increased lateral strength by a factor of 4 and, in the retrofit with shear links, energy dissipation capacity by a factor of 3. Chaulagain et al. [127] investigated three possible retrofit options for non-engineered buildings with deficient columns and walls in Nepal using pushover and dynamic analyses. They considered RC shear walls around columns, diagonal steel braces, and RC jacketing, and found all three improved lateral strength, stiffness, and deformation capacity. Shear walls and steel braces improved the performance of non-engineered structures most significantly, but the authors believe these

are impractical modifications for building owners as they limit access to floor area. Similarly, Timsina et al. [128] assessed the seismic performance and feasibility of seven potential retrofit options for soft-story buildings in Nepal, including adding infill or RC shear walls to the open story, increasing the size of the beam and/or columns, adding diagonal braces to open bays, and steel jacketing, or carbon fiber wrapping around columns. Using numerical simulation and static pushover analysis, they determined that diagonal braces, infill, and RC shear walls provide the most significant improvement to seismic performance but are least desirable for building usability [128]. Steel jacketing and carbon fiber wraps also improve performance, but the necessary materials are not widely available. Increasing column size improved lateral strength, but not deformation capacity, when compared to the bare frame [128]. Holliday and Kang [7] identified solutions to improve seismic performance through static pushover analysis of models of vulnerable houses. This included additional reinforcement in columns and beams, the use of a structural confining beam at the top of the wall, reinforced and confined masonry walls, and the avoidance of tall walls.

A method for the comprehensive assessment that incorporates typical informal building practices, considers susceptibility to natural hazards, and offers recommendations for increased safety is needed to improve community resilience in vulnerable communities worldwide. This work outlines such a methodology, and presents results for a seismic risk assessment of informally-constructed houses in Puerto Rico.

### 3.3 Methods

This framework includes the development of a set of archetype houses to represent Puerto Rican informally-constructed houses based on interviews and observations. This set represents a range of construction methods, material strengths, steel detailing, and gravity loads to assess the impact of each building characteristic on seismic performance. I modeled each archetype in the open-source nonlinear seismic analysis platform, *OpenSees*, and analyzed using IDA, focusing on collapse risk and damage states as measures of performance.

### 3.3.1 Development of archetype houses

I began by identifying common construction practices associated with informal construction in Puerto Rico. This process involved interviews with residents and local builders, visits to hardware stores, and observations of construction characteristics and damage from the 2020 earthquakes in conjunction with Goldwyn et al. [35]. Through these interviews (detailed in Appendix A and Goldwyn et al. [35]), I aimed to identify commonly available materials, associated strengths (including concrete mixes, reinforcing bars, and masonry blocks), and building design characteristics that could be used to define archetype buildings and element designs. These questions included:

- **Materials:** Which types of cement and aggregate are most popular for house construction? What masonry blocks are typically purchased?
- **Detailing:** What size rebar is used in columns? What size pre-formed ties are most popular?
- **Safety:** If a homeowner is seeking to improve the safety of their house, what products do you recommend? What improvements do homeowners usually choose?

Additionally, we asked about the motivations for building informally and/or incrementally, the process of building or expanding a house, and perceptions of safe and unsafe design. A complete list of questions can be found in Appendix A. Figure 3.4 shows some of the available materials used in concrete mixes. Figure 3.5 shows some typical RC houses in Puerto Rico. In total, about 12 interviews were conducted, 50 houses surveyed or photos reviewed, and eight hardware stores were visited in this phase of the work.

I then developed a set of 50 concrete and masonry archetype houses from these interviews and field observations that are representative of common house designs, based on the rationale outlined in Table 3.1. Figure 3.6 shows the floor plan and elevation views for the archetype houses in this study. Story heights are 10 ft (3 m) and bay widths are 10 ft in the NS direction and 12 ft (3.6 m) in the EW direction. Slab foundations are common in Puerto Rico, though I also observed concrete



Figure 3.4: Commonly available concrete materials, including coarse and fine aggregate and cement, at a hardware store in San Juan, Puerto Rico. [Photos: Polly B. Murray]



Figure 3.5: Typical RC houses in Guánica and Humacao, Puerto Rico. [Photos: Polly B. Murray]

footings and foundations built from concrete masonry blocks. The archetype houses considered in this study all have a concrete slab foundation for simplicity, as well as reinforced concrete floor and roof slabs. I considered houses with 4, 8, and 12 in (10, 20, 30 cm) slabs, and houses with wood second stories.

Some of the archetype buildings are elevated buildings, with an open ground story. These houses were particularly susceptible to damage and collapse during the past earthquakes because the first story is significantly weaker than upper stories, and the lateral loads are concentrated in these columns [24]. Figure 3.7a shows an open ground story building that was collapsed and damage to masonry walls during the January 7, 2020 earthquake. I also studied one- and two-story houses



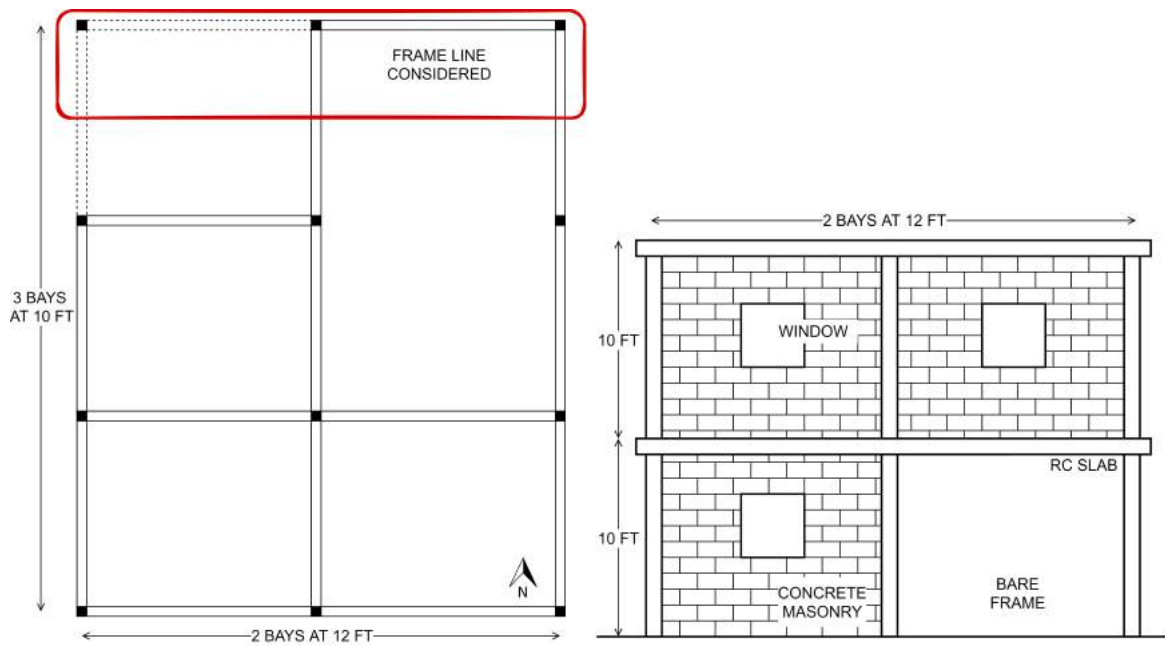


Figure 3.6: Typical floor plan (showing building frame of interest) and elevation views for archetype houses. The infill configuration and the number of stories are two of the variations considered.

with masonry walls with various sizes of openings, illustrated in Figure 3.8. In the earthquakes, typical damage to these structures is shown in Figure 3.7b. I analyzed houses with infilled and confined masonry walls, as both methods of construction were frequently cited as correct by local builders with whom I met [35].



Figure 3.7: Houses in Guánica that were damaged during the January 7, 2020 earthquake. (a) failure in first story columns, (b) shear cracks in masonry walls. [Photos: Polly B. Murray]

Table 3.1: Archetype design variations and assumptions

Parameter	Values	Rational
Story height	10 ft	Field observations
Bay width	10 - 12 ft	Field observations
Slab thickness	4 - 12 in	Field observations
Slab direction	one-way	Field observations
Foundation	slab	Field observations
Soil conditions	site class B	USGS Vs30 data [129]
Column size	8 x 14 in	Interviews, field observations
Longitudinal bars	4 or 6 bars, no. 4 or no. 5	Interviews, field observations
Transverse ties	no 3 bars at 6 or 14 in	Interviews, field observations
Corrosion	0 to 20% <sup>1</sup>	Field observations, prior studies [115, 116]
PVC pipe	3 in diameter gutter	Field observations
Retrofit	Infill panels, RC jacketing	Interviews, prior studies [130, 127]
Window and door size	3 x 3 ft, 7 x 3 ft	Field observations
Wall thickness	6 in	Interviews, field observations
Wall construction	Infilled or confined	interviews
Wall configuration	0, 1, or 2 filled bays	Field observations
Concrete strength	1.5 to 3 ksi	Interviews
Masonry unit strength	0.4 to 1.5 ksi	Interviews, drop tests
Steel strength	40 ksi	Hardware stores
Dead loads	100 – 200 psf	Calculated from roof and floor slabs, masonry walls
Live loads	40 psf (floor), 20 psf (roof) <sup>2</sup>	ASCE 7-16 [84]

<sup>1</sup> Cross-sectional area lost by corrosion

<sup>2</sup> Live loads assumed for “design”; 25% of live load used in determining applied loads in seismic assessment

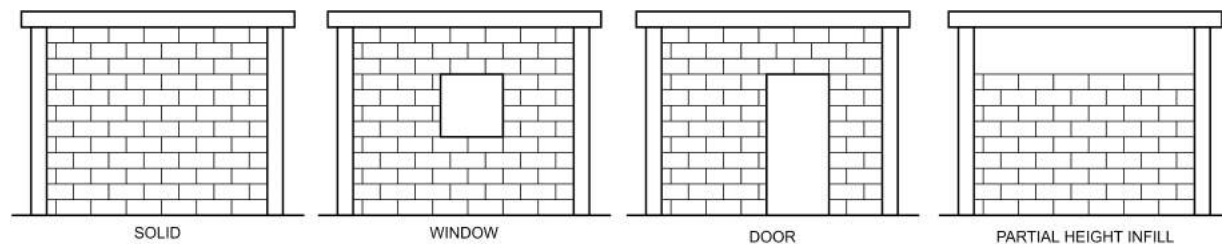


Figure 3.8: Masonry wall configurations with and without openings

### 3.3.2 Open ground story houses

Variations in the open-ground-story houses considered columns that differ in terms of concrete strength, longitudinal bar detailing, transverse tie spacing, and the thickness of the floor and roof slab, and longitudinal PVC gutters embedded in columns. I also considered variation in low, moderate, and high gravity loads associated with 4, 8, and 12 in (10, 20, and 30 cm) RC floor and roof slabs, respectively. In all cases, I determined gravity loads with infilled walls in the second story. All open-ground-story columns are for 8 x 14 in columns (20 x 36 cm) and oriented in the weak-axis direction in the frame line considered. I identified these typical column cross-section size, shown in Figure 3.9, based on the availability and popularity of pre-formed transverse ties measuring 6 x 12 in (15 x 30 cm). I assumed a clear cover of 1 in (2.5 cm). I determined sizes and placement of steel reinforcing bars through interviews with local builders, field observations, and visits to hardware stores. Builders commonly use no. 4 and no. 5 bars for longitudinal bars, and no. 3 bars for transverse ties. Figure 3.11 shows the steel reinforcing available at most hardware stores, the nominal strength of this steel is 40 ksi (276 MPa). Builders reported a typical tie spacing around 6 inches (15 cm), but I observed much larger spacing in some of the collapsed houses in Guánica (see Figure 3.10).

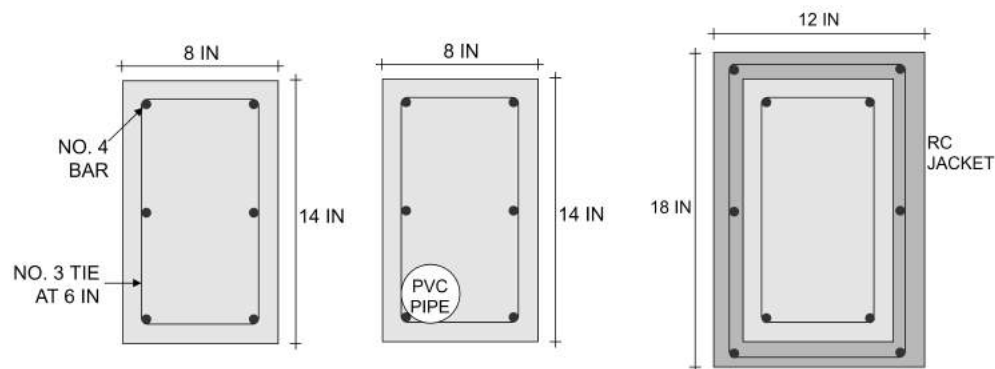


Figure 3.9: Baseline column configuration, and two variations (PVC gutter and RC jacket)

I considered a range of concrete strengths to reflect the variety of concrete mixes reported by builders. Some concrete mix decisions reduce bond strength, *e.g.*, “we add water until it’s easy

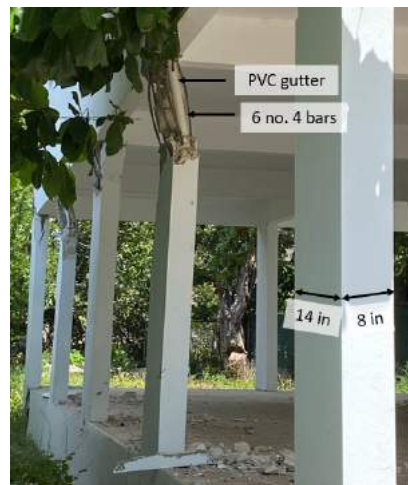


Figure 3.10: Column damaged during the January 7, 2020 earthquake (Guánica, Puerto Rico)



Figure 3.11: Steel reinforcing bars used in home construction. Transverse ties are sold in pre-defined bent shapes; the 6 x 12 in bars are most common. The most common longitudinal bars are no. 4 and no. 5, and are often stored outside (Humacao, Puerto Rico). [Photos: Polly B. Murray]

to work with” or the use of smooth river sand [111, 10]. The range of concrete strengths used in this study reflects tested values from other areas where informal construction is common [10] and my interviews with builders, and are consistent with the range of methods reported for mixing concrete. In some houses, a gutter made with PVC is embedded in the column to prevent water accumulation on the roof. I included some columns with this PVC gutter in this analysis. Table 3.2 summarizes the open-ground-story archetypes considered in this study.

### 3.3.3 Houses with masonry walls

In Puerto Rican construction, external masonry walls are typically built using 6 x 8 x 16 in (15 x 20 x 40 cm) concrete blocks. Blocks measuring 4 x 8 x 16 in (10 x 20 x 40 cm) are commonly used in internal walls, as shown in Figure 3.12. These blocks are typically from the same manufacturer, in northwest Puerto Rico. Hardware stores report the strength of these blocks as 2200 psi (15 MPa). However, I assessed block quality through drop tests, conducted according to the Build Change test [107]. These tests revealed brittle failure in blocks purchased from a hardware store, suggesting a range of values should be considered to capture variation in block quality. From interviews, I estimated mortar is typically type N or S, which correspond to strengths of  $f'm = 750$  and 1500 psi (5 and 10 MPa), respectively [131]. To account for the brittle block failure observed in the drop test, I also considered walls with  $f'm = 400$  psi (3 MPa).

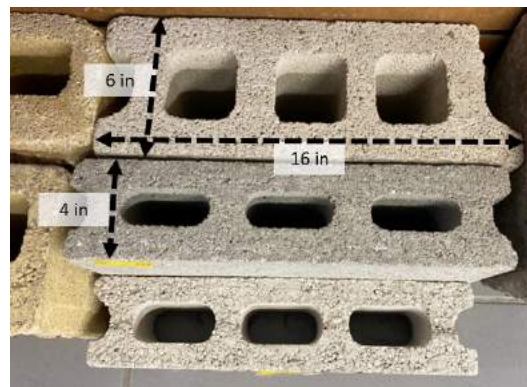


Figure 3.12: Masonry blocks used in home construction available at a hardware store in Puerto Rico. [Photos: Polly B. Murray]

RC frames with both infill and confined methods of masonry construction are considered. These frames have 8 x 8 in (20 x 20 cm) columns, which are typical of houses with walls. I considered walls with different openings, including 3 x 3 ft (90 x 90 cm) windows and 7 x 3 ft (210 x 90 cm) doors (Figure 3.8). I also considered walls with partial height infill, where the top 2 ft (61 cm) are open. This wall is susceptible to shear failure in the section of the column adjacent to the window. These houses have either 4 or 8 in RC floor and roof slabs, as gravity loads are more influenced by masonry walls than slab thickness.

Table 3.3 summarizes house archetypes with concrete masonry walls, including variation in material strength, construction method, distribution of walls, opening type, and gravity loading. For each archetype, I assessed key seismic performance measures, including strength and deformation capacity through pushover analysis, stiffness (period) through eigenvalue analysis, and collapse risk through IDA.

Table 3.2: Open-ground-story houses, including design parameters and performance measures

ID	Column design parameters						Seismic performance measures				
	Column height, h (in)	Column width, b (in)	Conc. strength, $f'_c$ (ksi)	Num. of longi- tudinal bars	Tie spacing, s (in)	Slab thickness, t (in)	Period, $T_1$ (s)	Strength ( $V_{max}/W$ )	Def. capacity (% drift) <sup>1</sup>	Med. Collapse Sa( $T=0.8s$ ) (g)	Med. Collapse Sa/ $MCE_R$
OGS1	8	14	3.0	6	6	4	0.6	0.14	4.7	0.65	1.1
OGS2	8	14	3.0	6	14	4	0.6	0.14	3.0	0.54	0.9
OGS3	8	14	3.0	6	6	8	0.7	0.11	4.4	0.65	1.1
OGS4	8	14	3.0	6	14	8	0.7	0.11	3.3	0.55	0.9
OGS5	8	14	3.0	6	6	12	0.8	0.10	4.0	0.64	1.1
OGS6	8	14	3.0	6	14	12	0.8	0.10	3.2	0.55	0.9
OGS7	8	14	1.5	6	6	4	0.6	0.13	4.6	0.62	1.1
OGS8	8	14	1.5	6	14	4	0.6	0.13	2.5	0.51	0.9
OGS9	8	14	1.5	6	6	8	0.7	0.10	3.9	0.56	1.0
OGS10	8	14	1.5	6	14	8	0.7	0.10	3.0	0.47	0.8
OGS11	8	14	1.5	6	6	12	0.8	0.08	3.5	0.58	1.0
OGS12	8	14	1.5	6	14	12	0.8	0.08	2.6	0.48	0.8
OGS13	8	14	3.0	4	6	4	0.6	0.11	4.3	0.57	1.0
OGS14	8	14	3.0	4	14	4	0.6	0.11	3.3	0.49	0.8
OGS15	8	14	3.0	4	6	8	0.7	0.09	3.8	0.58	1.0
OGS16	8	14	3.0	4	14	8	0.7	0.09	3.1	0.49	0.8
OGS17	8	14	3.0	4	6	12	0.8	0.08	3.4	0.58	1.0
OGS18	8	14	3.0	4	14	12	0.8	0.08	3.0	0.51	0.9
OGS19	8	14	1.5	4	6	4	0.6	0.11	4.1	0.53	0.9
OGS20	8	14	1.5	4	14	4	0.6	0.11	2.2	0.45	0.8
OGS21	8	14	1.5	4	6	8	0.7	0.08	3.5	0.51	0.9
OGS22	8	14	1.5	4	14	8	0.7	0.08	2.8	0.43	0.7
OGS23	8	14	1.5	4	6	12	0.8	0.07	3.1	0.50	0.8
OGS24	8	14	1.5	4	14	12	0.8	0.07	2.5	0.43	0.7
OGS25-P <sup>2</sup>	8	14	3.0	4	6	8	0.7	0.09	3.6	0.59	1.0
OGS26-R <sup>3a</sup>	12	18	3.0	12	2	8	0.3	0.14	4.6	0.59	1.0
OGS27-R <sup>3b</sup>	12	18	3.0	12	2	8	0.3	0.13	4.4	0.58	1.0
OGS28-C <sup>4</sup>	8	14	3.0	6	6	8	0.7	0.11	4.4	0.47	0.8
OGS29 <sup>5</sup>	8	8	1.5	4	6	8	0.8	0.1	5.4	0.31	0.5

<sup>1</sup> Story drift when 20% of strength is lost in pushover<sup>2</sup> PVC gutter<sup>3</sup> Retrofit with (a) full (b) partial RC jacket<sup>4</sup> Corroded reinforcing steel<sup>5</sup> Column with smaller cross section used in wall archetypes

Table 3.3: One- and two-story houses with masonry walls and their seismic design parameters

ID	Design parameters				Seismic performance measures							
	Wall construction <sup>1</sup>	Conc. strength, $f'_c$ (ksi)	Masonry strength, $f'_m$ (ksi)	Num. of stories	Slab thickness (in)	First story, bays <sup>2</sup>	Second story bays <sup>2</sup>	Period, $T_1$ (s)	Strength ( $\frac{V_{max}}{W}$ )	Def. capacity <sup>3</sup> (% drift)	Median Collapse Sa (T=0.1s) (g)	Median Col-lapse Sa $/MCE_R$
W1	I	1.5	0.75	1	8	S   S	-	0.05	1.04	0.58	1.9	1.6
W2	I	1.5	0.75	2	4	S   B	S	0.11	0.42	0.67	0.6	0.6
W3	I	1.5	0.75	2	4	W   B	S	0.11	0.39	0.63	0.6	0.5
W4	I	1.5	0.75	2	4	D   B	S	0.13	0.33	0.63	0.5	0.5
W5	I	1.5	0.75	2	8	S   S	S	0.10	0.67	NC <sup>4</sup>	0.9	0.8
W6	C	1.5	0.75	1	8	S   S	-	0.05	1.87	0.6	3.4	2.9
W7	C	1.5	0.75	2	8	S   S	S	0.09	1.15	0.67	1.1	1.2
W8	I	3.0	1.5	1	8	S   S	-	0.04	1.58	0.5	2.8	2.4
W9	I	3.0	1.5	2	8	S   S	S	0.08	0.82	0.63	1.0	0.9
W10	C	3.0	1.5	1	8	S   S	-	0.04	2.18	0.42	4.3	3.6
W11	C	3.0	1.5	2	8	S   S	S	0.08	0.75	0.46	1.8	1.2
W12	I	1.5	0.75	2	4	S   S	S	0.10	1.16	0.63	1.0	0.8
W13	I	1.5	0.75	1	8	PHI   PHI	-	0.12	1.14	0.57	0.5	0.5
W14	I	3.0	1.5	1	8	PHI   PHI	-	0.12	0.58	NC	0.5	0.5
W15	I	1.5	0.75	2	8	PHI   PHI	S	0.10	0.57	0.57	0.5	0.5
W16	I	3.0	1.5	2	8	PHI   PHI	S	0.09	0.7	NC	0.5	0.5
W17	I	1.5	0.75	2	4	W   W	S	0.10	0.59	0.61	0.9	0.8
W18	I	1.5	0.75	2	4	D   D	S	0.10	0.06	0.61	0.8	0.7
W19C <sup>5</sup>	I	1.5	0.75	2	8	S   S	B	1.00	0.07	6.67	1.5	1.3
W20	I	1.5	0.75	2	8	S   S	B	1	0.75	7.5	0.9	0.8
W21	I	1.5	0.4	2	8	S   S	S	0.13	0.67	NC	0.8	0.7

<sup>1</sup> I: Infilled, C: Confined<sup>2</sup> S: Solid, W: Window, D: Door, PHI: Partial height infill, B: Bare frame<sup>3</sup> Story drift when 20% of strength is lost in pushover<sup>4</sup> Analysis did not converge<sup>5</sup> Corroded reinforcing bars



### 3.3.4 Incremental construction

I considered the effects of incremental construction in two ways. First, I compared the performance of one-story buildings with masonry walls or a second story that is lightweight (wood, which is common in Puerto Rico) and a heavy second story that built with RC and masonry. The weight of the moderate and heavy second stories correspond to masonry walls and RC columns with roof and floor slabs that are 4 and 8 in (10 and 20 cm) thick, respectively. Builders will often leave reinforcing bars extending above columns to facilitate the addition of an additional story, as shown in Figure 3.3a. This practice is common, and, from field observations and interviews, I determined splices are typically 24 in (60 cm) in length. These bars, when not protected from exposure by coating, corrode and may impair the seismic performance of the house. The level of corrosion varies with time and proximity to the coast [116, 132, 115, 133]; I incorporated an anticipated upper bound of bar area loss due to corrosion, 20%, to capture a scenario where a bar may be exposed for more than a decade and is close to the coast, as is the case in much of Puerto Rico, and a lower bound in which no corrosion has occurred. Table 3.4 summarizes the archetypes used in this study to assess the effects of incremental construction on collapse capacity.

Table 3.4: Archetype houses used to assess effects of incremental construction

ID	Description
W1	One-story, 8 in roof slab OR two-story, 4 in slab with wood frame second story
W2	Two-story, 4 in floor and roof slabs and infill walls
W5	Two-story, 8 in floor and roof slabs and infill walls
W20	Two-story, RC frame second story (no infill) with corrosion
W21	Two-story, RC frame second story (no infill) without corrosion

### 3.3.5 Retrofit

Local builders and community organizations with whom I met expressed interest in building modifications that could improve seismic performance, especially for open ground story buildings. I have investigated the potential benefits of two retrofit options in this study: RC jacketing and

infill walls. In the RC jacket retrofits, additional concrete and longitudinal and transverse steel reinforcement are added to vulnerable columns to increase strength and deformation capacity [127]. The RC jacket is 2 in (5 cm) thick with 6 no. 5 longitudinal bars and ties consisting of no. 3 bars at 2 in and is applied to all columns in the soft story. I assessed two cases to capture variation in construction quality. In the first, a “full” RC jacket, the jacket is well connected to the existing column through dowels and a roughened surface and the entire length of the column acts as an equivalent monolithic element [134, 135]. In the second, a “partial” RC jacket. This jacket still extends the full height of the column, but the connection between the jacket and the existing column is not as strong, and only the lower portion of the column sees a performance improvement. RC jacketing maintains the open story, which may be desirable to homeowners. Filling some or all open bays with masonry blocks can significantly increase strength and stiffness of open ground stories, but potentially reduces access to floor area [128]. I selected retrofits that use readily available and affordable materials [101]. Martinez Cruzado et al. proposed retrofit methods for Puerto Rican houses on stilts (*i.e.*, open-ground-story houses) including adding RC walls and strengthening foundations [130]. RC walls require engineered design and may be beyond the scope of informal construction. Many of the homes identified by Martinez Cruzado et al. [130] were vulnerable because of their location on a hillside, the archetypes in this study do not have this vulnerability as they are assumed to be built on level ground.

### 3.4 Nonlinear simulation models

I developed nonlinear 2D *OpenSees* [89] models to capture the seismic performance of the archetype informally-constructed houses up to the point of collapse. The 2D models described subsequently represent the building orientation and frame line that is expected to control the structural response (*i.e.*, the weaker direction), as shown in Figure 3.6a. Figure 3.13 shows a typical model for the archetype houses, including lumped plasticity hinges to represent the nonlinear behavior of columns and diagonal struts to represent the behavior of infill or confined masonry panels. These elements are calibrated as described below.

In all building models, I applied 3% Rayleigh damping at the first and third modes, assuming a cracked initial stiffness [54, 136]. I determined gravity loads based on estimated weights of walls, roof, and floor slabs, and beams and columns, along with 25% of design live loads for residential buildings [84]. These loads were applied as masses to generate inertial seismic forces and as distributed and point loads on beams and at the top of columns. I used a fixed base in these models, as slab foundations are common and the focus of this work is on structure response. I considered P- $\Delta$  effects in this analysis through the *PDelta* geometric transformation [137].

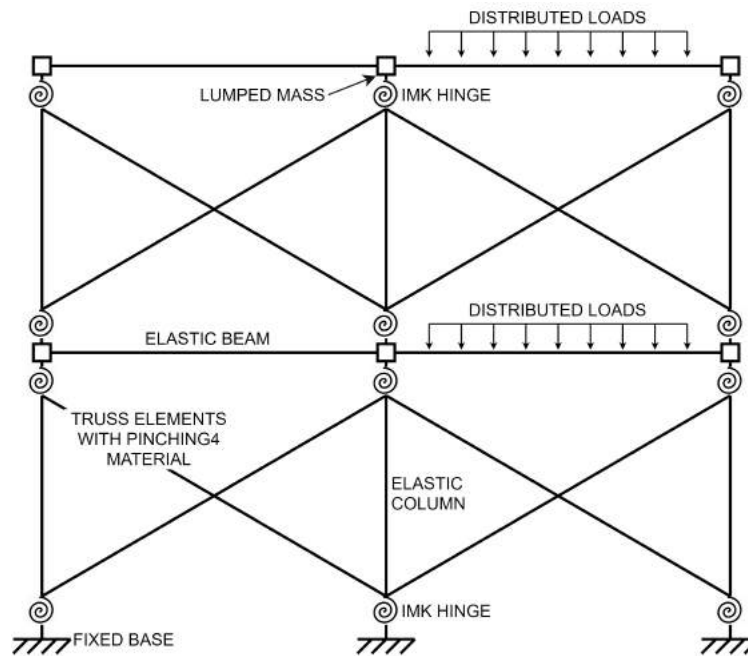


Figure 3.13: Diagram of models of a two-story, two-bay house with infilled or confined masonry walls.

The relative stiffness of the open ground story is significantly lower than an infilled story, generating a weak and soft first story. Under pushover loading, all lateral displacement occurs in the first story. To reduce computational time, I modeled open-ground-story houses as shown in Figure 3.14 with lumped masses representing the stiff second story. The rigid beam captures the stiffness of the second story, while the lumped masses account for its weight. This simplification can obscure the distribution of mass and damage to the second story, but these effects in both pushover and dynamic analysis are minor and are outweighed by the significant reduction in computational

time.

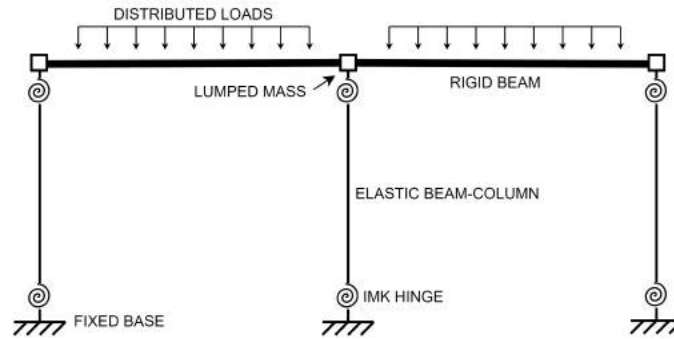


Figure 3.14: Diagram of models of the open-ground-story houses. The lumped masses account for the weight of a second story with masonry walls.

### 3.4.1 RC columns

Due to their design details, the columns in this study are flexure-critical, with ratios of flexural to shear strength between 0.2 to 0.5 (except those considered with the partial height infill). Columns are modeled using a lumped plasticity approach with rotational spring defined using the Peak-Oriented Ibarra, Medina, Krawinkler (IMK) material [90]. The IMK model parameters for each column are based on equations by [54], which considers each column's reinforcement, axial load ratio, transverse tie spacing, and account for bar slip. An elastic beam-column element connects rotational spring and accounts for the elastic response, considering cracked sections.

I also modified the analytical model for the columns to account for reinforcing bar corrosion due to several years of exposure (see Figure 3.11b). The response of the IMK hinges was modified based on a review of the literature for this level of exposure in a coastal environment, which indicated a moderate reduction (30%) in yield and ultimate strength (*e.g.*, Zhang et al. [138], DiCarlo et al. [133], Meda et al. [139]). Based on field observations that showed the length of exposed rebar typically exceeds minimum splice length requirements per ACI 318 [140], I did not consider vulnerabilities associated with short lap splices. In addition, Meda et al. [139] tested the cyclic response of concrete columns with corroded and uncorroded bars, and found that deformation capacity was reduced by 50%. Ou et al. [132] developed equations to capture the effect of corrosion

on the force-deformation response of concrete sections and found a similar reduction in strength and deformation capacity. The backbone defining the nonlinear response of the corroded columns was modified based on Meda et al. [139].

I also modeled the seismic performance of RC columns with PVC gutters, or longitudinal holes, in this study. The response of RC components with longitudinal holes has been studied analytically and experimentally. Murugesan and Narayanan [141] tested 86 RC beams with longitudinal holes of various sizes and positions, and found that beams with holes were slightly weaker and less stiff than those without holes. Kassim and Ahmad [142] evaluated RC columns with longitudinal rainwater pipes through compression testing, and found that a 5% decrease in the cross-sectional area reduced axial capacity by 20%. Informed by these experimental studies, I determined the strength, stiffness, and deformation capacity of an RC column with a longitudinal hole using a distributed plasticity fiber analytical model. I defined the column cross-section using *OpenSees* materials *Concrete02*, which captures linear tension softening, and *Steel02*, which follows the Giuffr -Menegotto-Pinto model for steel behavior and captures strain hardening [137]. In the case with PVC, I omitted fibers to represent the hole. I calibrated a lumped plasticity (IMK) model so its static pushover response matched that of the fiber model, and used the lumped plasticity model to determine the effect of PVC gutters on collapse capacity. PVC gutters slightly reduce the strength of columns, as illustrated by Figure 3.15d, though this is relatively inconsequential when compared to other column details (*e.g.*, tie spacing, gravity load).

Well-connected RC jackets respond as an equivalent monolithic section [134, 135], the full RC jacket cases are modeled as larger columns in place of smaller sections. The response is calibrated following Haselton et al. [54]. In the partial RC jacket case, only the bottom of the column is modified. This approach captures a case in which vertical loads in the column are not distributed to the jacketed portion over the entire length of the column. If the existing column is not modified through doweling or surface roughening, the RC jacket does not significantly improve performance [134, 135]. As a result, I have not considered houses with poorly-built RC jackets.

Figure 3.15 shows the effect of design variation on the pushover response of individual

columns, illustrating the changes in strength, stiffness, and deformation capacity associated with each configuration. Longitudinal reinforcement, both the number of bars and the level of corrosion, has the most significant effect on the flexure capacity of columns. Deformation capacity is most influenced by corrosion and the spacing of transverse ties in the columns and the gravity (axial) load level. RC jacket retrofit significantly increases strength, stiffness, and deformation capacity.

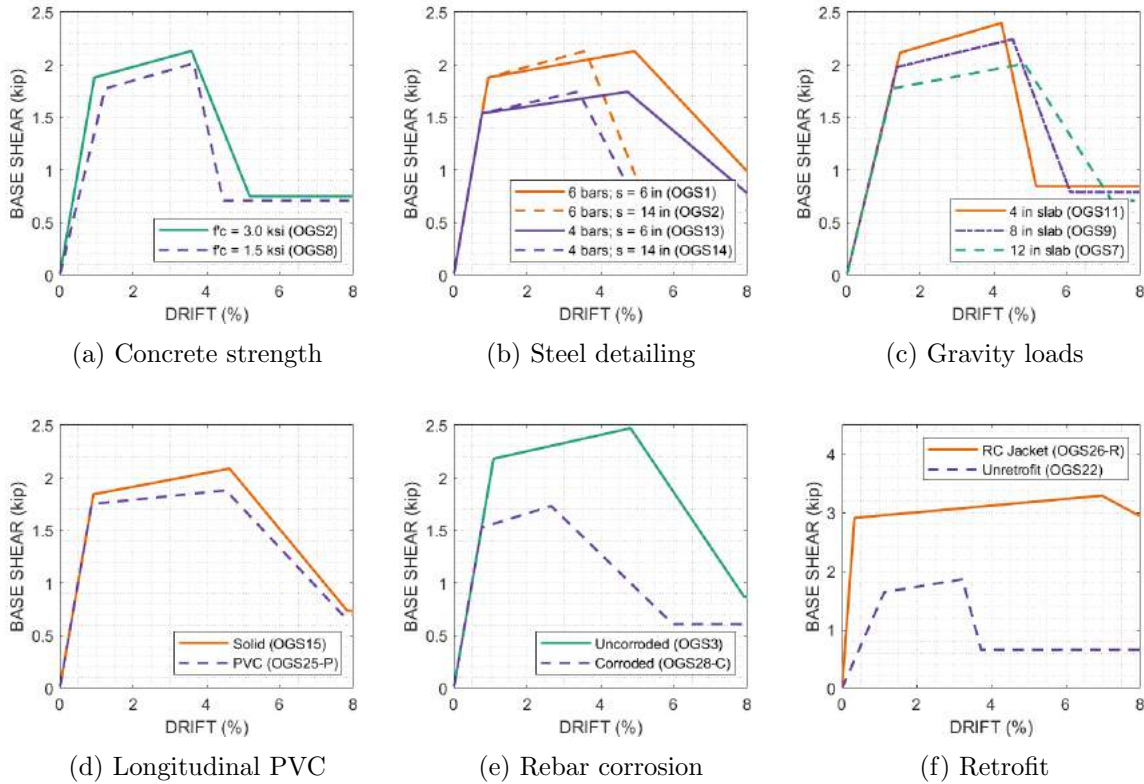


Figure 3.15: Static pushover response of columns configurations.

### 3.4.2 Masonry walls

Several methods exist for numerical modeling of infill and confined walls in RC frames; researchers have considered approaches that balance detail (*e.g.*, micro-modeling and finite element (FE) modeling) with computational efficiency (*e.g.*, strut models). Burton and Deierlein [143] calibrated equivalent struts to represent the behavior of infill walls in 3D analysis models used to assess collapse capacity. Their work illustrated methods for incorporating the various failure

mechanisms typical of infilled frames, including shear failure, infill sliding and crushing, and flexural hinging. Sattar and Liel [59] used FE modeling to calibrate strut models in nonductile RC frames with infill walls, balancing model accuracy and computational efficiency.

Recently, micro-models and experimental testing have been aggregated to develop empirical equations to calibrate diagonal compression struts to predict the response of masonry walls in RC frames. Huang et al. [55] developed a database of experimental responses of infilled frames and used it to create empirical equations to define the response of struts. Bose et al. [117] developed analytical backbone equations to capture the force-displacement response of infilled bays of RC frames. They used the developed model to assess a multi-story RC frame and masonry wall building that was damaged in the 2015 Ghorka earthquake in Nepal [144], showing the efficacy of the analytical model in predicting damage in an informally-constructed building. Mohammad Noh et al. [52] assessed efforts to capture the cyclic response of masonry infill walls through numerical simulation, and found that the behavior can reliably be captured with a hysteretic model that includes pinching in struts.

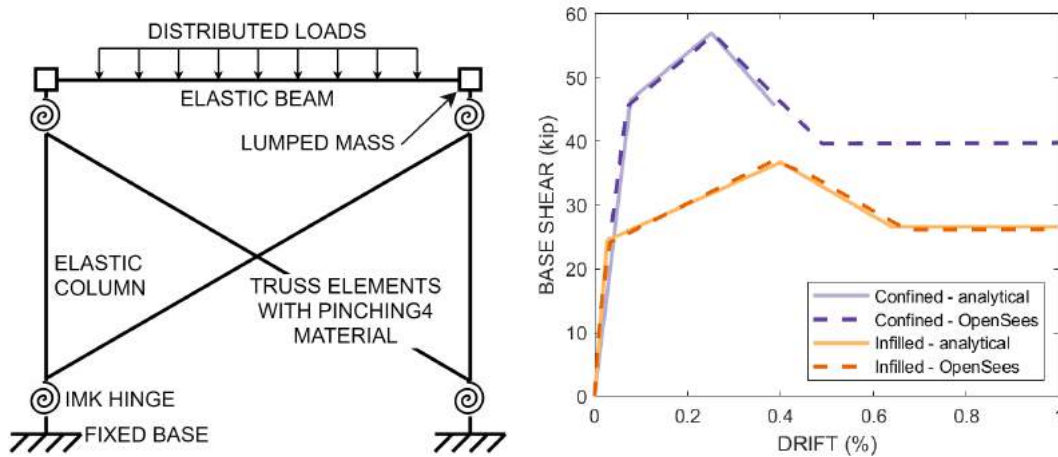


Figure 3.16: (a) Diagram of the model of a single bay with RC columns and a concrete masonry panel, illustrating the adopted modeling approach; and (b) analytical backbone and static pushover response of one bay calibrated for infilled and confined construction.

Figure 3.16a shows the modeling approach adopted for a single bay of RC frame with infilled or confined masonry implemented in *OpenSees*. The diagonal struts represent the behavior of the

masonry panel and are modeled using truss elements defined by a uniaxial material with a pinched hysteretic response, *Pinching4* [137]. For infill walls, I followed the methodology proposed by Bose et al. [117] to define the material model parameters in the strut, because it captures the variety of potential of failure modes in infill walls-RC frame systems and considers the effects of vertical (gravity) loading, concrete and masonry strength, and openings on the lateral capacity of infilled RC frames. Bose et al. [117] developed this approach based on experimental tests, including infilled RC frames with concrete blocks, similar to those built informally in Puerto Rico. Following the Bose et al. [117] approach, I first identify the anticipated force-deformation response using empirical equations developed by Martín Tempestti and Stavridis [145]. These equations consider multiple possible failure mechanisms in masonry infilled RC frames, and the interaction between columns and infill, including bed joint sliding, shear or flexural failure in columns, masonry toe crushing, and shear cracking within the masonry panel, and were validated through comparison with experimental testing [145]. This backbone is defined by three points: force and deformation at yielding, maximum strength, and residual capacity. This model only considers the in-plane response of infill walls; based on observations of damage following the January 2020 earthquake, this failure mode is more common in RC houses with masonry walls in Puerto Rico [24]. The identified failure mechanism for a particular case depends on the relative strength and stiffness of the RC frame and masonry panel. The RC frame is classified as ductile or nonductile by the ratio of shear demands corresponding to flexure strength and shear strength [146, 145]. The infill panel is classified as strong or weak based on its stiffness relative to the column considering masonry unit strength  $f'_m$  and geometric properties. The configurations considered in this study are all ductile frames, except for cases with partial height infill, which is nonductile because of the induced short columns. The analytical backbone for each bay is a function of the failure mechanism classification, gravity load distribution, and wall and column characteristics. In this approach, the distribution of gravity loads between the walls and columns depends on the connection between the beam and the top of the infill panel and affects the lateral strength and failure mechanism of the wall system. I assumed there was no connection based on field observations of under-construction houses and discussion



with builders, and thus no gravity load on the infill panel.

To match the *OpenSees* model response of each RC frame bay with infill to the Bose et al. [117] analytical backbones, first, the input parameters for this material are determined following the empirical equations developed by Huang et al. [55]. Columns are modeled as described above. I adjusted these parameters so the pushover response of the bay (*i.e.*, columns, beam, and infill panel) matches the analytical backbone defined by Martín Tempestti and Stavridis [145], accounting for openings and the gravity load distribution. Figure 3.16b shows the analytical backbone for one typical infilled bay in the Puerto Rico archetype houses.

The backbone equations account for openings in the middle of infilled bays, by reducing the expected strength and stiffness proportionally to the area of the opening. However, in archetypes where the opening is within 2 feet (61 cm) of the column, the length of the column is modified to match the height of the opening, following Stavridis [147]. In this study, I consider the heightened risk of shear failure in short columns induced by partial height infill, illustrated in Figure 3.8. This configuration increases seismic vulnerability through brittle shear failure in columns adjacent to the opening [119]. I determined the shear strength of the short column using the formulation in ASCE/SEI 41-17 [95] and modified the column force-displacement response to degrade sharply when shear force demands exceed capacity. I modeled the behavior of the partial height infill panel as a solid panel tied from the base of the frame to the bottom of the opening with no gravity loads to determine the Martín Tempestti and Stavridis [145] backbone.

For the confined masonry systems, I again calibrated diagonal struts to represent the behavior of the walls, following recommendations of Ghaisas et al. [148]. The force-deformation backbones for confined walls are calibrated following equations developed by Riahi et al. [56]. These equations were developed based on a database of 102 confined masonry wall tests. These equations define response up to the ultimate drift capacity, defined as the level of drift at which 20% of lateral strength is lost. I assumed this to be the residual capacity of the wall system, though this level of drift typically coincides with the collapsed limit state. For systems with similar details (*e.g.*, column detailing, masonry and mortar strength, axial loads), a bay of confined masonry construction is

stronger than an infilled frame, as illustrated by Figure 3.16b.

### 3.5 Seismic performance assessment methods

Tables 3.2 and 3.3 summarize the house configurations and results of the seismic performance assessment. Building period is determined using eigenvalue analysis considering a cracked stiffness assumption in columns [54]. Strength and deformation capacity are determined using static pushover analysis conducted with a displacement-controlled analysis and an applied inverted triangular lateral load. Building strength is presented as maximum lateral base shear from pushover normalized by building weight ( $V_{max}/W$ ). Deformation capacity is quantified as the level of story drift when 20% of strength has been lost [86]. Collapse capacity, obtained through dynamic analysis, is used to quantify differences in performance among the building types.

The collapse safety performance is assessed using IDA, as illustrated in Figure 3.17. For each ground motion record, the ground motion input was scaled at increasing intensity—quantified as spectral acceleration ( $S_a$ ) at the structure’s first mode period—until a collapse threshold was reached. For houses with infilled or confined walls, I considered a building collapsed if story drifts exceed 1.5% [149]; for open-ground-story houses, the collapse threshold is 5% drift [53]. Because the IDA curves have flatlined by the time these thresholds are reached, the collapse assessment is not sensitive to the precise value. This process is then repeated for other ground motion records to capture record-to-record variability in the response. I used the FEMA P-695 [86] record set in IDA because the ground motion records are representative of typical far-field records from crustal earthquakes, which is consistent with the seismic hazard in Puerto Rico [102]. This set contains record pairs from 22 ground motions; I applied each horizontal motion record, 44 in total, to each 2D frame of the archetype building. These records contain variation in duration and frequency content and have been widely used to assess collapse capacity.

I derive collapse fragility curves from the motion intensity at which the collapse threshold is reached for each ground motion. For open-ground-story houses, I evaluated collapse at  $S_a(T=0.8s)$ , and for houses with walls, at  $S_a(T=0.1s)$ . These periods are typical of each building type and allow

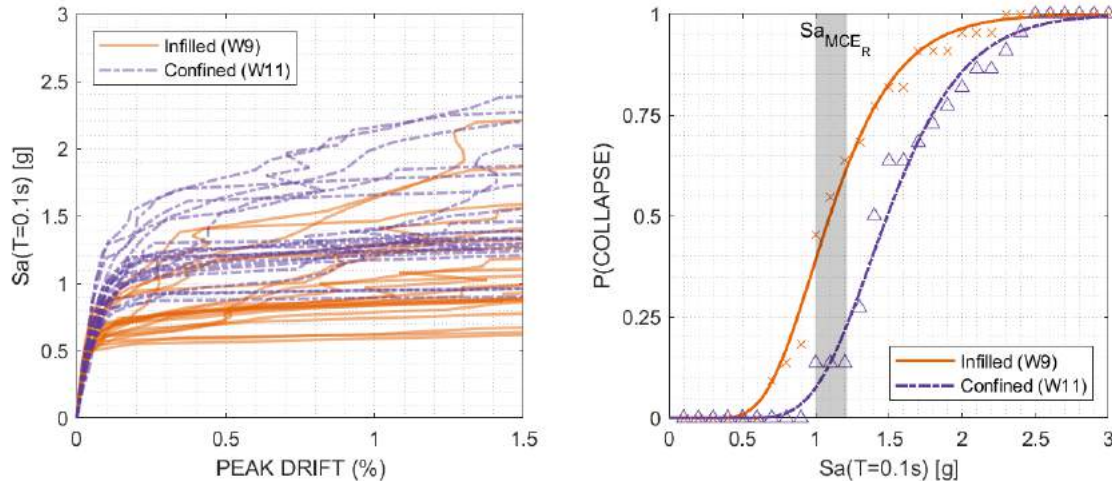


Figure 3.17: (a) IDA results for a single-story house with infilled and confined construction, and (b) corresponding fragility curves (both empirical and fitted distribution).

for a more direct comparison of seismic performance within each subgroup (open-ground-story and houses with walls). For each archetype, I fit the  $S_a$  collapse intensity values from each record with a lognormal cumulative distribution function (CDF) to obtain the probability of collapse associated with each intensity level. Figure 3.17 shows the collapse fragilities for two single-story houses and the IDA from which they were derived. The median collapse capacity is the ground motion intensity at which analysis indicates a 50% probability of collapse. Only record-to-record variability is considered in the fragility of each building. For context, I show the  $S_a$  range for the risk-targeted maximum considered earthquake ( $MCE_R$ ) values on the island from ASCE 7-16 [84] assuming site class B [129].

In addition to collapse, I investigated the likelihood that a ground motion will cause a structure with masonry walls to reach different damage states, including slight, moderate, extensive, and collapse, based on the extent of cracking and crushing in the masonry panel. These limits are defined as 0.15, 0.4, 1.0, and 1.5% story drift, respectively, and were calibrated based on aggregated experimental testing [149]. Slight damage indicates the presence of small cracks for which repair is only cosmetic. Moderate damage indicates larger, repairable cracks. Extensive damage typically requires the demolition of some building elements. Similar limit states are used to assess confined

masonry walls (*e.g.*, Ruiz-García and Negrete [150] and Tomažević and Klemenc [151]). Following a procedure similar to the definition of collapse fragilities, I identified the probability of exceedance of each damage state at a range of ground motion intensities using a cumulative distribution function. The focus of this work is on collapse risk, but limit states can be beneficial in identifying expected repair needs, which correlate with downtime, and costs. For example, slight damage may only require patching of cracks, while extensive damage may require demolition of building elements, which may make the space uninhabitable until repairs are complete [149].

### 3.6 Seismic performance results for informally-constructed houses

Figure 3.18 shows the collapse assessment results of the archetype houses in this study, with results for all buildings detailed in Table 3.2 and Table 3.3. Generally, houses with masonry walls perform better in earthquakes than those with open ground stories due to the strength and stiffness provided by the concrete block walls, as will be explored in more detail below. In the United States, a code-conforming building is expected to have a 10% probability of collapse during an  $MCE_R$ -level ground motion [84]. As illustrated by Figure 3.18b, most archetype buildings in this study do not meet that criteria. Generally, one-story houses with walls, particularly those built as confined masonry panels, perform well, with a low risk of collapse at  $MCE_R$  levels. Open-ground-story houses and those with partial height infill are most vulnerable to collapse in an  $MCE_R$ -level event, with a median collapse probability of 80%. The ratio of the median collapse  $S_a$  to  $S_a$   $MCE_R$  indicates that collapse is likely in open-ground-story buildings during an  $MCE_R$  level ground motion. The results following illustrate the effects of individual building characteristics (*e.g.*, material strength, construction type, detailing) on overall collapse capacity when other properties are kept the same.

#### 3.6.1 Collapse risk of open-ground-story RC houses

The collapse risk is high ( $P(\text{collapse} \mid MCE_R) > 0.75$  and median collapse  $S_a/MCE_R$   $S_a$  around 1.0) for all open-ground-story houses, listed in Table 3.2, considered in this study. These houses consistently fail in a soft-story mechanism in the first story.

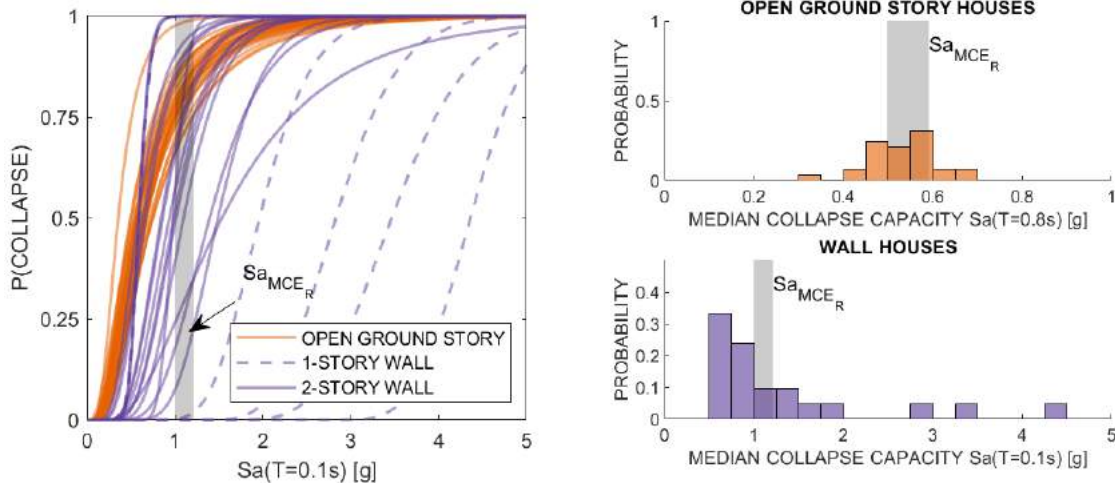


Figure 3.18: (a) Summary of collapse fragilities for all archetype houses; (b) distribution of median collapse capacities for informally-constructed RC open-ground-story houses and houses with masonry walls.

### 3.6.1.1 Effect of house weight and gravity loads

To explore the building characteristics that most influence this collapse risk, Figure 3.19 shows the collapse fragilities for open-ground-story houses of low, moderate, and high weight. These houses have relatively weak ( $f'_c = 1.5$  ksi, 5 MPa) concrete and 6 in (15 cm) tie spacing. In all three cases, houses are vulnerable to collapse in an  $MCE_R$ -level ground motion (illustrated in gray). The columns see an increase in flexural capacity with the increased gravity load due to moment-axial interaction. However, the increased gravity load and seismic weight reduce the deformation capacity of columns, generate larger inertial forces, and amplifies P- $\Delta$  effects, which translates to a higher probability of collapse, particularly at higher motion intensities.

### 3.6.1.2 Effect of column detailing

I then assessed the effect of column steel reinforcement on the seismic performance of these houses. Figure 3.20 illustrates the effect of the number of longitudinal bars and transverse tie spacing on collapse capacities for archetypes that all have weak concrete strength and moderate gravity loading. Columns perform better in columns with 6 longitudinal bars (reinforcement ratio,

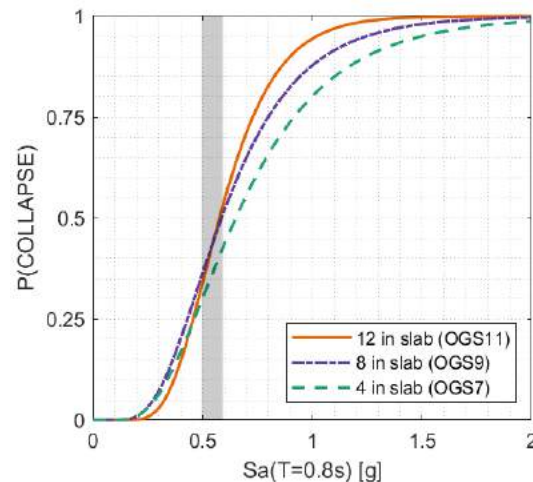


Figure 3.19: Collapse fragilities of open-ground-story houses with variation in weight, induced by floor and roof slab thicknesses listed in the legend.

$\rho = 0.011$ ) when compared to columns with 4 longitudinal bars ( $\rho = 0.007$ ). Similarly, collapse risk is reduced by closer spacing of transverse ties. Columns with 6 in (15 cm) spacing ( $\rho_{sh} = 0.003$ ) have better seismic performance than columns with 14 in (26 cm) spacing ( $\rho_{sh} = 0.001$ ). Transverse tie spacing increases deformation capacity and, when small enough, provides additional strength in confined concrete. I only included tie spacings typical of informal construction in Puerto Rico, which does not provide any confinement in columns.

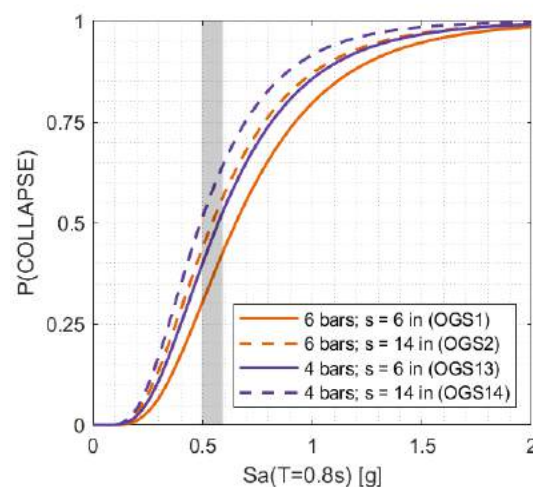


Figure 3.20: Collapse fragilities of open-ground-story houses with variation in weight, induced by floor and roof slab thicknesses listed in the legend.

### 3.6.1.3 Effect of reinforcing bar corrosion and PVC gutters

Figure 3.21a shows the difference in collapse fragility for a column with and without an embedded PVC gutter. Prior research [141, 142] has illustrated the slight change in strength and stiffness for columns with longitudinal holes, and this slight change is reflected in the collapse capacity. Figure 3.21b shows the effect of reinforcing steel corrosion. The behavior of the corroded model is defined considering 20% mass loss [139], which represents an upper bound on material quality available in Puerto Rican hardware stores 3.3.1. The lost cross-sectional area of reinforcing bars reduces the strength and deformation capacity of RC columns [116, 132, 115, 133]. Jiang et al. [152] developed a model for the effect of corrosion on bond slip based on a database of experimental testing, and found that as the level of corrosion increases, the level of stress at which slip occurs on the concrete-steel interface. The lost bond strength is accounted for in the modified force-deformation curve used to define the corroded column response. When critical columns, such as those in an open-ground-story, are affected by corrosion, this reduction in strength and deformation capacity manifests as a higher collapse risk during an earthquake. This is illustrated in Figure 3.21b, which compares the response of archetype houses with corroded and uncorroded reinforcing bars.

### 3.6.1.4 Effect of retrofit strategies

The retrofit strategies described in Section 3.3.5 increase the strength and stiffness of the vulnerable open-ground-story houses, and in cases where infill is added to previously empty bays, change the failure mechanism. Houses that have been retrofit with RC jackets still fail in a soft-story mechanism; houses that have been retrofit with infill may fail through masonry crushing or column failure, depending on the relative strength and stiffness. These failure mechanisms are discussed in Section 3.4.2, depending on the configuration of the frame. Figure 3.22 b shows the reduction in collapse risk of full RC jacketing, approximately a 10% reduction in the probability of collapse during an  $MCE_R$ -level ground motion, while partial RC jacketing does not improve

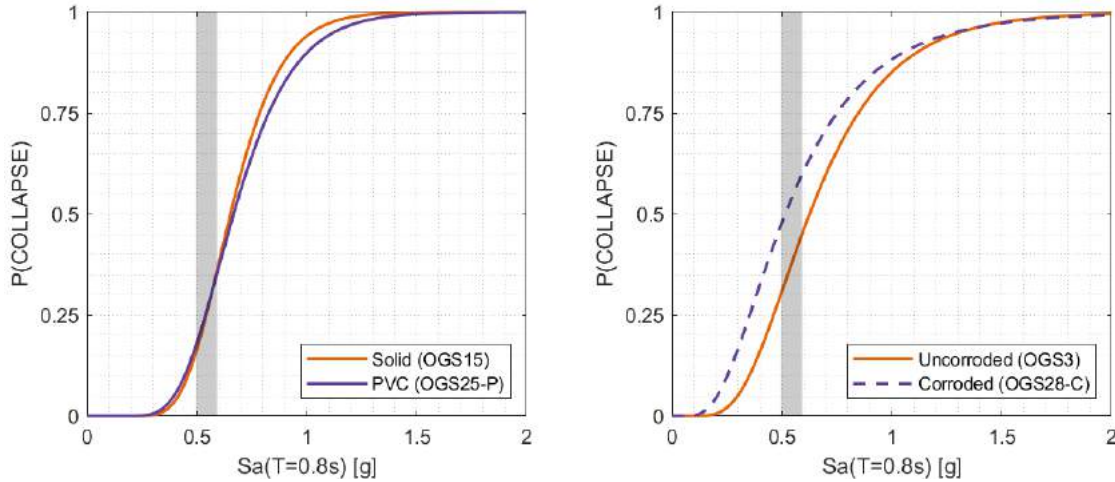


Figure 3.21: Collapse fragilities of open-ground-story houses with (a) longitudinal PVC gutter, and (b) corroded reinforcing steel. Corroded reinforcing steel in vulnerable columns reduces collapse capacity.

outcomes. Partial RC jacketing, in this case, is a result of construction methods that do not adequately improve the full column.

Retrofitting one or both bays of an open-ground-story building increases the strength and stiffness of the structure, and reduces the probability of collapse from approximately 85% to 50% if all bays are filled, but also reduces deformation capacity and leads to failure at lower levels of drift. Figure 3.22 suggests that infill panels provide the most significant reduction of collapse risk, but none of the retrofit strategies investigated here reduce collapse risk to an acceptable level ( $P(\text{collapse}) = 10\%$  in an  $MCE_R$ -level motion) [84].

### 3.6.2 Assessment of RC houses with walls

The collapse risk in houses with masonry walls varies more widely than in open-ground-story houses. In one-story houses or two-story houses built using confined construction,  $P(\text{collapse} | MCE_R)$  is  $< 0.25$ . In houses with partial height infill,  $P(\text{collapse} | MCE_R)$  approaches 1.0. Table 3.3 summarizes all house archetypes with masonry walls considered in this study, along with the associated collapse intensity.



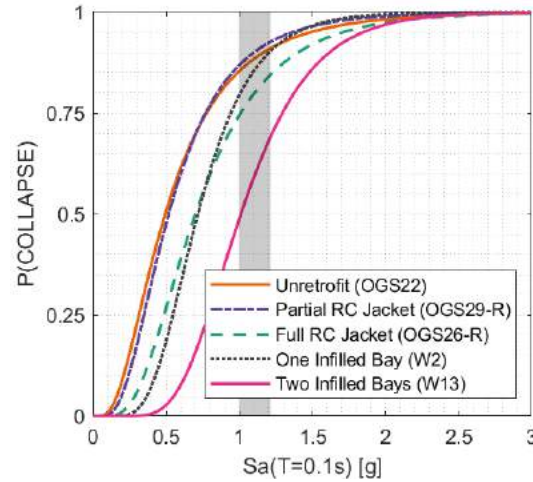


Figure 3.22: Collapse fragilities of open-ground-story house retrofit with full or partial RC jackets, one, and two bays of infill, illustrating the largest reduction in collapse capacity is provided by two bays of infill

### 3.6.2.1 Effect of construction method

Figure 3.23 illustrates the collapse fragilities for one- and two-story houses with infilled and confined masonry walls, to explore the effect of the construction method. In all cases, confined construction performed approximately 50% better than infilled, because of the gravity load distribution through the masonry panel and the confined masonry panel's capacity to act as a shear wall [153].

Additionally, I looked at the probability that non-collapse damage states will be exceeded for a given ground motion intensity for two-story masonry wall houses. The limit states, which have been defined by Cardrone et al. [149] for infilled walls, indicate the level of story drift associated with slight, moderate, and extensive damage. Figure 3.24a illustrates the IDA response for a two-story infill wall house, and the level of drift at which each limit state is achieved. Figure 3.24b shows the probability of exceedance for each limit state of infilled (I) and confined (C) masonry wall houses. The construction method does not affect initial stiffness; infilled and confined masonry reach the slight damage state at the same ground motion intensity. Houses built with infilled panels are more likely to experience moderate to extensive damage or collapse during  $MCE_R$ -level ground

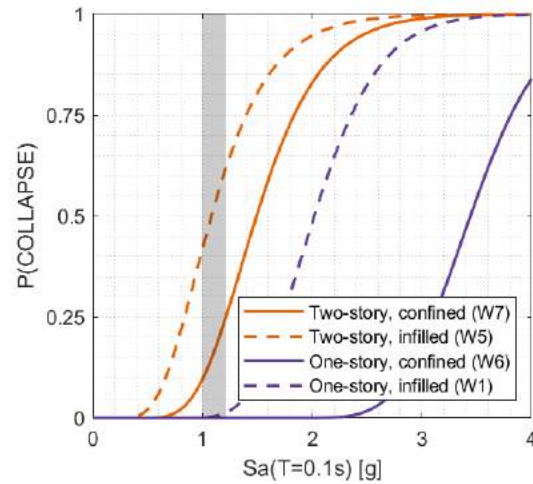


Figure 3.23: Collapse fragilities for one- and two-story houses with infilled and confined masonry walls, showing the large benefit from the confined construction technique.

motions than houses with confined masonry panels.

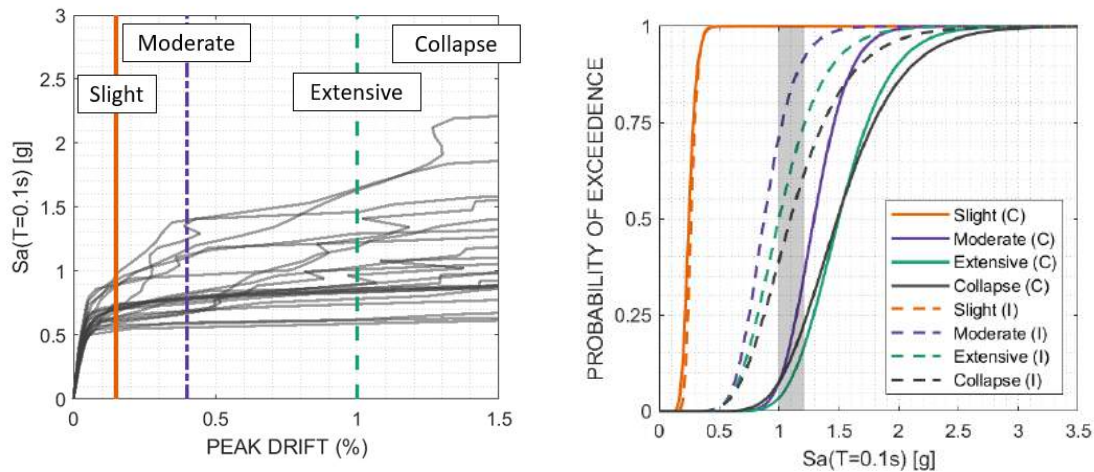


Figure 3.24: (a) Damage states, defined by the level of peak story drift. (b) Probability of exceedance for slight, moderate, extensive, and collapsed damage states in a two-story house with infilled (I) and confined (C) masonry walls.

### 3.6.2.2 Effect of material strengths

I assessed archetypes with a range of concrete and masonry unit strengths to represent the available materials on the island. Figure 3.25 shows the collapse fragilities for two-story houses with

infilled panels of varied strength. Stronger masonry units increase the strength and deformation capacity of wall panels and can rescue collapse risk, *i.e.*,  $P(\text{collapse} \mid MCE_R)$  by 10 – 20%.

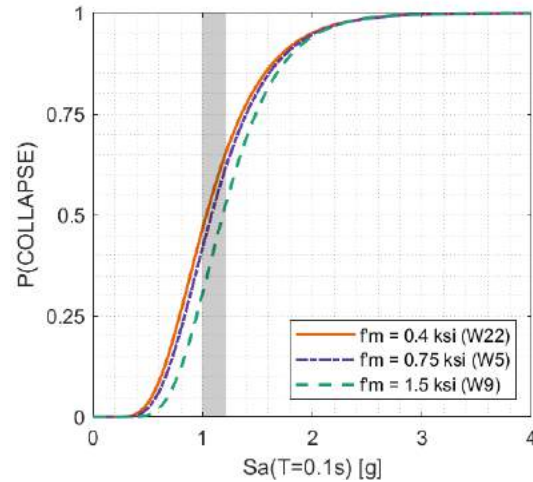


Figure 3.25: Collapse fragilities two-story houses with variation in masonry unit strength. Stronger masonry units reduce collapse risk.

### 3.6.2.3 Effect of openings

Figure 3.26 shows the collapse fragilities of two-story houses with window or door openings, with a solid infill panel, and with a partial height infill panel that induces a short column (see Figure 3.8). The reduced strength and stiffness of the houses with window and door openings (on the order of 15 and 10%) leads to a modest reduction in collapse capacity (around 10%). Notably, the house with partial height infill in the first story is far more vulnerable to collapse in an earthquake. This configuration is susceptible to brittle shear failure and has suffered extensive damage in recent earthquakes [120].

### 3.6.3 Collapse risk of incrementally-constructed houses

I considered the effect of incremental construction on seismic performance in two ways: (1) the change in collapse risk with the addition of a second story, and (2) corrosion of reinforcing bars from exposure. Figure 3.27 summarizes the effect of these configurations. One-story houses

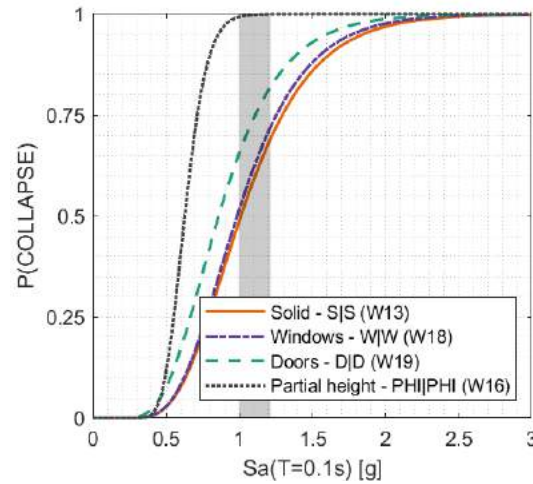


Figure 3.26: Collapse fragilities for walls with openings

have significantly lower collapse risks than two-story houses due to the lower seismic mass. In two-story cases, failure occurs in the first story, and the increased weight generates larger lateral demands. This is consistent with research by Lallemand et al. [114]. Corrosion of bars does not have a significant effect when limited to second story columns, as these columns only support the roof slab, and lateral demands are relatively small as a result.

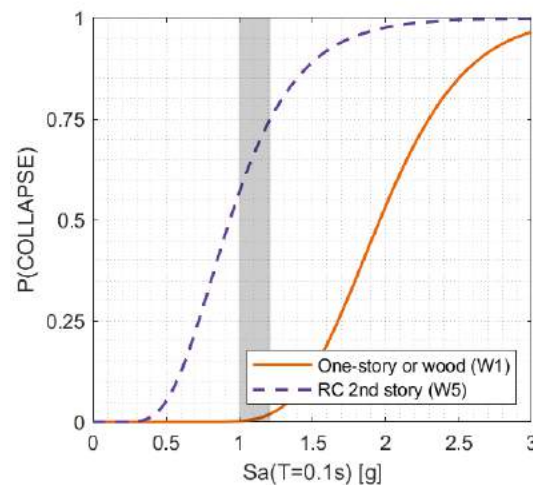


Figure 3.27: Collapse fragilities for one- and two-story houses. The addition of an RC second story drastically increases collapse risk, while a wood frame second story, which does not increase building weight significantly, does not.

### 3.7 Comparison with reconnaissance data

This work was informed by observations of damage by my team one month after the earthquake, and preliminary reconnaissance reports, including those by StEER [24], FEMA [154], and EERI [155]. These reports provide information regarding typical damage patterns and locations most affected by the earthquakes, but do not provide a detailed investigation of the extent of damage (*e.g.*, slight, moderate, extensive, or collapse) for a complete set of buildings or building components. Information can be gleaned from efforts to rehabilitate communities affected by the earthquake; FEMA has allocated more than 100 million USD to aid Puerto Ricans in recovery, including loans for nearly more than 1300 homeowners and renters [154], as of July 2021, more than 40,000 individuals have applied for disaster assistance. This indicates the broad need for repair or rebuilding.

USGS reports shaking intensities, peak spectral acceleration (PSA) at 0.3 s, around 0.50g in the most heavily affected municipalities during the largest of the January 2020 earthquake. For many of the open-ground-story houses, which are most vulnerable to ground shaking, the probability of collapse at this intensity from this assessment is approximately 50%. Based on observations of damage, these models are in general agreement with the extent of damage, but more detailed damage reports could improve this comparison. Observations indicated collapse or significant residual drift in many open-ground-story houses. Masonry walls in first stories of two-story houses tended to see more damage than one-story houses with masonry walls. Typically, this damage was in the form of in-plane shear cracking in masonry panels, which is consistent with the strong-infill-ductile-frames assessed in this study [145]. Damage to second stories was uncommon. My analytical models reflect this: building components in first stories have a much larger effect on overall seismic performance.

Many of the damaged columns in collapsed houses in Guánica featured very large transverse tie spacing or PVC gutters embedded in columns. I investigated both column configurations given the frequency of these column characteristics among collapsed buildings. Through numerical simu-

lation, I found that lateral tie spacing has a larger effect on seismic performance. It is important to note that the presence of PVC gutters or transverse tie spacing in undamaged houses is unknown.

In future reconnaissance efforts, it would be beneficial to generate a database with the locations of affected buildings, extent of damage, and construction details, including building and component dimensions, characteristics (*i.e.*, confined or infilled construction). This information would be beneficial in assessing the seismic safety of houses, and offering recommendations for improved performance.

### 3.8 Limitations and future work

There are some limitations to this study. First, materials used in informal construction can be highly variable, and depend on manufacturing (*e.g.*, concrete masonry blocks), available raw materials (*e.g.*, source of sand or rounded river aggregate), storage (*e.g.*, corrosion of steel reinforcement from exposure), and craftsmanship (*e.g.*, concrete and mortar mix and preparation). I accounted for many of these variations through parametric assessment of archetypes, but the uncertainty of this assessment could be reduced through material testing of typical materials. In this study, I used analytical assessments and test data to quantify the effects of PVC gutters in columns. I found that they do not significantly influence performance, but physical testing under cyclic loading could reinforce this claim. Paired with this, modeling the investigation of the effect of the PVC exiting the column may provide further insight into the vulnerability of this configuration. Other building variations could provide insight on seismic performance, including different foundations (*e.g.*, spread footings and hillside foundations), wood roofs, and different masonry block types (*e.g.*, clay brick, 4 in concrete blocks). This work did not consider failure in foundations or hillside cases, both of which have been shown to exacerbate collapse risk [156, 130] and are common in Puerto Rico. I observed limited cover in RC slabs and columns, and in some cases, deterioration and spalling failure of these elements, which is not fully considered.

In this seismic performance assessment, I used analytical models to determine the dynamic response of structures. Developing these models requires assumptions to be made regarding the

behavior of concrete and masonry components. These assumptions introduce uncertainty [53], which can be reduced with physical testing or more complex models. In this study, I used 2D models of a single frame line. I selected a frame line that is likely to control the behavior of the building, but it does not consider torsion or out-of-plane effects. These effects could be investigated using 3D models of masonry wall and open-ground-story buildings. The models in this study represent a lower bound of infilled construction, where no gravity load is transferred to the blocks, but careful construction of an infill panel could provide increased safety in a future earthquake.

The models in this study assume a fixed foundation, but soil-structure interaction should be considered in stiff structures (*i.e.*, those with masonry walls) and may increase displacements during ground shaking [157]. Further, I assessed the performance of informally-constructed houses using a generalized set of far-field ground motions [86]. Ground motions appropriate for a building site can be selected to match a target conditional mean spectrum [81]. This method requires hazard deaggregation, which is not currently available for Puerto Rico [83].

I investigated potential retrofit options in this study, including RC jacketing and infill walls. These options were selected because they employ readily available and inexpensive materials. Given the interest in seismic performance upgrades in Puerto Rico [35], I recommend further study into retrofit options and benefits.

### 3.9 Conclusions and recommendations

This study develops and demonstrates a framework for evaluating the earthquake risk of informally-constructed RC houses, with results for housing in Puerto Rico. I sought to identify which building elements and characteristics most affect seismic performance with the aim of recommending improvements or modifications to decrease collapse risk. I began by developing archetype buildings representative of RC houses in Puerto Rico through interviews with local builders and hardware store owners and reconnaissance following the damaging January 2020 earthquakes. I then modeled these archetype houses and quantified the strength, stiffness, and deformation capacity of each configuration. I used dynamic analysis to determine the collapse fragility associated

with building characteristics, including material strength, reinforcing bar detailing, gravity loads, and masonry wall construction.

I found that, generally, lighter houses perform better than heavier houses in earthquakes. While both RC columns and masonry walls see a benefit in terms of strength and deformation capacity from additional gravity load—particularly confined masonry walls—the increase in seismic mass outweighed this benefit, leading to two-story houses to have 60% lower median collapse capacity than one-story houses. Houses with masonry walls typically have lower collapse risks than open-ground-story houses (by, on average, 57%), and confined masonry performed better than infilled (an improvement of 100 to 200%). Among the open ground story houses, the most important building characteristics are column detailing, including transverse and longitudinal reinforcing and reinforcing bar corrosion, and building weight, which alters the collapse capacity by up to 30%.

Houses built incrementally have increased seismic risk as a result of expansion, and the additional demands on existing structures. A two-story house, built incrementally or at once, has a collapse risk 80% higher than a one-story house. Corrosion of reinforcing bars at the base of the second story does not significantly impair performance, when compared to the same frame with uncorroded bars.

I assessed two retrofit options, RC jacketing and infill walls, and found that both improved seismic performance of vulnerable houses. The most effective solution included in this work is the addition of infill walls in all open bays. RC jacketing can reduce collapse risk by 10% if the jacket is well-connected to the existing column and vertical loads are distributed throughout the jacket and the existing column.

This work aims to reduce the uncertainty around the seismic performance of informally-constructed homes to improve resilience through viable and feasible solutions [101]. Based on these findings, recommendations for improved seismic safety in informally-built residential construction in Puerto Rico are summarized in Table 3.5. These recommendations are rated based on their reduction of collapse risk and cost of implementation. For new construction, costs are estimated based on the price of materials; for existing construction, costs are estimated based on materials and



construction time as a proxy for labor costs. The costs presented in Table 3.5 are approximate, and further study is needed to develop community-specific cost estimates for improved seismic resilience. Costs associated with new and existing construction are considered separately. For many of these interventions, it is difficult to quantify the cost of implementation. For example, confined masonry construction may require additional training, but this cost may not be directly translated to the homeowner. Similarly, RC jacketing requires training that may not be available to all builders, but the material costs may be lower than retrofit by infill. For homeowners looking to expand their homes, a vertical expansion is typically less expensive as additional land is not required. The cost associated with procuring more land is highly variable.

Table 3.5: Recommendations for improved seismic safety in new and existing houses

Recommendation	Cost	Impact on collapse risk
<i>New construction</i>		
Lighter weight construction where possible, including thinner roof and floor slabs	L	M
Use confined construction instead of infilled when building with masonry	L	H
Place transverse ties close together in columns, and use uncorroded steel reinforcing bars	M	M
<i>Existing construction</i>		
Retrofit vulnerable columns using RC jackets	M	L
Retrofit open ground story houses by adding infill panels	M	M
Expand horizontally, rather than vertically, if space allows	H	H
Build vertical expansions using wood (with strong connections for hurricane resistance) [158]	M	H

<sup>1</sup> Impact on collapse risk is based on the change in the probability of collapse in an  $MCE_R$  level event. L indicates a change in  $P(\text{collapse})$  is less than 10%, H indicates a change in  $P(\text{collapse})$  greater than 50%

For those who work in the construction industry in Puerto Rico, including local organizations and those who manage hardware stores, I recommend the following:

- (1) Advise homeowners to avoid open-ground-story construction, unless adequate seismic strength and deformation capacity is provided through larger, well-detailed (*i.e.*, sufficient transverse

and lateral reinforcement) columns.

- (2) Provide guidelines for retrofit using RC jacketing or infill walls.
- (3) Encourage and train builders to use confined masonry construction, rather than infilled, for new house construction.
- (4) Demonstrate the importance of high-quality materials, including uncorroded reinforcing bars well-manufactured masonry blocks (quality can be demonstrated through drop testing, poorly-manufactured blocks typically shatter when dropped from 4 ft (1.2 m)).
- (5) Illustrate the cost-benefit of building with higher quality materials or larger columns by quantifying typical repair and rebuilding costs.

These recommendations may help improve the seismic resilience in informally-constructed houses, in combination with other strategies that (1) increase awareness of seismic hazard [113], (2) increase knowledge of the importance of material and construction quality [159], and (3) policy making to increase construction oversight [113, 114]. For Puerto Rico, timing is good as interest in safe building methods is high, particularly after the recent earthquake.

## Chapter 4

### Conclusions

In this dissertation, I investigated the seismic performance of reinforced concrete (RC) structures with a particular focus on the future performance of damaged buildings and collapse risk of informally-constructed homes. For each study, I developed a framework for assessing seismic performance, defined damage metrics of interest, and exercised the framework for a set of archetype structures to determine the influence of building components and characteristics. Together, these frameworks offer improved assessment techniques of RC buildings that increase the understanding of the seismic performance of RC structures to improve community outcomes in major earthquakes. Additionally, I tested and implemented computationally-efficient analysis methods that can be applied to future related studies, reducing run-time while maintaining or improving the breadth of analysis. I also developed 2D and 3D nonlinear numerical models that can easily be adapted to model other buildings. The contributions of this dissertation are summarized in Table 4.1.

#### 4.1 A framework for assessing impaired seismic performance as a trigger for repair

##### 4.1.1 Summary

In *Chapter 2*, I developed and exercised a framework for quantifying the effect of earthquake damage on the seismic performance of RC buildings. The framework involves a comparison of seismic performance—quantified as peak story drift demands—of a building in its damaged and undamaged state in a set of  $MCE_R$ -level ground motion records. I assessed drift demands using

Table 4.1: Summary of studies collected in this dissertation, including research gaps and contributions

Chapter	Research Questions	Contributions
<b>Chapter 2.</b> A framework for assessing impaired seismic performance as a trigger for repair	When does damage matter? How do building characteristics affect how damage changes future performance? How can the computational efficiency of these assessments be improved?	<i>Theoretical:</i> Methodology for assessing the effect of damage future seismic performance. <i>Practical:</i> Identification of the level of damage at which performance is impaired and safety repairs needed. Numerical models for library of nonlinear dynamic analysis.
<b>Chapter 3.</b> Seismic safety assessment of informally-constructed houses in Puerto Rico	How does informal construction affect the earthquake risk of homes? What building elements most influence seismic performance? What improvements could be made to houses to reduce collapse risk?	<i>Theoretical:</i> Framework for assessing seismic performance of informally-constructed houses. Quantification of effects of building characteristics on collapse risk. <i>Practical:</i> Recommendations for safer building and retrofit strategies for Puerto Rico

back-to-back nonlinear dynamic analysis in *OpenSees*; the first motion damages the building model in the simulation, and the second motion is used to assess the change in performance due to damage. This chapter provides results for 50 single-degree-of-freedom and five 3D models of modern RC frame buildings, and uses machine learning strategies to improve computational efficiency in the selection of analyses to include in back-to-back analysis. For each building, I considered the magnitude and distribution of drift amplifications to identify a threshold at which seismic performance may be impaired, indicating repairs are needed.

The results of *Chapter 2* illustrate the benefit of building deformation capacity in repeated earthquakes in that they are able to sustain more damage before having impaired future performance. Future seismic performance of code-conforming, longer-period ( $T > 1$ s) structures is not significantly impaired by earthquakes in which story drifts do not exceed 2%. The undamaged short

period building in this study had the lowest drift demands in the  $MCE_R$ -level ground motions, but was the most sensitive to damage in terms of drift amplifications. Ductile buildings were the least sensitive to damage. Strong buildings had lower drifts in the undamaged building, so saw relatively higher amplifications in the damaged state.

#### 4.1.2 Contributions

This work is part of the FEMA-funded project that seeks to address the lack of guidelines for post-earthquake repair in the U.S. [39]. The current guideline for repair, FEMA 306 [45] is more than 20 years old, and only applies to a subset of buildings. This framework and the results of this study contribute to system-level checks which, when paired with component-level assessment and visual inspection, can reduce unnecessary repair or demolition and identify which buildings may have insufficient capacity to resist future earthquakes. Using computational models to evaluate performance, this framework accounts for cyclic loading effects, including strength and stiffness deterioration, in evaluating performance. Historically, extensive nonlinear dynamic analysis is computationally-intensive. I address this by applying machine learning strategies and computationally-efficient models to reduce run-time. This framework illustrated the relationship between damage and future performance, which measures of damage best capture impaired seismic performance, and how different building characteristics (*e.g.*, stiffness, deformation capacity, and strength) affect a structure's capacity to withstand damage. The results of this framework for a set of modern RC buildings revealed which building characteristics are likely to contribute to impaired performance, which can improve post-earthquake decision-making.

#### 4.1.3 Limitations and future work

There are some limitations to this work. First, the buildings in this study are all modern RC frame buildings with significant deformation capacity. While I considered non-conforming buildings, I did not consider highly non-ductile frames. As the aim of this work is to assess the future performance of buildings, I first focused on ductile buildings for which repair is a likely

post-earthquake outcome, rather than non-ductile buildings which are likely in need of significant repairs or demolition in the aftermath of an earthquake [99]. I focused on drift amplifications in  $MCE_R$ -level motions as an indicator of seismic performance and proxy for safety. However, lower levels of damage may impair the serviceability of a building. This study does not consider cosmetic repairs. Additionally, I assessed the system-level performance of buildings, but repair may be needed to address damage to components that may not be evident through a system-level analysis. This framework could be paired with component-level analysis (*e.g.*, checks of low-cycle fatigue) to more thoroughly understand the extent of damage and determine a repair strategy. Finally, several elements of this framework require judgment. I quantified drift amplifications relative to drift demands for an undamaged building, but this can obscure the actual seismic performance of a building when the undamaged building has poor performance. In using this framework to guide post-earthquake decision-making, it is important to consider how amplified drift demands relate to design limits. More discussion is needed to determine whether the limits chosen are appropriate for other structural systems.

In future studies, this framework could be applied to a wider range of building types, including non-ductile RC, wood, or steel buildings. The repair trigger threshold detailed in this chapter, which is defined by a 15% change in demands, is based on historical thresholds for building repair [14], and a conservative estimate of the upper bound of performance (*i.e.*, the 90<sup>th</sup> percentile of drift amplifications). This definition of when repair is needed is intentionally conservative, but could be refined through assessment of more buildings and building types.

## 4.2 Seismic safety assessment of informally-constructed houses in Puerto Rico

### 4.2.1 Summary

In *Chapter 3*, I evaluated the seismic performance of residential construction in Puerto Rico. More than half of houses there are built informally; the lack of explicit engineering design poten-

tially increases vulnerability in earthquakes. I developed a framework for defining a set of archetype RC houses based on interviews, field work, and reconnaissance reports. For each archetype, I developed a nonlinear *OpenSees* model and assessed the seismic performance using incremental dynamic analysis (IDA). From the IDA, I calculated the collapse fragilities for each archetype, and compared fragilities to evaluate the effect of building characteristics on seismic performance. Informal construction has a wide range of performance, but is generally worse than code-conforming due to the lack of ductile detailing, low-quality and highly variable materials, and vulnerable building configurations. I found that open-ground-story houses, which offer strong flood resistance, are most vulnerable to collapse in earthquakes due to the weak and poorly-detailed columns. Incremental construction, a house expansion practice that is common worldwide, increases vulnerability of homes through additional gravity loads/seismic weight, and weakened connections. The presence of a PVC gutter in a column did not significantly affect seismic performance, as other column details dominated response. Houses with masonry walls, either confined or infilled construction, have lower collapse risk than open-ground-story houses as they add strength and stiffness. However, confined construction offers better performance than infilled construction because the panel shares the gravity loads and acts as a unified system, increasing strength and stability. Heavier buildings, from large floor and roof slabs or additional stories, have higher collapse risk as they generate large inertial seismic forces. I assessed two retrofit options, RC jacketing and infill panels, and found that both improve seismic performance. RC jacketing reduces collapse risk moderately while maintaining deformation capacity. Infill panels increase strength and stiffness, and reduce collapse risk more drastically. I considered the cost and benefit of design decisions and retrofit strategies to make recommendations for homeowners, builders, and local organizations.

#### 4.2.2 Contributions

Despite the ubiquity of informal construction in many parts of the world, particularly areas of high seismic hazard, limited work has been done to assess the seismic performance of these houses. Seismic performance is often assessed retrospectively in the aftermath of earthquakes;

this work provides a framework for assessing seismic safety apriori. I demonstrate the utility of this framework for identifying collapse risk associated with house configurations, materials, and construction methods. I exercise this framework for a set of 50 archetype houses in Puerto Rico and identify recommendations for homeowners, builders, and local organizations that will improve seismic safety. I considered reconnaissance reports, local knowledge, material availability, and feasibility of implementation in selecting archetype houses and variations as I sought to provide culturally-appropriate recommendations [101]. These recommendations are related to construction methods, materials, and expansion practices, and are presented alongside estimated implementation costs and impact on collapse risk.

### 4.2.3 Limitations and future work

There are several limitations to this work that could be addressed in future study. First, I determined material properties based on limited data. To address this, I incorporated a range of material properties (*e.g.*, concrete and masonry strengths) in the set of archetype houses. However, material testing should be conducted to improve the alignment of simulation models to real world conditions. Also, the simulation models in this study are two-dimensional and contain a single frame line that is likely to govern response; a 3D model could capture torsion and out-of-plane effects. Limited ground motion data is available for Puerto Rico, so this assessment was conducted using a generic set of ground motion records appropriate for far-field analysis [86]. Site-specific and hazard consistent ground motions could improve the accuracy of the assessment should hazard deaggregation become available for the region.

The methods described in *Chapter 3* can be applied to informal housing in other areas of the world, or other types of housing. This work could be made more broadly applicable through study of additional archetypes, including houses with wood roofs, the effects of spread or hillside foundations, and other masonry types that are more common elsewhere (*e.g.*, clay brick). Two retrofit strategies are considered in this work—RC jacketing and infill panels—but additional study of other retrofit methods is needed [127, 130].



### 4.3 Proposed future work

In this work, I have developed nonlinear simulation models to capture the earthquake response of RC buildings. These models feature lumped-plasticity elements that have been calibrated for each building of interest. In recent years, researchers, including Ghannoum et al. [160], have sought to improve nonlinear modeling of RC buildings. These efforts include capturing the multiaxial interaction of demands within the column, integrated prediction of failure mechanism, and calibration of column strength to account for changes in demands at each step of analysis. I am working to incorporate the new column model that is under development by Ghannoum et al. [160], and this work is detailed in Appendix B.

This dissertation focuses on the behavior of RC buildings in earthquakes. Motivated by the complexity of response of RC buildings to ground motions, and the uncertainty surrounding the effects of damage and informal construction, I developed frameworks to assess the seismic performance of RC buildings. In my study of informal construction, I assessed the seismic performance of RC houses in Puerto Rico and identified vulnerabilities with the current state of practice. This work, and the recommendations for builders, homeowners, and local organizations can aid in reducing damage from earthquakes. However, wood-frame construction that is well-detailed for high winds could reduce vulnerability in earthquakes without increasing hurricane risk. Wood houses saw extensive damage, particularly in roofs, during recent hurricanes in Puerto Rico [93]. This damage could be mitigated through design modifications [158], but the intersection of damage assessments in RC and wood homes in hurricanes in earthquakes has not been fully explored. I propose a multi-hazard assessment of wood and RC houses to identify building configurations with limited risk of damage or collapse during both hurricanes and earthquakes.

Further, while there are many advantages to concrete as a building material, the environmental impacts associated with its production are significant. Production of cement, a key ingredient in concrete, accounts for 8% of global carbon dioxide emissions [161]. Further, widespread demolition and rebuilding of buildings in the aftermath of an earthquake comes with a high environmental

cost [162]. The framework for assessing impaired seismic performance is intended to aid in post-earthquake decision-making, but could be applied in other contexts. Welsh-Huggins and Liel [162] demonstrated the capacity for increased lateral strength to reduce the lifetime environmental impact of a building. This framework could also serve to reduce environmental impacts by reducing the need for conservative decision-making that leads to excess demolition. For buildings in which additional lateral strength was not considered in the initial building design, retrofits could prove beneficial in terms of improved repeated earthquake performance and reduced environmental cost.

Additionally, the modeling and analysis strategies for seismic performance assessment used in this study could be applied to other building types with lower environmental impacts, such as cross-laminated timber (CLT). The use of CLT in larger buildings and seismic applications is relatively new, but the analysis methods used in this dissertation could be used to accelerate its adoption.

## References

- [1] Kam WY, Pampanin S, Elwood K. Seismic performance of reinforced concrete buildings in the 22 February Christchurch (Lyttelton) earthquake. *Bulletin of the New Zealand Society for Earthquake Engineering* 2011; 44(4): 239–278.
- [2] Marquis F, Kim JJ, Elwood KJ, Chang SE. Understanding post-earthquake decisions on multi-storey concrete buildings in Christchurch, New Zealand. *Bulletin of Earthquake Engineering* 2017; 15(2): 731–758.
- [3] Government of Nepal . Nepal Earthquake 2015 Post Disaster Needs Assessment—Vol. A: Key Findings. 2015.
- [4] Lang AF, Marshall JD. Devil in the Details: Success and Failure of Haiti’s Nonengineered Structures. *Earthquake Spectra* 2011; 27(S1): 345–372.
- [5] Pokharel T, Goldsworthy HM. Lessons learned from the Nepal earthquake 2015. *Australian Journal of Structural Engineering* 2017; 18(1): 11–23.
- [6] Gagg CR. Cement and concrete as an engineering material: An historic appraisal and case study analysis. *Engineering Failure Analysis* 2014; 40: 114–140.
- [7] Holliday L, Kang THK. Low-cost earthquake solutions for nonengineered residential construction in developing regions. *Journal of Performance of Constructed Facilities* 2015; 29(5): 04014141.
- [8] FEMA P-2020: Mitigation Assessment Team Report. Hurricanes Irma and Maria in Puerto Rico: Building performance, Observations, Recommendations, and Technical Guidance. Federal Emergency Management Agency (FEMA); 2018.
- [9] Kijewski-Correa TL, Kennedy AB, Taflanidis AA, Prevatt DO. Field reconnaissance and overview of the impact of Hurricane Matthew on Haiti’s Tiburon Peninsula. *Natural Hazards* 2018; 94(2): 627–653.
- [10] Marshall JD, Lang AF, Baldridge SM, Popp DR. Recipe for disaster: Construction methods, materials, and building performance in the January 2010 Haiti earthquake. *Earthquake Spectra* 2011; 27(S1): 323–343.
- [11] Arslan M, Korkmaz HH. What is to be learned from damage and failure of reinforced concrete structures during recent earthquakes in Turkey?. *Engineering Failure Analysis* 2007; 14(1): 1–22.

- [12] Gulkan P, Sozen MA. Inelastic responses of reinforced concrete structure to earthquake motions. In: *Proceedings of the American Concrete Institute*. . 71. ; 1974: 604–610.
- [13] Elwood K, Filippova O, Noy I, Paz JP. Seismic Policy, Operations, and Research Uses for a Building Inventory in an Earthquake-Prone City. *International Journal of Disaster Risk Science* 2020; 11(6): 709–718.
- [14] Polese M, Di Ludovico M, Marcolini M, Prota A, Manfredi G. Assessing reparability: simple tools for estimation of costs and performance loss of earthquake damaged reinforced concrete buildings. *Earthquake Engineering & Structural Dynamics* 2015; 44(10): 1539–1557.
- [15] Safiey A, Pang W. A new approach to assessing reparability for seismic risk assessment of buildings. *Earthquake Spectra* 2021; 37(1): 284–303.
- [16] Burton HV, Deierlein GG. Integrating visual damage simulation, virtual inspection, and collapse capacity to evaluate post-earthquake structural safety of buildings. *Earthquake Engineering & Structural Dynamics* 2018; 47(2): 294–310.
- [17] Hulsey AM, Deierlein GG, Baker JW. Quantifying the post-earthquake downtime induced by cordons around damaged tall buildings. In: *Proceedings of the 11th US National Conference on Earthquake Engineering, Los Angeles, California*. ; 2018.
- [18] Kim JJ, Elwood KJ, Marquis F, Chang SE. Factors influencing post-earthquake decisions on buildings in Christchurch, New Zealand. *Earthquake Spectra* 2017; 33(2): 623–640.
- [19] Potter SH, Becker JS, Johnston DM, Rossiter KP. An overview of the impacts of the 2010–2011 Canterbury earthquakes. *International Journal of Disaster Risk Reduction* 2015; 14: 6–14.
- [20] Hosseinpour F, Abdelnaby AE. Fragility curves for RC frames under multiple earthquakes. *Soil Dynamics and Earthquake Engineering* 2017; 98: 222–234.
- [21] Raghunandan M, Liel AB, Luco N. Aftershock collapse vulnerability assessment of reinforced concrete frame structures. *Earthquake Engineering & Structural Dynamics* 2015; 44(3): 419–439.
- [22] Dorahy MJ, Rowlands A, Renouf C, Hanna D, Britt E, Carter JD. Impact of average household income and damage exposure on post-earthquake distress and functioning: A community study following the February 2011 Christchurch earthquake. *British Journal of Psychology* 2015; 106(3): 526–543.
- [23] USGS . M 6.4 - 13km S of Indios, Puerto Rico. United States Geological Survey (USGS); 2020. <https://earthquake.usgs.gov/earthquakes/eventpage/us70006vll/executive>. Accessed May 2021.
- [24] Miranda E, Acosta Vera A, Aponte L, et al. StEER - 07 Jan. 2020 Puerto Rico Mw6.4 Earthquake: Preliminary Virtual Reconnaissance Report (PVRR). tech. rep., DesignSafe-CI; 2020.
- [25] Mazzei P, Ayala E, Robles F. After Homes Collapse in Earthquake, Puerto Ricans Ask: Are We Safe?. The New York Times; 2020. <https://www.nytimes.com/2020/01/08/us/puerto-rico-earthquake.html>. Accessed May 2021.

- [26] Robles F. Months After Puerto Rico Earthquakes, Thousands Are Still Living Outside. The New York Times; 2020. <https://www.nytimes.com/2020/03/01/us/puerto-rico-earthquakes-fema.html>. Accessed May 2021.
- [27] Puerto Rico Department of Housing . Puerto Rico Disaster Recovery Action Plan. 2018.
- [28] Samper J. Toward an epistemology of the form of the informal city: Mapping the process of informal city making. *Informal Settlement Research ISR* 2014.
- [29] Talbot J, Poleacovschi C, Hamideh S, Santos-Rivera C. Informality in Postdisaster Reconstruction: The Role of Social Capital in Reconstruction Management in Post–Hurricane Maria Puerto Rico. *Journal of Management in Engineering* 2020; 36(6): 04020074.
- [30] Ferguson B, Smets P. Finance for incremental housing; current status and prospects for expansion. *Habitat International* 2010; 34(3): 288–298.
- [31] World Bank . World Development Report 2010: Development and Climate Change. 2010.
- [32] Zorn M. Natural disasters and less developed countries. In: *Nature, Tourism and Ethnicity as Drivers of (De)Marginalization*. Springer. 2018 (pp. 59–78).
- [33] USGS . M 7.0 - 10 km SE of Léogâne, Haiti. United States Geological Survey (USGS); 2020. <https://earthquake.usgs.gov/earthquakes/eventpage/usp000h60h/executive>. Accessed May 2021.
- [34] Mix D, Kijewski-Correa T, Taflanidis AA. Assessment of residential housing in Leogane, Haiti, and identification of needs for rebuilding after the January 2010 earthquake. *Earthquake Spectra* 2011; 27(S1): 299–322.
- [35] Goldwyn B, Javernick-Will A, Liel A. Dilemma of the Tropics: Changes to Housing Safety Perceptions, Preferences, and Priorities in Multihazard Environments. *Natural Hazards Review* 2021; 22(3): 04021012.
- [36] Suárez LE, López RR, Torres DV, Caraballo MEA. Topographic amplification of earthquakes in Puerto Rico and its effects in residential construction. Federal Emergency Management Agency (FEMA); 2003.
- [37] Mittrani-Resier J, Wu S, Beck JL. Virtual Inspector and its application to immediate pre-event and post-event earthquake loss and safety assessment of buildings. *Natural Hazards* 2016; 81(3): 1861–1878.
- [38] (ATC) ATC. ATC-20: Procedures for Post-Earthquake Safety Evaluation of Buildings. 1989.
- [39] Elwood K, Sarrafzadeh M, Pujol S, et al. Impact of Prior Shaking on Earthquake Response and Repair Requirements for Structures – Studies from ATC-145. In: *Proceedings of the NZSEE Conference, New Zealand Society for Earthquake Engineering, Christchurch, New Zealand.* ; 2021.
- [40] Zhang Y, Burton HV, Shokrabadi M, Wallace JW. Seismic Risk Assessment of a 42-Story Reinforced Concrete Dual-System Building Considering Mainshock and Aftershock Hazard. *Journal of Structural Engineering* 2019; 145(11): 04019135.

- [41] Jeon JS, DesRoches R, Brilakis I, Lowes L. Aftershock Probabilistic Seismic Demand Model of Damaged Non-Ductile Reinforced Concrete Frames in California. In: *ASCE Structures Congress 2013*. ; 2013: 2638–2649.
- [42] Ruiz-García J, Aguilar JD. Aftershock seismic assessment taking into account postmainshock residual drifts. *Earthquake Engineering & Structural Dynamics* 2015; 44(9): 1391–1407.
- [43] Ramirez C, Liel A, Mittrani-Reiser J, et al. Expected earthquake damage and repair costs in reinforced concrete frame buildings. *Earthquake Engineering & Structural Dynamics* 2012; 41(11): 1455–1475.
- [44] Holmes WT. Policies and standards for reoccupancy repair of earthquake-damaged buildings. *Earthquake Spectra* 1994; 10(1): 197–208.
- [45] FEMA 306 . *Evaluation of Earthquake Damaged Concrete and Masonry Wall Buildings: Basic Procedures Manual*; Redwood City, CA: Federal Emergency Management Agency (FEMA) . 1998.
- [46] Brando G, Rapone D, Spacone E, et al. Damage reconnaissance of unreinforced masonry bearing wall buildings after the 2015 Gorkha, Nepal, Earthquake. *Earthquake Spectra* 2017; 33(S1): 243–273.
- [47] O'Brien P, Eberhard M, Haraldsson O, et al. Measures of the seismic vulnerability of reinforced concrete buildings in Haiti. *Earthquake Spectra* 2011; 27(S1): 373–386.
- [48] Hassan AF, Sozen MA. Seismic vulnerability assessment of low-rise buildings in regions with infrequent earthquakes. *ACI Structural Journal* 1997; 94(1): 31–39.
- [49] Brzev S, Pandey B, Maharjan DK, Ventura C. Seismic vulnerability assessment of low-rise reinforced concrete buildings affected by the 2015 Gorkha, Nepal, earthquake. *Earthquake Spectra* 2017; 33(S1): 275–298.
- [50] Gautam D, Chaulagain H. Structural performance and associated lessons to be learned from world earthquakes in Nepal after 25 April 2015 (MW 7.8) Gorkha earthquake. *Engineering Failure Analysis* 2016; 68: 222–243.
- [51] Elwood KJ, Moehle JP. Evaluation of existing reinforced concrete columns. In: *Proceedings of the 13th World Conference on Earthquake Engineering. 13WCEE, Vancouver, B.C., Canada*. ; 2004.
- [52] Noh NM, Liberatore L, Mollaioli F, Tesfamariam S. Modelling of masonry infilled RC frames subjected to cyclic loads: State of the art review and modelling with OpenSees. *Engineering Structures* 2017; 150: 599–621.
- [53] Liel AB, Haselton CB, Deierlein GG, Baker JW. Incorporating modeling uncertainties in the assessment of seismic collapse risk of buildings. *Structural Safety* 2009; 31(2): 197–211.
- [54] Haselton CB, Liel AB, Taylor-Lange SC, Deierlein GG. Calibration of model to simulate response of reinforced concrete beam-columns to collapse.. *ACI Structural Journal* 2016; 113(6).
- [55] Huang H, Burton HV, Sattar S. Development and utilization of a database of infilled frame experiments for numerical modeling. *Journal of Structural Engineering* 2020; 146(6): 04020079.

- [56] Riahi Z, Elwood KJ, Alcocer SM. Backbone model for confined masonry walls for performance-based seismic design. *Journal of Structural Engineering* 2009; 135(6): 644–654.
- [57] Krawinkler H, Seneviratna G. Pros and cons of a pushover analysis of seismic performance evaluation. *Engineering structures* 1998; 20(4-6): 452–464.
- [58] Ellingwood B. *Development of a probability based load criterion for American National Standard A58: Building code requirements for minimum design loads in buildings and other structures*. 13. US Department of Commerce, National Bureau of Standards . 1980.
- [59] Sattar S, Liel AB. Seismic performance of nonductile reinforced concrete frames with masonry infill walls—II: collapse assessment. *Earthquake Spectra* 2016; 32(2): 819–842.
- [60] Sattar S, Mahoney M, Kersting R, et al. Recommended options for improving the functional recovery of the built environment. In: *17th World Conference on Earthquake Engineering. 17WCEE, Sendai, Japan.* ; 2020.
- [61] Polese M, Marcolini M, d’Aragona MG, Cosenza E. Reconstruction policies: explicating the link of decisions thresholds to safety level and costs for RC buildings. *Bulletin of Earthquake Engineering* 2017; 15(2): 759–785.
- [62] Gokkaya BU, Baker JW, Deierlein GG. Quantifying the impacts of modeling uncertainties on the seismic drift demands and collapse risk of buildings with implications on seismic design checks. *Earthquake Engineering & Structural Dynamics* 2016; 45(10): 1661–1683.
- [63] FEMA 307 . *Evaluation of Earthquake Damaged Concrete and Masonry Wall Buildings: Technical Resources*; Redwood City, CA: Federal Emergency Management Agency (FEMA) . 1998.
- [64] Abdelnaby AE, Elnashai AS. Performance of degrading reinforced concrete frame systems under the Tohoku and Christchurch earthquake sequences. *Journal of Earthquake Engineering* 2014; 18(7): 1009–1036.
- [65] Hatzigeorgiou GD, Liolios AA. Nonlinear behaviour of RC frames under repeated strong ground motions. *Soil Dynamics and Earthquake Engineering* 2010; 30(10): 1010–1025.
- [66] Zhang Y, Burton HV, Sun H, Shokrabadi M. A machine learning framework for assessing post-earthquake structural safety. *Structural Safety* 2018; 72: 1–16.
- [67] Jeon JS, DesRoches R, Lowes LN, Brilakis I. Framework of aftershock fragility assessment—case studies: older California reinforced concrete building frames. *Earthquake Engineering & Structural Dynamics* 2015; 44(15): 2617–2636.
- [68] Uma S, Ryu H, Luco N, Liel A, Raghunandan M. Comparison of main-shock and aftershock fragility curves developed for New Zealand and US buildings. In: *Proceedings of the Ninth Pacific Conference on Earthquake Engineering. Auckland, New Zealand.* ; 2011: 14–16.
- [69] Li Y, Song R, Lindt V. dJ, Nazari N, Luco N. Assessment of wood and steel structures subjected to earthquake mainshock-aftershock. In: *15th World Conference on Earthquake Engineering. 15WCEE, Lisbon, Portugal.* ; 2012.

- [70] Fairhurst M, Bebamzadeh A, Ventura CE. Effect of Ground Motion Duration on Reinforced Concrete Shear Wall Buildings. *Earthquake Spectra* 2019; 35(1): 311–331.
- [71] Raghunandan M, Liel AB. Effect of ground motion duration on earthquake-induced structural collapse. *Structural Safety* 2013; 41: 119–133.
- [72] Belejo A, Barbosa AR, Bento R. Influence of ground motion duration on damage index-based fragility assessment of a plan-asymmetric non-ductile reinforced concrete building. *Engineering Structures* 2017; 151: 682–703.
- [73] Park YJ, Ang AHS. Mechanistic seismic damage model for reinforced concrete. *Journal of Structural Engineering* 1985; 111(4): 722–739.
- [74] Chandramohan R, Baker JW, Deierlein GG. Quantifying the influence of ground motion duration on structural collapse capacity using spectrally equivalent records. *Earthquake Spectra* 2016; 32(2): 927–950.
- [75] Hwang SH, Mangalathu S, Jeon JS. Quantifying the effects of long-duration earthquake ground motions on the financial losses of steel moment resisting frame buildings of varying design risk category. *Earthquake Engineering & Structural Dynamics* 2020.
- [76] Mahin SA. Effects of duration and aftershocks on inelastic design earthquakes. In: *Proceedings of the 7th World Conference on Earthquake Engineering. Istanbul, Turkey.* . 5. ; 1980: 677–680.
- [77] Amadio C, Fragiocomo M, Rajgelj S. The effects of repeated earthquake ground motions on the non-linear response of SDOF systems. *Earthquake Engineering & Structural Dynamics* 2003; 32(2): 291–308.
- [78] Liapopoulou M, Bravo-Haro MA, Elghazouli AY. The role of ground motion duration and pulse effects in the collapse of ductile systems. *Earthquake Engineering & Structural Dynamics* 2020; 49(11): 1051–1071.
- [79] Ji D, Wen W, Zhai C, Katsanos EI. Maximum inelastic displacement of mainshock-damaged structures under succeeding aftershock. *Soil Dynamics and Earthquake Engineering* 2020; 136: 106248.
- [80] PEER . PEER Ground Motion Database. 2020. <https://ngawest2.berkeley.edu/site>. Accessed August 2020.
- [81] Baker JW. Conditional mean spectrum: Tool for ground-motion selection. *Journal of Structural Engineering* 2011; 137(3): 322–331.
- [82] ATC . ATC Hazards by Location. 2020. [hazards.atcouncil.org](https://hazards.atcouncil.org). Accessed August 2020.
- [83] USGS . Unified Hazard Tool. 2020. [earthquake.usgs.gov/hazards/interactive](https://earthquake.usgs.gov/hazards/interactive). Accessed August 2020.
- [84] ASCE/SEI . ASCE 7-16: Minimum design loads and associated criteria for buildings and other structures. In: American Society of Civil Engineers. ; 2017.
- [85] Vamvatsikos D, Cornell CA. Incremental dynamic analysis. *Earthquake Engineering & Structural Dynamics* 2002; 31(3): 491–514.



- [86] FEMA P-695 . *Quantification of Building Seismic Performance Factors*; Washington, DC: Federal Emergency Management Agency (FEMA) . 2009.
- [87] Parsons VL. Stratified sampling. *Wiley StatsRef: Statistics Reference Online* 2014: 1–11.
- [88] Kullback S, Leibler RA. On information and sufficiency. *The Annals of Mathematical Statistics* 1951; 22(1): 79–86.
- [89] McKenna F, Scott MH, Fenves GL. Nonlinear finite-element analysis software architecture using object composition. *Journal of Computing in Civil Engineering* 2009; 24(1): 95–107.
- [90] Ibarra LF, Medina RA, Krawinkler H. Hysteretic models that incorporate strength and stiffness deterioration. *Earthquake Engineering & Structural Dynamics* 2005; 34(12): 1489–1511.
- [91] Sozen MA. The velocity of displacement. In: *Seismic Assessment and Rehabilitation of Existing Buildings*. Springer. 2003 (pp. 11–28).
- [92] Haselton CB, Liel AB, Deierlein GG, Dean BS, Chou JH. Seismic collapse safety of reinforced concrete buildings. I: Assessment of ductile moment frames. *Journal of Structural Engineering* 2011; 137(4): 481–491.
- [93] FEMA P-2012 . *Assessing Seismic Performance of Buildings with Configuration Irregularities*; Washington, DC: Federal Emergency Management Agency . 2018.
- [94] Haselton CB, Liel AB, Deierlein GG. Simulating structural collapse due to earthquakes: model idealization, model calibration, and numerical solution algorithms. *Computational methods in structural dynamics and earthquake engineering (COMPDYN)* 2009.
- [95] ASCE/SEI . ASCE 41: Seismic Evaluation and Retrofit of Existing Buildings. In: American Society of Civil Engineers. ; 2017.
- [96] Ruiz-Garcia J, Miranda E. Probabilistic estimation of residual drift demands for seismic assessment of multi-story framed buildings. *Engineering Structures* 2010; 32(1): 11–20.
- [97] Paal SG, Jeon JS, Brilakis I, DesRoches R. Automated damage index estimation of reinforced concrete columns for post-earthquake evaluations. *Journal of Structural Engineering* 2015; 141(9): 04014228.
- [98] Bommer JJ, Martinez-Pereira A. The effective duration of earthquake strong motion. *Journal of Earthquake Engineering* 1999; 3(02): 127–172.
- [99] Polese M, Di Ludovico M, Prota A. Post-earthquake reconstruction: A study on the factors influencing demolition decisions after 2009 L’Aquila earthquake. *Soil dynamics and earthquake engineering* 2018; 105: 139–149.
- [100] Murray MW. Shelter after disaster: Facts and figures. 2015. <https://www.scidev.net/global/features/shelter-after-disaster-facts-figures-spotlight/>. Accessed May 2021.
- [101] Kijewski-Correa T, Taflanidis AA, Mix D, Kavanagh R. Empowerment model for sustainable residential reconstruction in Léogâne, Haiti, after the January 2010 earthquake. *Leadership and Management in Engineering* 2012; 12(4): 271–287.

- [102] Mueller C, Frankel A, Petersen M, Leyendecker E. New seismic hazard maps for Puerto Rico and the US Virgin Islands. *Earthquake spectra* 2010; 26(1): 169–185.
- [103] McCann WR. On the earthquake hazards of Puerto Rico and the Virgin Islands. *Bulletin of the Seismological Society of America* 1985; 75(1): 251–262.
- [104] Pérez Méndez O. Partial number of refugees rises to more than 8,000. Primera Hora; 2020. <https://www.primerahora.com/noticias/puerto-rico/notas/cifra-parcial-de-refugiados-asciende-a-mas-de-8000>. Accessed May 2021.
- [105] Acevedo N. Puerto Ricans displaced by earthquakes wait for a safe home amid roadblocks, delays. NBC News; 2020. <https://www.nbcnews.com/news/latino/puerto-ricans-displaced-earthquakes-wait-safe-home-amid-roadblocks-delays-n1120941>. Accessed June 2021.
- [106] Blondet M, Garcia GV. Earthquake resistant earthen buildings. In: *13th World Conference on Earthquake Engineering, Paper*. No. 2447. ; 2004.
- [107] Change B. Example of a drop test for concrete blocks. 2013. <https://youtu.be/wexpHM3VYaM>. Accessed May 2021.
- [108] Barakat S. Housing reconstruction after conflict and disaster. *Humanitarian Policy Group, Network Papers* 2003; 43: 1–40.
- [109] Chen H, Xie Q, Li Z, Xue W, Liu K. Seismic damage to structures in the 2015 Nepal earthquake sequences. *Journal of Earthquake Engineering* 2017; 21(4): 551–578.
- [110] Barbosa AR, Fahnestock LA, Fick DR, et al. Performance of medium-to-high rise reinforced concrete frame buildings with masonry infill in the 2015 Gorkha, Nepal, earthquake. *Earthquake Spectra* 2017; 33(S1): 197–218.
- [111] Bothara JK, Dhakal R, Dizhur D, Ingham J. The challenges of housing reconstruction after the April 2015 Gorkha, Nepal earthquake. *Technical Journal of Nepal Engineers' Association, Special Issue on Gorkha Earthquake 2015, XLIII-EC30* 2016; 1: 121–134.
- [112] Manandhar S, Hino T, Soralump S, Francis M. Damages and causative factors of 2015 strong Nepal Earthquake and directional movements of infrastructures in the Kathmandu Basin and along the Araniko Highway. *Lowland Technol Int* 2016; 18(2): 141–164.
- [113] Dixit AM. Promoting safer building construction in Nepal. In: *13th World Conference on Earthquake Engineering*. ; 2004.
- [114] Lallemand D, Burton H, Ceferino L, Bullock Z, Kiremidjian A. A framework and case study for earthquake vulnerability assessment of incrementally expanding buildings. *Earthquake Spectra* 2017; 33(4): 1369–1384.
- [115] Yu XH, Dai KY, Li YS. Variability in corrosion damage models and its effect on seismic collapse fragility of aging reinforced concrete frames. *Construction and Building Materials* 2021; 295: 123654.
- [116] McKee C, Sideris P, Hubler M. Seismic performance of reinforced concrete structures considering steel corrosion. 2020.

- [117] Bose S, Martin J, Stavridis A. Simulation Framework for Infilled RC Frames Subjected to Seismic Loads. *Earthquake Spectra* 2019; 35(4): 1739–1762.
- [118] Han SW, Lee CS. Cyclic behavior of lightly reinforced concrete moment frames with partial- and full-height masonry walls. *Earthquake Spectra* 2020; 36(2): 599–628.
- [119] Guevara LT, Garcia LE. The captive-and short-column effects. *Earthquake Spectra* 2005; 21(1): 141–160.
- [120] Duran B, Tunaboyu O, Avşar Ö. Structural failure evaluation of a substandard RC building due to basement story short-column damage. *Journal of Performance of Constructed Facilities* 2020; 34(4): 04020053.
- [121] Brzev S, Mitra K. *Earthquake-resistant confined masonry construction*. NICEE, National Information Center of Earthquake Engineering . 2007.
- [122] Nguyen L. *Confined Masonry: Theoretical Fundamentals, Experimental Test, Finite Element Models, and Future Uses*. PhD thesis. University of Colorado at Boulder, 2014.
- [123] Yepes-Estrada C, Silva V, Valcárcel J, et al. Modeling the residential building inventory in South America for seismic risk assessment. *Earthquake spectra* 2017; 33(1): 299–322.
- [124] Calderon A, Silva V. Probabilistic seismic vulnerability and loss assessment of the residential building stock in Costa Rica. *Bulletin of Earthquake Engineering* 2019; 17(3): 1257–1284.
- [125] Antonopoulos T, Anagnostopoulos S. Seismic evaluation and upgrading of RC buildings with weak open ground stories. *Earthquake and Structures* 2012; 3(3-4): 611–628.
- [126] Sahoo DR, Rai DC. Design and evaluation of seismic strengthening techniques for reinforced concrete frames with soft ground story. *Engineering structures* 2013; 56: 1933–1944.
- [127] Chaulagain H, Rodrigues H, Spacone E, Varum H. Assessment of seismic strengthening solutions for existing low-rise RC buildings in Nepal. *Eartquakes and Structures: An Int'l Journal*, 8 (3) 2015: 511–539.
- [128] Timsina K, Krishna CG, Meguro K. Sociotechnical Evaluation of the Soft Story Problem in Reinforced Concrete Frame Buildings in Nepal. *Journal of Performance of Constructed Facilities* 2021; 35(4): 04021019.
- [129] McPhillips D, Herrick J, Ahdi S, Yong A, Haefner S. Updated compilation of VS 30 data for the United States. *US Geol. Surv. Data Release* 2020.
- [130] Martínez Cruzado JA, López Rodríguez RR, González Avellanet Y. Rehabilitación sísmica de casa en zancos. 2013.
- [131] ASTM . ASTM C270-19ae1 Standard specification for mortar for unit masonry. 2019.
- [132] Ou YC, Susanto YTT, Roh H. Tensile behavior of naturally and artificially corroded steel bars. *Construction and Building Materials* 2016; 103: 93–104.
- [133] Di Carlo F, Meda A, Rinaldi Z. Numerical evaluation of the corrosion influence on the cyclic behaviour of RC columns. *Engineering Structures* 2017; 153: 264–278.

- [134] Bousias SN, Biskinis D, Fardis MN, Spathis AL. Strength, stiffness, and cyclic deformation capacity of concrete jacketed members. *ACI Structural Journal* 2007; 104(5): 521.
- [135] Palieraki V, Vintzileou E. Cyclic behaviour of interfaces in repaired/strengthened RC elements. *Architecture Civil Engineering Environment* 2009; 2(1): 97–108.
- [136] Moaveni B, Stavridis A, Lombaert G, Conte JP, Shing PB. Finite-element model updating for assessment of progressive damage in a 3-story infilled RC frame. *Journal of Structural Engineering* 2013; 139(10): 1665–1674.
- [137] Mazzoni S, McKenna F, Scott MH, Fenves G, Jeremic B. OpenSees command language manual. Pacific Earthquake Engineering Research Center. *University of California, Berkeley* 2007.
- [138] Zhang Wp, Chen H, Gu Xl. Tensile behaviour of corroded steel bars under different strain rates. *Magazine of Concrete Research* 2016; 68(3): 127–140.
- [139] Meda A, Mostosi S, Rinaldi Z, Riva P. Experimental evaluation of the corrosion influence on the cyclic behaviour of RC columns. *Engineering Structures* 2014; 76: 112–123.
- [140] 318-14 A. Building code requirements for structural concrete (ACI 318-14). In: American Concrete Institute Farmington Hills, MI. ; 2015.
- [141] Murugesan A, Narayanan A. Deflection of reinforced concrete beams with longitudinal circular hole. *Practice Periodical on Structural Design and Construction* 2018; 23(1): 04017034.
- [142] Kassim MM, Ahmad SA. Strength evaluation of concrete columns with cross-sectional holes. *Practice Periodical on Structural Design and Construction* 2018; 23(4): 04018027.
- [143] Burton H, Deierlein G. Simulation of seismic collapse in nonductile reinforced concrete frame buildings with masonry infills. *Journal of Structural Engineering* 2014; 140(8): A4014016.
- [144] Bose S, Rai DC. Lateral load behavior of an open-ground-story RC building with AAC infills in upper stories. *Earthquake Spectra* 2016; 32(3): 1653–1674.
- [145] Tempestti JM, Stavridis A. Simplified method to assess lateral resistance of infilled reinforced concrete frames. In: ; 2017.
- [146] Sattar S, Liel AB. Collapse indicators for existing nonductile concrete frame buildings with varying column and frame characteristics. *Engineering Structures* 2017; 152: 188–201.
- [147] Stavridis A. *Analytical and experimental study of seismic performance of reinforced concrete frames infilled with masonry walls*. University of California, San Diego . 2009.
- [148] Ghaisas KV, Basu D, Brzev S, Gavilán JJP. Strut-and-Tie Model for seismic design of confined masonry buildings. *Construction and Building Materials* 2017; 147: 677–700.
- [149] Cardone D, Perrone G. Developing fragility curves and loss functions for masonry infill walls. *Earthquakes and Structures* 2015; 9(1): 257–279.
- [150] Ruiz-García J, Negrete M. Drift-based fragility assessment of confined masonry walls in seismic zones. *Engineering Structures* 2009; 31(1): 170–181.

- [151] Tomažević M, Klemenc I. Seismic behaviour of confined masonry walls. *Earthquake Engineering & Structural Dynamics* 1997; 26(10): 1059–1071.
- [152] Jiang C, Wu YF, Dai MJ. Degradation of steel-to-concrete bond due to corrosion. *Construction and Building Materials* 2018; 158: 1073–1080.
- [153] Brzev S, Astroza M, Moroni O. Performance of confined masonry buildings in the February 27, 2010 Chile earthquake. *Earthquake Engineering Research Institute, Oakland, California* 2010.
- [154] Federal Disaster Assistance for Puerto Rico Earthquakes Tops \$104 Million. Federal Emergency Management Agency (FEMA); 2020. <https://www.fema.gov/news-release/20200716/federal-disaster-assistance-puerto-rico-earthquakes-tops-104-million>. Accessed July 2021.
- [155] EERI . Puerto Rico Earthquake Sequence. Earthquake Engineering Research Institute (EERI); 2020. <http://www.learningfromearthquakes.org/2020-01-07-puerto-rico/>. Accessed June 2021.
- [156] Welsh-Huggins S, Rodgers J, Holmes W, Liel A. Seismic vulnerability of reinforced concrete hillside buildings in Northeast India. In: *Proc. of the 16th World Conference on Earthquake Engineering, Santiago, Chile. ; 2017*.
- [157] Dutta SC, Bhattacharya K, Roy R. Response of low-rise buildings under seismic ground excitation incorporating soil–structure interaction. *Soil Dynamics and Earthquake Engineering* 2004; 24(12): 893–914.
- [158] Lochhead M, Goldwyn B, Venable C, Liel A, Javernick-Will A. Assessment of and recommendations for hurricane wind performance of informally-constructed housing in Puerto Rico. *Natural Hazards Review* Under review.
- [159] Chmutina K, Rose J. Building resilience: Knowledge, experience and perceptions among informal construction stakeholders. *International journal of disaster risk reduction* 2018; 28: 158–164.
- [160] Ghannoum W, Matamoros A, Breña S, et al. Decision-oriented column simulation capabilities for enhancing disaster resilience of reinforced concrete buildings. In: *17th World Conference on Earthquake Engineering. 17WCEE, Sendai, Japan. ; 2020*.
- [161] Lehne J, Preston F. Making Concrete Change. *Innovation in Low-carbon Cement and Concrete* 2018.
- [162] Welsh-Huggins SJ, Liel AB. Evaluating multiobjective outcomes for hazard resilience and sustainability from enhanced building seismic design decisions. *Journal of Structural Engineering* 2018; 144(8): 04018108.

## Appendix A

### Interview questions for informal construction data collection

#### (1) Questions for hardware store owners

##### (a) Materials

##### (i) Concrete | *concreto*

- Are pre-made mixes commonly used? Do people make their own mix?
- What are typical mix ratios?
- Where are cement, sand, and gravel sourced from?
- What is the process for mixing and pouring concrete?
- Does anyone get concrete from a concreteria?
- How strong is the concrete?
- What mistakes are made in mixing concrete?

##### (ii) Masonry | *albañilería*

- What blocks are commonly used? Concrete or brick? Size?
- Where do the blocks come from?
- What reinforcement (if any) is used? What size and spacing?
- Is horizontal joint reinforcement used?
- What is used as mortar? Pre-made mix or made from scratch?
- What is used for grout?
- What strength testing (if any) is done?

(iii) Steel | *acero*

- What size bars are used in columns, beams, foundations, walls?
- How strong are the bars?
- Where do the bars come from?
- Is epoxy coated rebar used? Or other precautions for rebar that will be exposed?
- Is anything done to remove rust or otherwise maintain exposed bars?

(iv) Wood | *madera*

- Is the wood treated?
- What sizes are typical for posts, beams, trusses?
- How are the posts connected to the foundation?
- Are the fasteners typically metal or wood?
- What type of screws or nails are used?

## (b) Perceptions of safety and material demand

- What differentiates a good contractor from a bad one?
- Have people changed the types of materials they're building with (i.e. wood vs concrete) since the hurricane? since the earthquake?
- Has the amount people are willing to spend on materials changed with the hurricane? earthquake?
- What precautions are people taking to prepare for storms?
- Is anyone retrofitting/strengthening their home in case of an earthquake?
- Have you noticed other changes in building practices from the storms or earthquakes?
- Where do people get their information about how to build?

## (c) Incremental construction

- What provisions are included in construction to allow for incremental construction?
- Why do homeowners build incrementally?
- Is there a best practice? What are signs that a house was well set up for incremental construction or not?

(2) Questions for builders

(a) Foundation

- How do you decide what type of foundation to use?
- What materials are used for the foundation?
- What are typical dimensions for a foundation?
- How are columns connected to the foundation?
- What reinforcement is present in the foundations?
- How much development of rebar is present in the base of the columns?

(b) Columns

- How do you decide where to put columns?
- How do you decide what size columns are appropriate?
- How are the columns connected to the foundation and roof/beams?
- What longitudinal/transverse reinforcement is present? (size and spacing?)

(c) Walls

- Where are the blocks sourced from?
- Is there reinforcement in the walls? What type and what spacing?
- How are the walls connected to the columns?
- How do you make decisions about wall types?

(d) Beams



- How are the beams connected to the columns? Walls?
- Typical reinforcement - transverse and longitudinal?
- How do you make decisions about beam dimensions?

(e) Roof

- How is the roof connected to the building frame?
- What is the construction process for a concrete slab roof?

(f) Connections

- how are beams connected to columns?
- how are walls connected to columns and beams?
- how are columns connected to foundations? (also above)
- what is used to connect other elements (nails, screws, hurricane straps, plates, etc)?

(g) Incremental Construction

- What provisions are included in construction to allow for incremental construction?
- Why do homeowners build incrementally?
- Is there a best practice? What are signs that a house was well set up for incremental construction or not?

## Appendix B

### Multi-axial column material

I developed 2D and 3D nonlinear simulation models in this dissertation to capture the dynamic response of RC buildings. These models feature lumped plasticity elements; this approach offers an advantage over fiber models in computational efficiency and the capacity to phenomenologically capture softening behavior in highly-nonlinear, near collapse states [94]. The materials are defined using empirical equations calibrated to experimental data and consider nonlinear force-deformation backbones and strength and stiffness deterioration. These models, which have been developed in the open-source earthquake engineering software platform *OpenSees* [89], include a set of code-conforming and non-conforming RC frame buildings, and can easily be modified to represent other buildings in an effort to reduce the barriers to earthquake engineering assessment. These models have been used by other researchers to assess the seismic performance of 1960s-era RC buildings and reparability assessments of RC frame buildings with vulnerabilities, including limited deformation capacity and shear critical columns.

In developing these nonlinear simulation models, I make assumptions related to material strengths, building configuration, and load distribution. Model components are calibrated using empirical equations that have been developed from physical testing [54, 56, 55]. Particularly with informal construction, which, by definition, has non-code-conforming elements that may deform brittly, these databases are somewhat limited and may not be representative of the building archetypes in the study. The calibration of model elements generally requires determining the controlling failure mechanism (*e.g.*, flexure, shear, splice critical) a priori because the nonlinear force-deformation

response is dependent on the limiting failure mechanism [51, 160]. Brittle (shear) failure modes are difficult to capture numerically because the sharp change in force-deformation often presents a convergence problem [51]. Also, in columns and walls, the flexural and shear capacities vary with gravity demands. In dynamic analysis, these gravity demands change constantly as the building deforms, but current lumped-plasticity numerical modeling strategies cannot account for this updating interaction.

Ghannoum et al. [160] have developed a RC column model that addresses some of these limitations. This column model is calibrated internally—the user inputs column dimensions and detailing rather than externally calculated strength and deformation capacities. The model determines force-displacement responses for shear, axial, and flexural demands, and determines the controlling failure mechanism internally and continuously through the analysis. These equations that define the behavior of this column model are derived from a database with more than 600 column tests [160]. The model incorporates a spline curve to better capture stiffness changes and energy dissipation during cyclic loading. At each step of the analysis, the interaction between axial, shear, and flexure demands is updated. This model has been developed to consider steel jacket or fiber-reinforced polymer (FRP) retrofits, based on physical laboratory testing, and can be used to more simply evaluate the benefits of retrofit for seismic performance. I have worked to test the functionality and implement this new column model into system-level dynamic analysis. Through this work, I have identified discrepancies between forces in adjacent elements during dynamic analysis and errors in the shear response backbone definition. Figure B.1 illustrates the hinge force time history for this material, before and after the discontinuity in the hinge responses was addressed.

The studies presented in this dissertation employ currently-available methods for modeling RC building components, which are not without limitations. The capability of the new Ghannoum et al. [160] column model to capture updating multi-axial interaction, while maintaining computational efficiency, allows researchers to analyze non-ductile buildings for reparability with fewer external modeling assumptions. In assessing the reparability of a building, it would be quite valuable to investigate the effect of retrofit on seismic performance. Some retrofit strategies (*e.g.*, RC

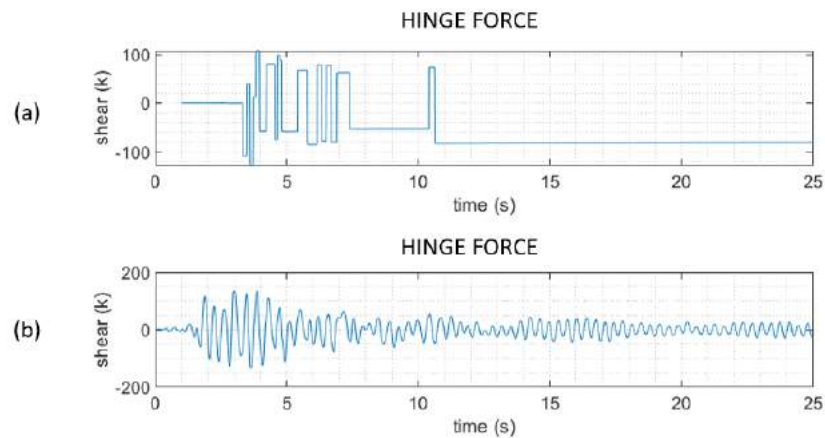


Figure B.1: Hinge response history (a) before and (b) after error generating discontinuity in the hinge was addressed

jacketing) can be incorporated into numerical models using existing strategies, but the implementation of other retrofit strategies such as steel jackets and FRP wraps is more difficult. Further, in my study of informally-constructed houses with RC columns that are susceptible to flexure and shear failure. Current methods dictate these be considered independently and a priori; the improvements offered by the Ghannoum et al. [160] model could simplify the modeling and assessment of informally constructed houses.